ÇUKUROVA UNIVERSITY
INSTITUTE OF NATURAL AND APPLIED SCIENCES

PhD THESIS

Ahmed ALAHMED

TEXTILE-BASED LITHIUM-ION BATTERY INVESTIGATION

DEPARTMENT OF TEXTILE ENGINEERING

ADANA, 2022

DEDICATION

To Allah, my Creator. I also recall my father (departed), mother, and siblings; their sacrifices and encouragements. Without your parenting, I would never be here where I am.

ÖZ

DOKTORA TEZİ

TEKSTİL BAZLI ESNEK LİTYUM-İON BATARYA GELİŞTİRİLMESİ

Ahmed ALAHMED

ÇUKUROVA ÜNİVERSİTESİ
FEN BİLİMLERİ ENSTİTÜSÜ
TEKSTİL MÜHENDİSLİĞİ ANABİLİM DALI

Danışman : Prof. Dr. Emel Ceyhun SABIR
Yıl: 2022, Sayfa: 126
Jüri : Prof. Dr. Emel Ceyhun SABIR
: Doç. Dr. Füsun DOBA KADEM
: Prof. Dr. Gülfeza KARDAŞ
: Prof. Dr. Oğuz DEMİRYÜREK
: Doç. Dr. Murat FARSAK

Giysilere, gözlüklere, saatlere ve hatta cilde entegre edilebilen akıllı tekstil, esnek elektronik cihazlar ve sensörlerin geliştirilmesi esnek bir enerji kaynağı gerektirir. Tekstil bazlı lityum iyon piller (LIB'ler) bu enerjiyi güvence altına almak için en önemli adaydır. Bu tezde, lityum piller için bir dizi mürekkep ve yapı incelenmiştir. Elektrot malzemelerinin seçiciliğine ve hazırlama yöntemlerine özel önem vurgu yapılmıstır.. Elektrotların elektrokimyasal özellikleri de Gamry cihazı kullanılarak incelenmiştir. Tekstil bazlı bir LIB de üretilmiş ve elektrokimyasal karakterizasyon, para tipi hücre pil test sistemi OPT-BST8-WA kullanılarak test edilmiştir. Üretilen madeni para hücrelerinin şarj ve deşarj kapasiteleri araştırılmıştır. Üretilen pilin kapasitansı 268.43 mAh g^{-1} olarak bulunmuş olup, bu kapasitans pil için kabul edilebilir düzeydedir .

Anahtar Kelimeler: Tekstil bazlı lityum iyon piller; Esnek elektrotlar; Oksit nanoparçacıkları; Tekstil depolama enerjisi.

ABSTRACT

PhD THESIS

TEXTILE-BASED LITHIUM-ION BATTERY INVESTIGATION

Ahmed ALAHMED

ÇUKUROVA UNIVERSITY
INSTITUTE OF NATURAL AND APPLIED SCIENCES
DEPARTMENT OF TEXTILE ENGINEERING

Supervisor: Prof. Dr. Emel Ceyhun SABIR
Year: 2022, Page: 126
Jury : Prof. Dr. Emel Ceyhun SABIR
: Assoc. Prof. Dr. Füsun DOBA KADEM
: Prof. Dr. Gülfeza KARDAŞ
: Prof. Dr. Oğuz DEMİRYÜREK
: Assoc. Prof. Dr. Murat FARSAK

The development of smart textile, flexible electronic devices and sensors that can be integrated into clothes, glasses, watches, and even skin requires a flexible source of energy. Textile-based lithium-ion batteries (LIBs) are the most important candidate to secure this energy. In this thesis, a series of inks and structures for lithium batteries were examined. Where special emphasis was placed on the selectivity of electrode materials and their preparation methods. The electrochemical properties of the electrodes were also examined using the Gamry device. A textile-based LIB was also manufactured and the electrochemical characterization has been tested by using the coin cell battery test system OPT-BST8-WA. The charge and discharge capacities of manufactured coin cells have been investigated. The capacitance of the produced battery was 268.43 mAh g^{-1}.

Keywords: Textile-based lithium ion batteries; Flexible electrodes; Oxide nanoparticles; Textile storage energy

EXTENDED SUMMARY

The development of smart textiles, flexible electronic devices, and sensors that can be integrated into clothes, glasses, watches, and even skin requires a flexible source of energy. This source should have the following properties: high specific capacitance wearability and long-term cyclability. The traditional energy sources are not able to be integrated into yarns and fabrics due to their rigid character.

Flexile batteries are considered an attractive power system that can supply smart textiles, flexible electronic devices, and sensors with energy due to their unique properties, such as their high energy density, high power density, high flexibility, lightweight, and wearability. Plastic batteries, flexible alkaline batteries, flexible rechargeable lithium-ion batteries (LIBs), polymer lithium-metal batteries, and other types of flexible batteries have been developed. In general, regardless of the composites/principle of the flexible battery, the design of a flexible battery must aim to achieve an optimal match between the electrode materials, electrolytes, and mechanically soft and strong current collectors. This is to ensure that the high capacity, robust flexibility, good conductivity, and high rate capability of the battery can be maintained. The optimization of the match between the battery components has been a challenge for researchers during the fabrication of flexible batteries.

Textile-based lithium ion batteries are considered the most suitable type of flexible battery to be easily integrated into smart textiles and garments. Textile-based batteries can be created by stacking coated fabrics layer by layer or weaving coated fibers to a fabric.

In this study, the materials used to produce electrodes and batteries have been described. The methods for assembling the electrodes and the battery also have been described, as will the methods for evaluating the electrochemical properties of electrodes and batteries, and the test tools and equipment used.

Cotton yarns and carbon yarns were used as the core material for fiber/yarn electrodes. Cotton fabric and carbon cloth were used as the core material for 2D

electrodes. Different metal oxides were used as active materials to obtain the positive and negative electrodes. Multi-Walled Carbon Nanotubes (MWCNTs) Carbon Black, Super P, and Graphite were used to increase the conductivity of the electrodes.

Several inks have been made that can be used to make conductive yarns and fabrics that store and release energy. Initially, yarns and fabrics were prepared to receive the inks. To ensure a good coating, various coating methods were used. The influence of different factors on the chemical properties of the resulting electrodes was investigated.

The electrodes are the basis for building flexible lithium-ion batteries (FLIBs), and many attempts have been made to develop flexible electrodes with high efficiency in terms of electrical conductivity, chemical and mechanical properties. The anode and cathode of the Li-ion coin cell were chosen from samples that had already been made based on the results of electrochemical tests.

Flexible substrate supported electrodes have been fabricated by using cotton yarns, cotton fabrics, carbon cloth, and carbon fiber paper. Both carbon cloth and carbon fiber paper have good conductivity, but cotton yarn and fabrics are considered insulating materials, so they have been coated with an electrical conductive material to obtain the required conductivity in order to make the battery.

The resistance of the produced samples was measured using a digital multimeter, and the conductivity was calculated. Where the conductivity is the reciprocal of the resistance.

The electrochemical characterization for produced electrodes has been tested and discussed by using Gamry Interface 1000 device. Where the 3-electrode method was used to obtain cyclic voltammetry CV and electrochemical impedance spectroscopy EIS curves for different electrode samples. Specific capacity (Cp) was calculated based on CV data.

The charge and discharge capacities of produced lithium ion batteries have been tested and investigated by using the coin cell battery test system. The

electrochemical characterization has been tested by using the coin cell battery test system OPT-BST8-WA. The charge and discharge capacities of manufactured coin cells have been investigated. The optimum results are given below.

A high flexible substrate supported anodes have been made using carbon fiber/Graphite /CMC, which shows an excellent electrochemical performance (a specific capacity of 412 mAh g^{-1}).

A high flexible substrate supported cathodes have been made using carbon fiber/LiFePO4 /Carbon Black, Super P/PVDF, which shows an excellent Li ion storage performance (a specific capacity of 225.785 mAh g^{-1}).

A textile-based LIB has been made and tested by using the coin cell battery test system OPT-BST8-WA. The capacitance of the produced battery was 268.43 mAh g^{-1}.

GENİŞLETİLMİŞ ÖZET

Giysilere, gözlüklere, saatlere ve hatta cilde entegre edilebilen akıllı tekstillerin, esnek elektronik cihazların ve sensörlerin geliştirilmesi esnek bir enerji kaynağı gerektirir. Bu kaynak, yüksek spesifik kapasitans giyilebilirliği ve uzun süreli döngülenebilirlik gibi özelliklere sahip olmalıdır. Geleneksel enerji kaynakları, katı karakterlerinden dolayı (esnek yapıda olmadıkları için) ipliklere ve kumaşlara entegre edilememektedir.

Esnek piller; yüksek enerji yoğunluğu, yüksek güç yoğunluğu, yüksek esneklik, hafiflik ve giyilebilirlik gibi benzersiz özelliklerinden dolayı akıllı tekstillere, esnek elektronik cihazlara ve sensörlere enerji sağlayabilen çekici bir güç sistemi olarak kabul edilir. Plastik piller, esnek alkali piller, esnek şarj edilebilir lityum iyon piller (LIB'ler), polimer lityum metal piller ve diğer esnek pil türleri geliştirilmiştir. Genel olarak, esnek pilin kompozitleri/prensibi ne olursa olsun, esnek bir pilin tasarımı, elektrot malzemeleri, elektrolitler ve mekanik olarak yumuşak ve güçlü akım toplayıcılar arasında en uygun eşleşmeyi sağlamayı amaçlamalıdır. Bu, pilin yüksek kapasitesinin, sağlam esnekliğinin, iyi iletkenliğinin ve yüksek hız kapasitesinin korunabilmesini sağlamak için gereklidir. Pil bileşenleri arasındaki uyumun optimizasyonu, esnek pillerin üretimi sırasında araştırmacılar için bir zorluk oluşturmuştur.

Tekstil bazlı lityum iyon piller, akıllı tekstil ve giysilere kolayca entegre edilebilecek en uygun esnek pil türü olarak kabul edilir. Tekstil bazlı piller, kaplanmış kumaşları katman katman istifleyerek veya kaplanmış elyafları bir kumaşa dokunarak oluşturulabilir. Bu tez çalışmasında elektrot ve pil üretiminde kullanılan tekstil bazlı malzemelere değinilmiştir. Aynı zamanda elektrotların ve pillerin birleştirilmesine yönelik yöntemler ile elektrotların ve pillerin elektrokimyasal özelliklerinin değerlendirilmesine yönelik yöntemler ve kullanılan test araçları ve ekipmanı da açıklanmıştır.

Elyaf/iplik bazlı elektrotları için çekirdek malzeme olarak pamuk iplikleri ve karbon ipliklerin kullanıldığı, 2D elektrotlar için ise ana malzeme olarak pamuklu kumaş ve karbon kumaş kullanıldığı görülmektedir. Tez çalışmasında pozitif ve negatif elektrotları elde etmek için aktif malzeme olarak farklı metal oksitler ve elektrotların iletkenliğini artırmak için çok duvarlı karbon nanotüpler (MWCNT'ler) Karbon Siyahı, Süper P ve Grafit kullanılmıştır.

Elektrotlar, esnek lityum iyon piller (FLIB'ler) oluşturmak için temel oluşturmaktadır. Tez çalışmasında elektriksel iletkenlik, kimyasal ve mekanik özellikler açısından yüksek verimli esnek elektrotlar geliştirmek için birçok denemelerde bulunulmuştur. Enerji depolayan ve serbest bırakan iletken iplik ve kumaşlarda kullanılmak üzere birkaç çeşit mürekkep hazırlanmıştır. İlk olarak, mürekkepleri bünyesine daha iyi alması (kaplanması) için iplikler ve kumaşlar süreksizlikleri gidermek için ütü gibi hazırlık aşamalarından geçirilmiştir. İyi bir kaplama sağlamak için çeşitli kaplama yöntemleri kullanılmıştır. Elde edilen elektrotların kimyasal özellikleri üzerinde farklı faktörlerin etkisi araştırılarak en iyi faktörler tespit edilmiştir.

Esnek substrat destekli elektrotlar, pamuk iplikleri, pamuklu kumaşlar, karbon kumaş ve karbon fiber kağıt kullanılarak üretilmiştir. Hem karbon kumaş hem de karbon fiber kağıt iyi iletkenliğe sahiptir, ancak pamuk ipliği ve kumaşlar yalıtım malzemesi olarak kabul edilir, bu nedenle pili yapmak için gerekli iletkenliği elde etmek için pamuk ipliği ve kumaşlar elektrik iletken bir malzeme ile kaplanmıştır. Üretilen numunelerin direnci dijital multimetre kullanılarak ölçülmüş ve iletkenlik hesaplanmıştır.

Üretilen elektrotların elektrokimyasal karakterizasyonu Gamry Interface 1000 cihazı kullanılarak test edilmiş ve tartışılmıştır. Farklı elektrot numuneleri için döngüsel voltametri CV ve elektrokimyasal empedans spektroskopisi EIS eğrilerini elde etmek için 3-elektrot yönteminin kullanıldığı yerlerdir. Özgül kapasite (Cp), CV verilerine göre hesaplanmıştır.

Üretilen lityum iyon pillerin şarj ve deşarj kapasiteleri madeni para pil test sistemi kullanılarak test edilmiş ve incelenmiştir. Elektrokimyasal karakterizasyon, düğme pil test sistemi OPT-BST8-WA kullanılarak test edilmiştir. Üretilen madeni para hücrelerinin şarj ve deşarj kapasiteleri araştırılmıştır. Tez çalışması sonucunda aşağıdaki optimum sonuçlar elde edilmiştir.

Karbon fiber/Grafit/CMC kullanılarak, mükemmel bir elektrokimyasal performans gösteren yüksek esnek bir alt tabaka destekli anotlar yapılmıştır (412 mAh g^{-1} özgül kapasite).

Karbon fiber/LiFePO4/Karbon Siyahı, Süper P/PVDF kullanılarak yüksek esnek alt tabaka destekli katotlar yapılmıştır ve bu mükemmel bir Li iyon depolama performansı gösterir (225.785 mAh g^{-1}spesifik kapasite).

Düğme pil test sistemi OPT-BST8-WA kullanılarak tekstil bazlı bir LIB yapılmış ve test edilmiştir. Üretilen pilin kapasitansı 268,43 mAh g^{-1} idi.

ACKNOWLEDGE

First and foremost, I am grateful to Allah, the Almighty, for keeping me fit and energized throughout my work. This study was made possible through contributions, support, and encouragement from many individuals. Unfortunately, it is not possible to acknowledge each of them here.

I especially would like to express my sincere gratitude to my supervisor, Prof. Dr. Emel Ceyhun SABIR, for offering me such a precious opportunity to conduct my PhD study under her supervision. Her wealth of knowledge and meticulous attitude inspire and motivate me a lot. Her patient guidance and encouragement supported me to move forward progressively.

I am also grateful to Prof. Dr. Gülfeza KARDAŞ and her group for the great lab environment as well as the helping group culture contributed by all of them.

I would give my thanks to Assoc. Prof.Dr. Füsun DOBA KADEM following up on the quarterly reports and for her wise guidance.

I also would give my thanks to Çukurova University for funding our project by the Scientific Research Projects Unit (BAP). Also I want to thank the administrative and academic staff in the Department of Textile Engineering, for the great support that I received during my doctoral study.

I'd also like to thank Assoc. Prof. Dr. Murat FARSAK, who welcomed me into his laboratory at Osmaniye Korkut Ata University and was instrumental in getting this project completed.

Last but not the least, I would like to thank my parents, brothers and sisters, parents-in-law, and brothers and sisters-in-law for their unending love and support, which translated into strength and guidance for me during my PhD studies. My heartfelt gratitude goes to my wonderful wife, Baraa Alabd, who is always supportive and inspiring me to complete my PhD, as well as to all of my beloved children, Abdullah and Sare. You are all an inspiration to me.

CONTENTS **PAGE**

ÖZ I
ABSTRACT II
EXTENDED SUMMARY III
GENİŞLETİLMİŞ ÖZET VII
ACKNOWLEDGE XI
CONTENTS XII
LIST OF TABLES XVI
LIST OF FIGURES XVIII
1. INTRODUCTION 1
1.1. Development of Batteries 1
1.2. The Battery's Main Components 2
1.3. Lithium-Ion Batteries 2
1.3.1. Working Principle of Lithium-Ion Batteries 2
1.3.2. Lithium-Ion Batteries Terminology 5
1.3.3. Advantages and Uses of Lithium Batteries 6
1.4. Flexible Batteries 9
1.4.1. Production of Flexible Batteries and Their Applications 9
1.4.2. Performance Evaluation of Flexible Batteries 13
1.5. Research Objectives 16
1.6. Research Originality 16
2. LITERATURE REVIEW 19
2.1. Flexible Electrodes 20
2.1.1. Flexible Substrate Supported Electrodes 23
2.1.1.1. Flexible Substrate Supported Anodes 25
2.1.1.2. Flexible Substrate Supported Cathodes 27
2.1.2. Flexible Freestanding Electrodes 30

2.1.2.1. Flexible Freestanding Anodes 31
2.1.2.2. Flexible Freestanding Cathodes 33
2.2. Solid-state Electrolytes 37
3. MATERIAL AND METHOD 39
3.1. Material 39
3.2. Method 41
3.2.1. Conductive Cotton-Based Electrodes Production 42
3.2.2. Anode Production 46
3.2.2.1. Preparation of Anode Inks 46
3.2.2.2. Coating Process for Anode Samples 49
3.2.2.3. Electrochemical Characterization of Anode Samples 55
3.2.2.4. Scanning Electron Microscopy (SEM) 62
3.2.3. Cathode Production 63
3.2.3.1. Preparation of Cathode Inks 63
3.2.3.2. Coating Process for Cathode Samples 65
3.2.3.3. Electrochemical Characterization of Cathode Samples 66
3.2.3.4. Scanning Electron Microscopy (SEM) 66
3.2.4. Battery Production 66
3.2.4.1. Lithium-Ion Battery Electrochemical Characterization 69
4. RESULTS AND DISCUSSION 71
4.1. Conductivity 71
4.2. The Effect of the Ink Preparation Method 73
4.3. The Effect of the Concentration of the Active Material 74
4.3. The Effect of the Carrier Material 77
4.4. Scanning Electron Microscopy (SEM) Results 79
4.5. Electrochemical Properties of Produced Lithium-Ion Batteries 80
5. CONCLUSIONS and RECOMMEDATIONS 81
5.1. Conclusion 81
5.2. Recommendation 82

REFERENCES 85
BIOGRAPHY 95
APPENDICES 97

LIST OF TABLES **PAGE**

Table 1.1. Advantages, disadvantages, and applications of various Li-ion battery types. 8
Table 3.1. The materials used to produce the electrodes and the battery and where they were purchased. 40
Table 3.2. The coating ink samples for conductive cotton yarns and fabrics 42
Table 3.3. The coating inks samples for textile-based LIBs anodes 49
Table 3.4. The 2D flexible substrate-based anodes that were made and the inks that were used. 54
Table 3.5. The coating inks samples for textile-based LIBs cathodes 64
Table 3.6. The 2D flexible substrate-based cathodes that were made and the inks that were used. 65
Table 3.7. The electrodes samples that used to produce Li-ion coin cell. 67

LIST OF FIGURES **PAGE**

Figure 1.1. The principle of the lithium-ion battery showing the intercalation of lithium-ions (yellow spheres) into the anode and cathode matrices upon charge and discharge, respectively 4
Figure 1.2. The energy density of lithium-ion batteries compared to other types of batteries 7
Figure 1.3. Wearable textile battery for smart textile applications. 10
Figure 2.1. The advantages and disadvantages of different types of flexible electrodes for LIBs. 22
Figure 2.2. An illustrative diagram of the flexible electrode production methods. 23
Figure 2.3. Flexible substrate supported anodes. A. Schematic for the 1 Si/TiO2-CC flexible anode, B. Schematic illustration of the preparation of composite VP@CFC., C. SEM images of Si-based anodes obtained by deposition using RF sputtering, C, D. Microfluidizer Schematic Diagram 27
Figure 2.4. Flexible substrate supported cathodes. A schematic of the V2O5 HoMSs/Ni-cotton fabric electrode fabrication process , B. schematic illustration of the fabrication processes for the CCF supported flexible organic cathodes and C. schematic illustration of the preparation process of the NFPP@NFP@C-CC flexible electrode. 30
Figure 2.5. Flexible freestanding anodes. A. Schematic illustration of the fabrication of SnS2/graphene/CC and graphene/SnS2/CC electrodes, B. Schematic illustration of the fabrication process of free-standing LTO-rGO film; C. Electrospun TiO2 and SiO2 nanofibers infused with TiO2 nanoparticles for lithium ion battery

anode: Schematic of the fabrication process for CB/Si/CB electrode..... 33
Figure 3.1. The materials used to fabricate the electrodes and the battery. 41
Figure 3.2. Photos of the procedure for preparing ink samples; A: CNTs weighing process, B: PVDF weighing process, C: The consistency of the final ink..... 43
Figure 3.3. Cotton yarns coating process..... 44
Figure 3.4. Yarn conductivity testing..... 45
Figure 3.5. Cotton fabrics samples..... 46
Figure 3.6. The first way for preparing inks samples for textile-based LIBs electrodes. 47
Figure 3.7. The second way for preparing anode inks samples 48
Figure 3.8. The used Mixers for preparing the coating inks 48
Figure 3.9. Coating Process for Yarn-Shaped LIBs anodes..... 50
Figure 3.10. Coating process for yarn-shaped anodes 51
Figure 3.11. Coating Process 2D LIBs anodes 52
Figure 3.12. 2D coated samples..... 53
Figure 3.13. 3-electrode cell setup..... 55
Figure 3.14. CV typical curve..... 58
Figure 3.15. The different areas in CV curve..... 59
Figure 3.16. Materials used to prepare the electrolyte..... 61
Figure 3.17. Measurement of electrochemical properties of electrodes using 3-electrode method..... 62
Figure 3.18. FEI Quanta model FEG 650 SEM analyzer. 63
Figure 3.19. The second way for preparing cathode inks samples 64
Figure 3.20. Circle sample cutting machine. 67
Figure 3.21. Glove box 68
Figure 3.22. Picture of battery components before assembly. **b.** Diagram showing the order of assembly. 68

Figure 3.23. Coin cell crimping machine. 69
Figure 3.24. Coin cell battery test system OPT-BST8-WA. 70
Figure 4.1. CV curve of a cotton fabric cathode sample coated on one side with cathode ink, scan rate of 0.1 mV·s-1. 72
Figure 4.2. CV curve of a cotton fabric cathode sample coated on both sides (first side with cathode ink and the second side with graphite), scan rate of 0.1 mV·s-1. 73
Figure 4.3. CV curves of the 3 different carbon cloth cathode samples, scan rate of 0.1 mV·s-1. 75
Figure 4.4. CV curves of the 2 different carbon fiber cathode samples, scan rate of 0.1 mV·s-1. 76
Figure 4.5. CV curves of the 3 different cotton fabric cathode samples, scan rate of 0.1 mV·s-1. 77
Figure 4.6. CV curves of the 3 different cathode samples of carbon cloth, carbon fiber, and cotton fabric, scan rate of 0.1 mV·s-1. 78
Figure 4.7. SEM morphology of 4 different samples (50000X) 79
Figure 4.8. SEM morphology of 4 different samples (50000X) 79
Figure 4.9. Charge-discharge curve for lithium-ion batteries 80

LIST OF SYMBOLS ABBREVIATIONS

1D	: One-dimensional
2D	: Two-dimensional
CC	: Carbon cloth
CCFs	: Carbonized cotton fibers
CMC	: Carboxymethyl cellulose sodium
CNTs	: Carbon nanotubes
CV	: Cyclic voltammetry DMC : Dimethyl carbonate
DMC	: Dimethyl carbonate
FEs	: Flexible electrodes
GO	: graphene oxide
CB	: carbon black
IR	: Internal resistance
Li	: Lithium
Li4Ti5O12	: Lithium Titanate Oxide
LIBs	: lithium-ion batteries
LiCoO2	: Lithium cobalt oxide
LiFePO4	: Lithium iron phosphate
LiMn2O4	: Lithium manganese oxide
LiNiCoAlO2	: Lithium nickel cobalt aluminum oxide
LiNiMnCoO2	: Lithium nickle manganese cobalt
Mo	: Metal oxide
MWCNT	: Multi-walled carbon nanotube
NMP	: N-Methylpyrrolidinone
NPs	: nanoparticles
NWs	: metal oxide nanowires
PAN	: polyacrylonitrile
PVD	: Physical vapor deposition

PVDF	: Polyvinylidene Fluoride
SEM	: Scanning Electron Microscope
SPEs	: Solid polymer electrolytes
SWCNTs	: Single-walled carbon nanotube
TiO2	: Titanium Dioxide
TPU	: Thermoplastic polyurethane

1. INTRODUCTION

Lithium-ion batteries (their components and principle of operation) will be discussed, as well as flexible lithium-ion batteries (their features and uses).Lithium-ion batteries (their components and principle of operation) will be discussed, as well as flexible lithium-ion batteries (their features and uses).

1.1. Development of Batteries

Humans have been dedicated to making full use of the various forms of energy available in nature since the first fire was lit. With technological advancements, not only chemical energy from biomass and fossil fuels, but also nuclear, solar, and wind energy, have been widely investigated. However, energy acquisition and release are typically transient, making storage and transport impossible. As a result, efforts to store energy have been made. Alessandro Volta, an Italian scientist, invented the first prototype of a battery, the voltaic pile, in 1799, using copper, silver, and zinc metal piles and salt solution as the electrolyte (Sun et al., 2017)(L. Li et al., 2021)(Cecchini & Pelosi, 1992). Since then, humanity has experimented with various types of batteries to store fleeting energy in the form of chemical energy for later use in the form of electrical energy at different times and places.

Regardless of the materials and mechanisms used, batteries are typically made up of two electrodes (a cathode and an anode), an electrolyte, and a separator. The energy is deposited in the electrodes via redox reactions of active materials. Mass transfer in the electrolyte enables the realization of redox reactions on separated electrodes. The separator is used to physically isolate the two electrodes in order to avoid a short circuit. During operation, ions in the electrolyte act as charge carriers and migrate within the internal circuit, while electrons transfer within the external circuit to generate current.

1.2. The Battery's Main Components

The battery's main components are:

Electrode: It is the charge-storing material, either through chemical bonds or a double layer capacitance.

Current collector: It is a sheet of metal that the electrode is rolled/adhered to in order to improve the electrical conductivity.

Electrolyte: a solution that transports ions from one electrode to another to perform ionic conductivity.

Separator: a device that separates two electrodes and current collectors so they do not short and allows electrolyte ions to pass through the membrane.

1.3. Lithium-Ion Batteries

Until now, lithium-ion batteries have unquestionably been the most commercialized batteries (Tarascon & Armand, 2001). After extensive research by John Goodenough, M. Stanley Whittingham, Rachid Yazami, and Koichi Mizushima in the 1970s and 1980s, Sony Inc. first commercialized lithium-ion batteries in the 1990s (M. Li et al., 2018). Today's lithium-ion batteries are typically made up of an anode made of graphitic carbon, a cathode made of Co, Mn, or FePO4-based materials, and a Li-rich electrolyte made of organic solvent.

1.3.1. Working Principle of Lithium-Ion Batteries

Lithium-ion batteries are a type of battery that generates electrical energy by converting chemical energy via redox reactions on the active materials, which are the negative (anode) and positive (cathode) electrodes in one or more electrically connected electrochemical cells. Lithium-ion batteries are classified as either primary (non-rechargeable) or secondary (rechargeable), depending on whether they can be recharged by applying an electric current (Anonymous, n.d.).

According to the "rocking chair" principle, Li-ions are shuttled between the positive electrode (typically a layered transition metal oxide material) and a graphite-based negative electrode in conventional lithium-ion batteries.

Figure 1.1 also shows the working principle of the lithium-ion battery. The negative electrode is typically composed of graphite. The positive electrode is typically made of a lithium metal oxide/phosphate, such as LiFePO4 or $LiMnO_2$. For electrical contact, a copper current collector on the negative side and an aluminum current collector on the positive side are typically used; the different metals are chosen based on the oxidation/reduction potentials to avoid side reactions such as oxygen evolution. An electrolyte is in charge of transporting ions between the electrodes.

It should have a high ionic conductivity and be electrically insulating. This is typically a lithium salt, such as $LiPF_6$, dissolved in organic carbonates, such as ethylene carbonate/diethyl carbonate mixtures. If the electrolyte is liquid, a separator is required to prevent short-circuiting; typically, this is micro-porous polyethylene with a thickness of around 30 μm. The electrolyte can also be solid, such as a polymer or gel electrolyte. In this case, the electrolyte acts as a separator and no additional one is required. Although the ionic conductivity of these electrolytes is typically lower, other benefits such as safety (no leakage) are achieved.

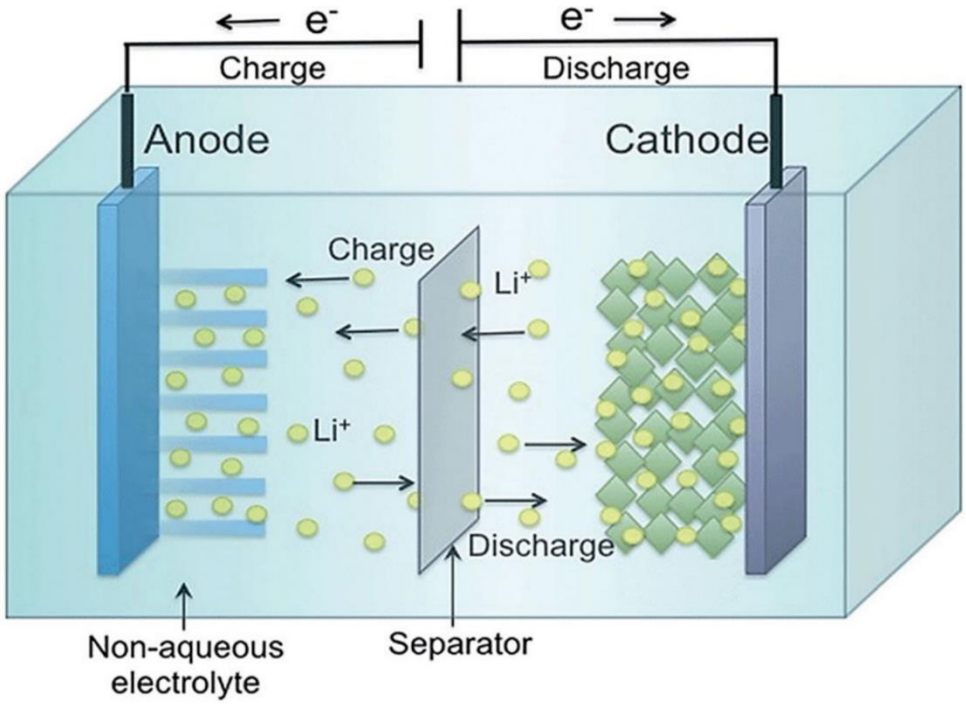


Figure 1.1. The principle of the lithium-ion battery showing the intercalation of lithium-ions (yellow spheres) into the anode and cathode matrices upon charge and discharge, respectively (Roy & Srivastava, 2015)

The process by which a battery supplies electrical energy to an external load is referred to as discharge. The electrolyte contains additional Li-ions to ensure rapid ionic charge transport within the cell.

The following equation expresses the working principle of LIBs:

Anode/Negative:

$$LiXXO_2 \rightarrow Li_{1-x}XXO_2 + Li^+ + xe^-$$

Cathode/Positive:

$$C + xLi^+ + xe^- \rightarrow Li_xC$$

Overall:

$$LiXXO_2 + C \rightarrow Li_xC + Li_{1-x}XXO_2$$

XX means various combining elements of the battery cathode material.

1.3.2. Lithium-Ion Batteries Terminology

Cut-off voltage (V): The cut-off voltage is the voltage at which the battery is considered "empty."

Capacity (Ah): The total amp-hours (Ah) available when the battery is discharged at a specific C-rate from 100 percent state of charge (full) to the cut-off voltage (empty) is known as the battery capacity, also known as the coulometric capacity.

Cycle life: Cycle life is the number of discharge and charge cycles that a battery can go through before failing to meet certain performance criteria.

Specific energy (Wh/kg): Specific energy is the nominal battery energy per unit mass, also known as gravimetric energy density. Along with how much energy is used in different situations, it tells how heavy a battery needs to be to reach a certain total energy.

Energy density (Wh/L): Energy density, also known as volumetric energy density, is the nominal battery energy per unit volume. Along with energy consumption of different applications, it determines the size of the battery required to achieve a certain total energy.

Internal resistance (IR) (Ω): The resistance that exists within the battery. It is usually different when charging and discharging, and it depends on the battery state of charge. The higher the internal resistance, the lower the battery efficiency.

Charge current (A): The constant current that charges the battery and raises the voltage (to approximately 70% state of charge) before switching to constant voltage charging (MIT Electric Vehicle Team., 2008).

Charge voltage (V): The voltage at which the battery is charged when it reaches full capacity. The charge voltage is generally reached when the battery is charged to about 70% state of charge by the charge current, and then becomes stable until the charge process ends (XIONG, 2019).

1.3.3. Advantages and Uses of Lithium Batteries

The benefits of lithium-ion batteries are self-evident. With high working voltages of 3. 3–4.2 V, the energy density of lithium-ion batteries can reach 150–200 $Whkg^{-1}$. Furthermore, the cycle longevity is excellent for more than 1,000 cycles. Figure 1.2 shows the energy density of lithium-ion batteries compared to other types of batteries.

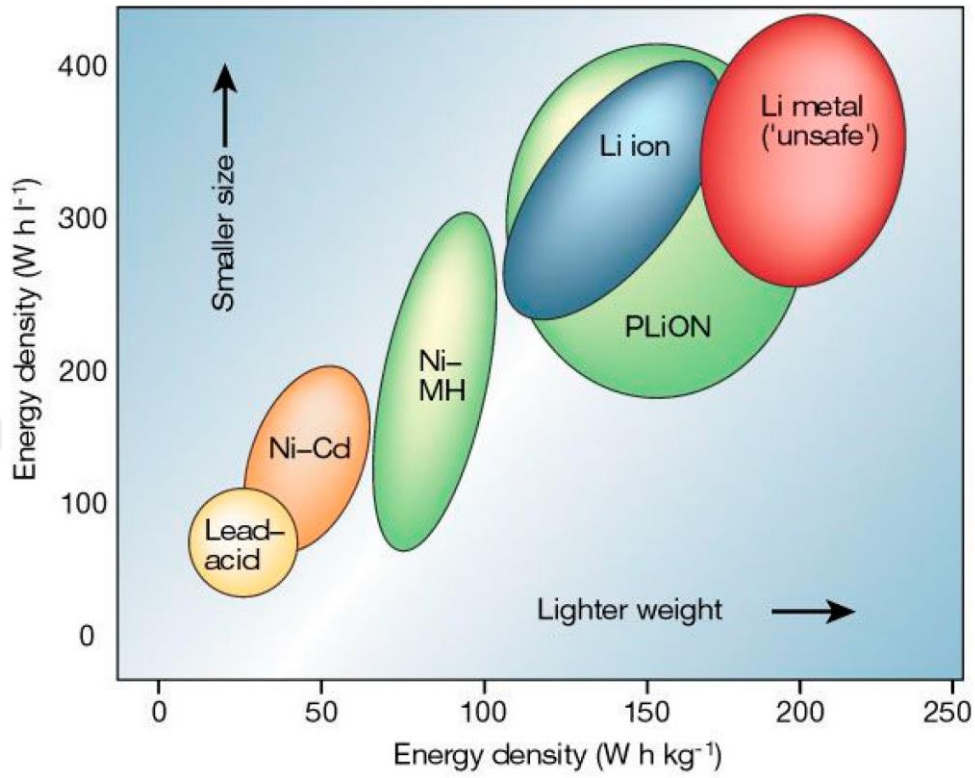


Figure 1.2. The energy density of lithium-ion batteries compared to other types of batteries (Tarascon & Armand, 2001).

Li-ion batteries come in a variety of shapes and sizes, with varying chemistries, but their basic components are the same: the cathode, anode, and electrolyte. The anode of Li-ion batteries is typically made of carbon/silicon and graphite. The cathode of Li-ion batteries, on the other hand, is made of different Lithium compounds, giving each battery distinct characteristics such as capacity, power density, cycle life, and safety. The five most common commercial Li-ion battery chemistries are shown in Table 2.1.

Table 1.1. Advantages, disadvantages, and applications of various Li-ion battery types (S. Wang et al., 2021).

Type	Advantages	Disadvantages	Applications
Lithium cobalt oxide LiCoO2	High specific energy	Unstable; Low specific power; Relatively short lifespan; Low thermal stability; Require built-in protective circuitry; Expensive	Energy cell; Digital portable devices such as mobile phones and laptop.
Lithium nickle manganese cobalt LiNiMnCoO2	High specific power; Safe, high thermal stability; Improved specific energy; Relatively large capacity; Long cycle life		Electric power train; Grid storage
Lithium nickel cobalt aluminum oxide LiNiCoAlO2	Stable; Long cycle life; Large capacity; High energy density	Low specific power	
Lithium iron phosphate LiFePO4	High thermal stability; Long cycle life; High capacity; High power; Safe, tolerate to abuse		Renewable energy storage(XIONG, 2019)
Lithium manganese oxide LiMn2O4	High specific power (load capability); Safe, high thermal stability;	Limited cycle and calendar life; Relatively low capacity	Electric vehicles; Power tools; Medical devices; Hybrid and electric vehicles

However, the development of lithium-ion batteries in the future is hampered by inherent issues. Combustion and explosion are serious safety concerns with

organic electrolytes. The scarcity of lithium reserves also portends a bleak future. Despite the relatively high energy density, efforts have been made to further increase the energy density in order to power electronics with higher energy demands.

1.4. Flexible Batteries

As with conventional batteries, a flexible LIB also needs five main components: an electrolyte, an anode, a cathode, current collectors, and a separator. However, this component must have specific properties, such as low self-discharge, high capacity, stable cycling performance, and high rate capability. Electrolytes should be non-liquid and have high ionic conductivity, mechanical flexibility, and electrochemical stability (Caiyun Wang & Wallace, 2015).

1.4.1. Production of Flexible Batteries and Their Applications

Many efforts have been made since the development of batteries to improve their electrochemical properties and design their shapes to fit various applications. Coin-type batteries, for example, have been developed for use in traditional watches, calculators, and thermometers, whereas cylinder, prismatic, and pouch-type batteries are used in smartphones and electric vehicles. All of these configurations, however, are bulky and rigid. The last decade has seen tremendous advancement in flexible electronic devices. Flexible and wearable electronic devices, such as the Huawei Mate X flexible smartphone, Apple Watch, and Mi band, have had a significant impact on human lifestyle. According to the most recent report from market research institute IDTechEx, the market will triple in size by 2026, reaching $150 billion. Furthermore, wearable sensors, implantable bioprobes, and interactive artificial intelligence (Galos et al., 2021) are examples of flexible electronic devices with enlightened perspectives(see Figure 1.3).

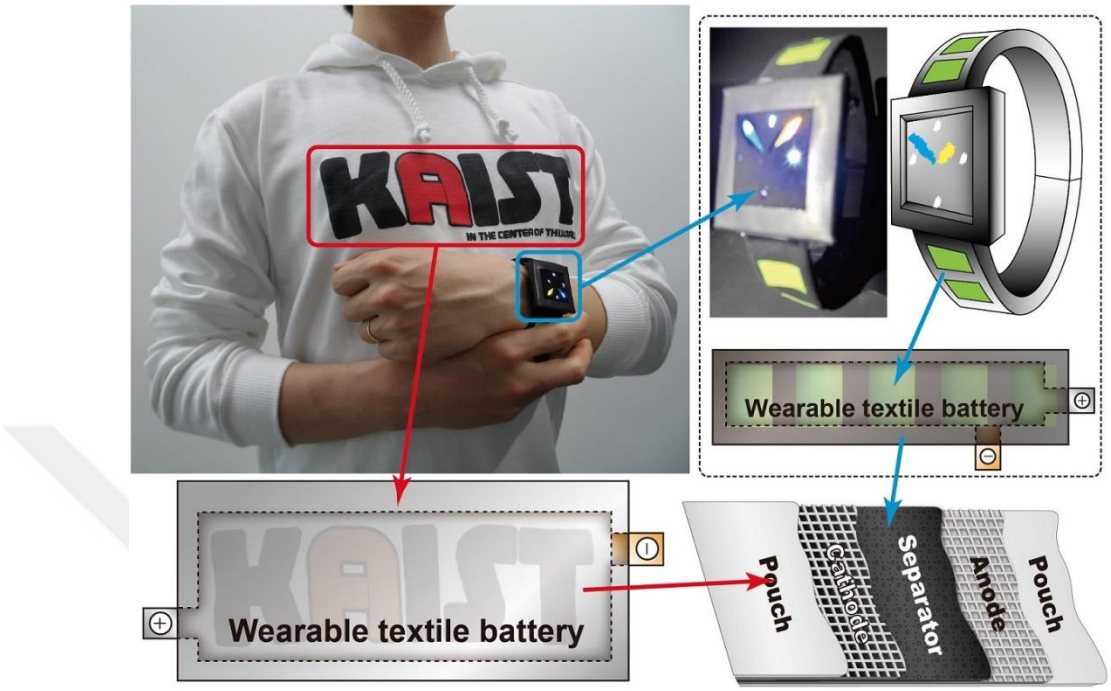


Figure 1.3. Wearable textile battery for smart textile applications (Y. H. Lee et al., 2013).

The batteries, on the other hand, appear in a rigid plate that cannot effectively meet the combined requirements of flexibility, light weight, miniaturization, and weaveability in modern electronics. As a result, the transition from traditional batteries to flexible batteries that are thin, lightweight, weavable, and even stretchable for integration has become a watershed moment in battery development.

Flexible batteries are typically manufactured in two forms: two-dimensional thin films and one-dimensional fibers. In 1993, Oak Ridge National Laboratory made the first attempt to fabricate two-dimensional thin-film batteries using lithium phosphorous oxynitride solid-state electrolytes prepared by vacuum deposition (Bates et al., 1993).

However, due to the high cost of fabrication and the time-consuming process, its potential for real-time applications has been limited. Furthermore, despite their high conductivity and cost-effectiveness, conventional aluminum and copper current collectors are typically too stiff to bend and fold. Carbonaceous current collectors have thus been developed as viable replacements for metal current collectors. Because of its structural stability, high conductivity, and commercial availability, carbon cloth has been regarded as a promising current collector.

The soft matrix allows for improved ion/ electron diffusion as well as high mechanical strength against various deformations and volume changes. Graphene, a two-dimensional monolayer of carbon atoms with packed honeycomb lattices, has a high surface area, thermal and chemical stability, conductivity, and flexibility.

These properties make graphene suitable for use as macroscopic self-standing electrodes. Carbon nanotube paper is another competitive substrate for flexible batteries due to its inherent advantages such as excellent electrical and thermal conductivity, large surface area, exceptional chemical stability, light weight, and impressive mechanical properties. As a result, carbon nanotubes can be formed into membranes that serve as substrates for active materials. Carbon nanotube electrodes have high cycling stability, good rate performance, and a high gravimetric energy density.

These carbonaceous substrates' free-standing electrodes are then loaded with active materials and sandwiched between a solid-state electrolytes to form thin-film flexible batteries. These thin-film flexible batteries are currently used in smart cards, radio frequency identification tags, implantable energy storage devices for neural stimulators, pacemakers, and defibrillators (Chunya Wang et al., 2019).

Despite significant efforts, the flexibility of thin-film flexible batteries remains limited. One-dimensional fiber batteries, on the other hand, have a number of intriguing advantages: (1) one-dimensional fiber batteries are compatible with the current textile industry and can be woven in textiles with multiple functions; (2) one-dimensional fiber batteries are permeable to air, which solves the critical issue of

thin-film batteries, which are impermeable to air; and (3) one-dimensional fiber batteries exhibit superior flexibility, compatibility, and miniaturization capability, which expands their working scenarios. Peng et al. created a wire-shaped micro-lithium-ion battery in 2013 by loading MnO2 nanoparticles on aligned multiwalled carbon nanotube fibers with lithium wires.

The specific volumetric capacity was 94.37 mAh.cm^{-3} and the specific gravimetric capacity was 174.40 mAh g^{-1} (J. Ren et al., 2013). Since then, enormous efforts have been made to develop additional battery systems and expand their applications. Fiber lithium-ion batteries have been thoroughly developed to date, and many novel battery systems, such as sodium-ion batteries, zinc-ion batteries, and metal-air batteries, have also been successfully converted into fiber batteries (Dong et al., 2021). Metal-organic frameworks and liquid metals have recently been investigated in fiber batteries, demonstrating their potential for next-generation fiber batteries (C. Zhang et al., 2018).

Aside from investigating novel materials and architectures, recent research has focused on the integration of flexible batteries with other functional components. One approach is to combine flexible batteries with supercapacitors or energy conversion devices, which can address the issues of low power density and self-power while also obtaining energy from the environment.

This strategy paves the way for greater energy efficiency and multifunctionality. Another approach would be to combine flexible batteries with other functional devices like bioprobes and biosensors. Flexible batteries can power biosensors while also serving as an integrated implant component. Currently, more effort is being made to design integrated systems with more functions and biocompatibility.

1.4.2. Performance Evaluation of Flexible Batteries

Flexible battery performance can be divided into two categories: electrochemical property and flexibility. Electrochemical properties, such as charge/discharge curves, cycle longevity, battery capacities, rate capability, temperature characteristics, and power/energy densities, generally follow the paradigm of conventional batteries. Charge/discharge curves represent battery characteristics such as charge/discharge voltage plateaus, specific capacities, and operation stability as represented by the curves' continuity.

Cycle life, expressed in cycle numbers, denotes the number of times a battery can be used under normal conditions. Battery capacity is the total charge stored in a charge/discharge cycle, expressed in milliampere-hours (mAh) or ampere-hours (Ah). For ease of comparison, battery capacity is typically normalized to gravimetric or volumetric specific capacities, which can be calculated using the following equations:

$$C_{\text{gravimetric}} = \frac{\int idt}{\text{m}}$$

$$C_{\text{volumetric}} = \frac{\int idt}{\text{v}}$$

Where I is the constant current applied, t is the charge/discharge time, and m (V) is the active materials' mass (volume). Rate capability refers to capacity retention (percent) with increasing charge/discharge rates, which is dependent on both fundamental component conductivity and reaction kinetics.

Temperature characteristics indicate battery reliability at extreme working temperatures, including temperatures above and below the normal temperature range. Energy density is the amount of energy stored gravimetrically or volumetrically, expressed in Whkg^{-1} or WhL^{-1}, whereas power density is the

amount of energy released per unit time, expressed in $Whkg^{-1}$ or WhL^{-1}. The following equation can be used to calculate energy density:

$$C_{\text{gravimetric}} = \frac{\int i * Udt}{\text{m}}$$
$$C_{\text{volumetric}} = \frac{\int i * Udt}{\text{v}}$$

Where I is the constant current applied, t is the charge/discharge time, U is the potential as a function of time, and m (V) is the active material's mass (volume).

The following equation can be used to calculate power density:

$$P = \frac{E}{\text{T}}$$

Where E denotes the gravimetric or volumetric energy density and T denotes the total charge/discharge time.

Flexibility, in addition to electrochemical properties, is an important parameter that must be evaluated. The ability of flexible batteries to maintain their electrochemical properties when subjected to various deformations such as bending, twisting, and stretching is commonly defined. Bending is the most commonly used working condition. Bending is typically characterized using two parameters:

Curvature bending angle (θ) and radius of curvature bending radius (r) as the substrate for flexible batteries, some evaluation systems use a cylinder with a fixed bending radius. The smaller r is thought to represent greater flexibility. The thickness and shape of the battery, on the other hand,

have a significant impact on its flexibility. As a result, the tensile strain calculated from the following equation is chosen to characterize the potential for flexible batteries in such application scenarios:

$$\varepsilon = h * r^{-1}$$

Where ε is the tensile strain, h is the thickness of the battery, and r is the bending radius.

The characterization of flexibility under twisting working conditions, on the other hand, is much cruder. Stabilizing the two ends of a flexible battery on a fixed actuator and a spinning actuator from the long side is a widely accepted testing method. The spinning actuator then spins at a fixed angle (e.g., ±15°) during certain twisting cycles (e.g., 1,000 cycles). The electrochemical property, which is typically capacity retention, is noted. The greater the flexibility under twisting deformation, the greater the twisting angle, the more twisting cycles, and the greater the capacity retention.

Stretching is the most difficult working condition for evaluating flexibility, and no standard measurement has been well established. This property is typically measured in the same way that twisting capability is.

A static actuator and a tensile actuator are attached to the two ends of a flexible battery from both the long and short sides. Following that, the tensile actuator stretches the flexible battery to a specific distance, which is normally expressed as a percentage of the flexible battery's length (e.g., 300 percent of the battery's length) for specific stretching cycles (e.g., 1,000 cycles). The electrochemical property, also known as capacity retention, is documented. The longer stretching distance, more stretching cycles, and

higher capacity retention indicate greater flexibility under stretching deformation.

1.5. Research Objectives

The aim of this research is to find the best way to fabricate Textile-bsed LIB that that can be integrated into yarns and fabrics. This involves:

Using the most suitable materials and producing methods to produce electrodes that provide high conductivity and specific capacitance.

Finding the best concentration of the active materials .

Enhancing the flexibility and texture characteristics to the electronic yarns selecting suitable packaging materials.

1.6. Research Originality

This research work develops three kinds' strategies/developments for fabricating high energy and high density and flexible textile-based electrode for wearable LIBs.

- A high flexible substrate supported anode has been made using carbon fiber/Graphite/CMC, which shows an excellent electrochemical performance (a specific capacity of 412 mAh g^{-1}).
- A high flexible substrate supported cathode has been made using carbon fiber/LiFePO4 /Carbon Black, Super P/PVDF, which shows an excellent Li ion storage performance (a specific capacity of 225.785 mAh g^{-1}) ,this result is higher than the highest result in the lecturer study which was 222.4 mAh g^{-1} In (Y. Zhu et al., 2020) study.

A textile-based LIB has been made and tested by using the coin cell battery test system OPT-BST8-WA. The capacitance of the produced battery was 268.43 mAh g^{-1}.

2. LITERATURE REVIEW

Flexible batteries are considered an attractive power system due to their unique properties, such as their high energy density, high power density, high flexibility, lightweight, and wearability. The development of flexible batteries is driven by the need for power systems for most of the developed soft portable electronic devices, such as wearable devices, rollup displays, integrated circuit smart cards, radio-frequency identification tags, etc. (Nathan et al., 2012).

The global wearable technology market was previously valued at USD 32.63 billion in 2019 and is expected to grow at a compound annual growth rate of 15.9% from 2020 to 2027 (Marriam et al., 2021).Numerous types of flexible batteries have so far been developed, such as plastic batteries (Prosini et al., 2001), flexible alkaline batteries (Gaikwad et al., 2011, 2012), flexible rechargeable lithium-ion batteries (LIBs) (Y. Zhao & Guo, 2020), polymer lithium-metal batteries (H. J. Kim et al., 2019; Mastragostino et al., 1999), etc. Generally, the design of a flexible battery must be aimed at achieving an optimal match between the electrode materials, electrolytes, and the mechanically soft and strong current collectors, irrespective of the composites/principle of the flexible battery (W. J. Zhang, 2011).

This is to ensure that the high capacity, robust flexibility, good conductivity, and high rate capability of the battery can be maintained. During the fabrication of flexible batteries, the optimization of the match between the electrode materials, electrolytes, and the soft & current collectors has been a challenge for researchers.

The history of flexible batteries dates back about 100 years ago, with flexible alkaline batteries (Gaikwad et al., 2011, 2012) and all-polymer batteries receiving early attention (Gofer et al., 1997; Nyholm et al., 2011; Sultana et al., 2012). In 2015, the global market for flexible batteries was worth USD 69.5 million, and it is expected to increase to USD 958.4 million by 2022 (Y. Zhao & Guo, 2020). Research interest in polymer lithium metal batteries only began recently (Mastragostino et al., 1999; Sannier et al., 2005; Shin et al., 2005), concentrating

more on flexible LIBs due to their high energy density, longer life, high voltage output, and environmentally friendly operation compared to other battery types(J. Wang & Sun, 2012). Both flexible LIBs and conventional LIBs share the same principles and concepts as already discussed in numerous studies (O'Heir, 2017).

Much progress has so far been made in core battery composite development; battery design has also been significantly advanced recently (Gwon et al., 2011). Numerous processes and new technologies have been introduced for the fabrication of high-performing full batteries (Flandrois & Simon, 1999). Nanoscience and nanotechnology have been the drivers of the advances in materials development as they enable the synthesis of different kinds of materials in different dimensions (1D and 2D) ((Bruce et al., 2008) (Liu et al., 2017)).

The innovation of new processes and technologies, such as sputtering, self-assembly, painting, printing, and deposition, has significantly advanced research in electrode materials (Ohta et al., 2013) (Liao & Fung, 2004). However, there are still many challenges for flexible LIBs research.

The currently existing batteries lack the capacity to withstand the stable power supply & cyclic stability necessary for operation under mechanical strains, mostly due to the following reasons: (i) The low strength and flexibility of the electrodes due to the use of intrinsically inflexible materials; (ii) The poor contact between the components of the battery , especially the active materials-substrate contact; (iii) Degradation of the mechanical and electrochemical properties due to operation in deformed states(normal use of textiles where many processes such as bending, tensile, friction, etc.).

2.1. Flexible Electrodes

The battery components and working principles of flexible rechargeable LIBs and conventional LIBs are similar. However, the design of flexible LIBs requires that the combination of the anode and cathode materials be done in a suitable medium that will ensure good mechanical strength and high flexibility.

For instance, a workable FE must have the active components combined with the basic current collector when twisting, bending, or folding a battery. The full battery design is somehow determined by the configuration of the flexible electrodes. Flexible electrodes are normally designed using two major approaches.

In the first approach, the active material is deposited or cast on a flexible substrate that has been pre-embedded with a current collector (Type-I).

In the second approach, the active material is bent with a second mechanically strong, electrically conductive, and electrochemically stable composite (normally 1D or 2D nanocarbon) to obtain the freestanding electrode (Type-II). This type of electrode does not need a flexible substrate as a backing composite. There are advantages and disadvantages to these two approaches. Type-I electrodes, for instance, exhibit strong mechanical strength due to the presence of a flexible substrate (yarn or fabric). But, this type of electrode requires a binder that can facilitate contact between the substrate and the active materials.

The overall energy density of the full battery is decreased due to the use of a non-conductive binder in combination with the substrate. This non-conductive binder adds nothing to the lithium storage but contributes to the weight of the electrode. The substrate also exhibits low surface area, which limits the contact between the active materials and the current collector. Hence, the active materials can be detached easily from the electrode upon deformation of the battery.

Most of the evaluations of Type-II electrodes are still at the laboratory scale due to their low mechanical stability despite their high energy density (due to the absence of a binder & substrate). Another limitation to the practical application of such electrodes is the low efficiency of their fabrication process.

Figure 2.1. shows the advantages and disadvantages of different types of flexible electrodes for LIBs.

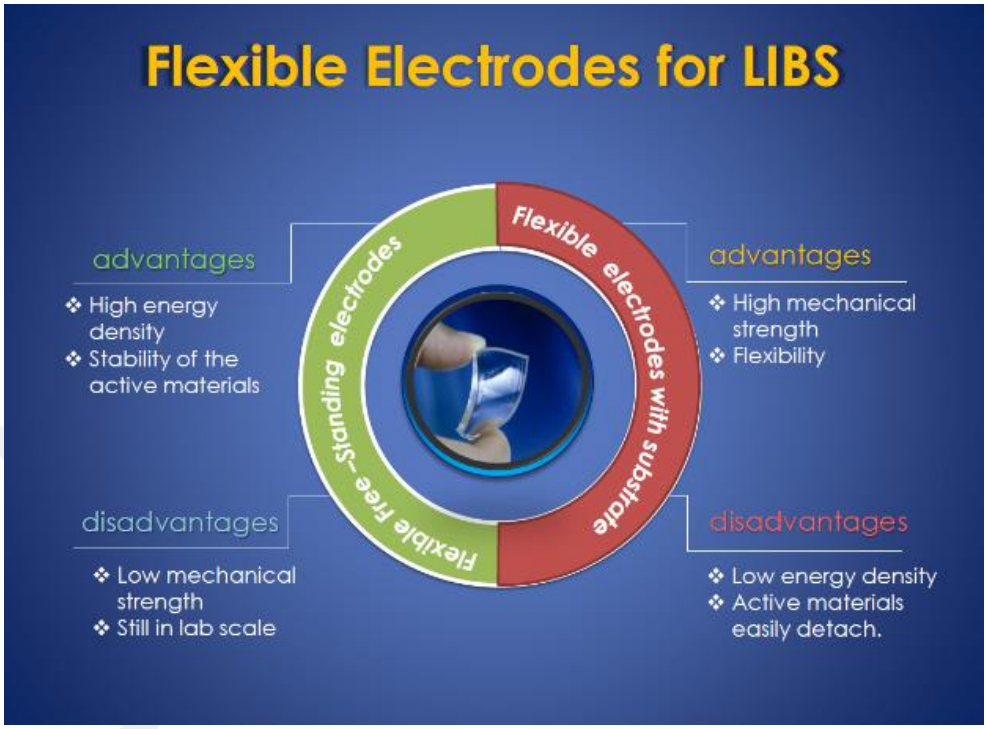


Figure 2.1. The advantages and disadvantages of different types of flexible electrodes for LIBs (Alahmed & Sabır, 2021).

Several attempts have been made to improve the mechanical and electrical properties of flexible freestanding electrodes by directing carbon nanofibers during the manufacturing process and reducing randomness in their placement (Downes et al., 2015). The alignment degree is widely thought to have a significant impact on the contact area and load transfer between neighboring carbon nanotubes (CNTs) due to the bulk resistivity dominated conduction, as opposed to contact resistance based conduction (Natarajan et al., 2019), resulting in dramatic changes in mechanical performance and linear changes in electrical performance (Vilatela et al., 2011)(Torres-Torres, C. Mercado-Zúñiga, C. Santos-Fernández, A. M. Martínez-González, C. L. Trejo-Valdez, M. Martínez-Gutiérrez, H. Vargas-García, J. R. Torres-Martínez, 2017). Regarding this, this review will focus on the development of two types of FEs.

Generally, Type-I Flexible electrodes (FEs) are classified into flexible anodes and flexible cathodes, but considering the substrate used, they are further classified into FEs on conductive and non-conductive substrates. Furthermore, Type-II electrodes are classified into flexible anodes and flexible cathodes; the flexible anodes are further classified into 2D and 3D carbon assemblies and high-capacity nanomaterials (see Figure 2.2) (K. T. Lee & Cho, 2011).

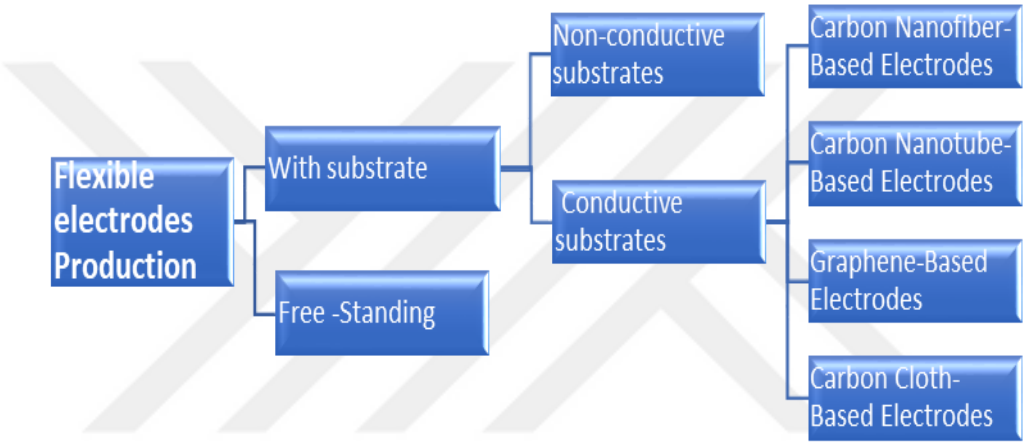


Figure 2.2. An illustrative diagram of the flexible electrode production methods.

2.1.1. Flexible Substrate Supported Electrodes

The mechanical strength and flexibility of this type of flexible electrode depend on the used substrate; note that both electrically conductive and non-conductive substrates can be used.

Some of the conductive substrates are metal foil (Jiang et al., 2012), carbon-based yarns /fabrics, and films, while substrates such as polycellulose, cotton yarns (B. Wang et al., 2020), silicon sheet (Kasavajjula et al., 2007), plastic films (Prosini et al., 2001), paper, and kapton are non-conductive. Regarding the need for a current collector to be fabricated during the electrode preparation, it is a function of the properties of the flexible substrate. For instance, a conductive substrate may act as a current collector, but using a non-conductive substrate demands the deposition of an

additional conductive composite (that will act as a current collector) onto the substrate.

The employed electrode preparation process is also determined by the selected substrate; printing or painting can be employed when the employed substrate is either paper, plastic (H. Kim et al., 2007), or metal foil. This part emphasized the flexible substrate and current collector in each of the considered examples. Considering flexibility and mechanical strength, metal foils, when thin enough, are suitable substrates for flexible LIBs, but their usage as a flexible substrate has several drawbacks. First, the density of metal foils, such as aluminum for cathodes and copper and iron for anodes (Park et al., 2010), is relatively higher than that of the other potential substrates.

The use of these foils can negatively affect the overall energy density of a full LIB as they will contribute about 15% of the total electrode mass without making any contribution to the lithium storage capacity of the electrode. Furthermore, the low surface area of these metal foils confers them with weak adhesion and low contact with the active material, leading to the formation of gaps at the electrode/metal interface and alteration of the volume of the active materials during the charging and discharging processes.

The consequence is a decline in battery performance, both in cyclic stability and capacity (Stenina et al., 2018). This problem is of great concern when fabricating flexible batteries due to the high possibility of this continuous deformation causing the separation of the metal foils from the active materials. Metal foils may also be prone to corrosion and chemical instability, which can cause an increase in the internal impedance, passivation of active materials, as well as reduced rate capability (He et al., 2013). This accounts for the low number of studies on metal foil utilization as flexible substrates compared to the carbon-based membranes which are being extensively researched.

Carbon-based sheets are theoretically better substrates for FE because they can serve as both support for the active materials and as a current collector. Several

new carbon 2D & 3D structures have so far been produced (C. Zhao et al., 2018); some have been reported to exhibit high mechanical strength and flexibility and have been investigated at lab scale as current collectors or substrates for flexible LIBs. Some of these novel carbon structures are graphene paper (Gwon et al., 2011), CNTs films (Wu et al., 2021), graphene foam (Yao et al., 2018), porous carbon films, carbon cloth, etc. (W. Ren et al., 2013). Another way of producing a current collector is the embedment of 1D nanostructured carbon into polymer-based films.

This approach has high practical application potential. This part of the review provides a summary of Type-I FEs based on the carbon arrangement in the current collectors.

2.1.1.1. Flexible Substrate Supported Anodes

Some of the studies on the fabrication of flexible substrate supported anodes are reviewed in this part. The study by Li et al., 2020, presented the fabrication of a carbon-doped anatase TiO2-based flexible Si anode for flexible LIBs.

The flexible silicon anode produced in this study exhibited high-performance and stability as shown in Figure 2.3 –a. A modified sol-gel impregnation method was used to prepare the Si/Ti O2-CC flexible anode. The TiO2 layer confers the flexibility feature on the integrated structure while Si expansion is prevented by the Si/TiO2 structure. The fabricated composite anode exhibited excellent stable cycle performance and areal capacity (B. Li et al., 2020).

C. Wang et al. (2020)(Chao Wang et al., 2020) prepared spherical VPO4 particles grown on carbon fiber cloth, as shown in Figure 2.3-b.The composite is used as a flexible binder-free anode for LIBs. In terms of reversible lithium-ion storage capacity (541.2 mAh g^{-1}at 0.1C), rate capability (350.2 mAh g^{-1} at 10C), and cycling stability (a capacity retention ratio of 91.8 percent after 250 cycles at 1C), the anode produced performs well(Chao Wang et al., 2020).

Another study reported the use of Multi-walled carbon nanotube (MWCNT) sheets as a substrate for the fabrication of flexible LIBs. In this approach, thin Si films were deposited via physical vapor deposition (PVD) using the Radio Frequency (RF) magnetron sputtering technique (Figure 2.3-c). The fabricated MWCNT-Si nanocomposites were evaluated as anode materials in full cells using LiFeP4O4 as the cathode and in half-cells using Li metal as counter and reference electrodes. Based on the analysis, the produced MWCNT-Si composites were electrochemically stable during 50 cycles; they also exhibited a good level of reversible capacity. In the full cell analysis, the MWCNT-Si//LiFePO4 exhibited satisfactory cycling performance during 50 cycles and delivered a voltage of 2.9 V (Bensalah et al., 2019).

Aziz A, 2020, published a study on the preparation of double-walled CNTs Ink for the fabrication of high-conductivity flexible electrodes. The study reported the suitability of water and sodium cellulose in producing scalable and conductive CNT-based ink provided the solution is micro-fluidized (see Figure 2.3-d). Acid-free materials were used, hence, no post-processing step was needed. The produced electrodes exhibited a conductivity of $3.6 \pm 0.2 \times 105\ Sm^{-1}$ and a sheet resistance of $0.11\ \Omega^{-1}\ mil^{-1}$. Further, the free-standing carbon films achieved a thermal conductivity of $43 \pm 4\ W\ m^{-1}\ K^{-1}$. With this approach, the study reported successful production of uniformly dispersed CNT inks of >1 Pa·s viscosity (Aziz et al., 2020).

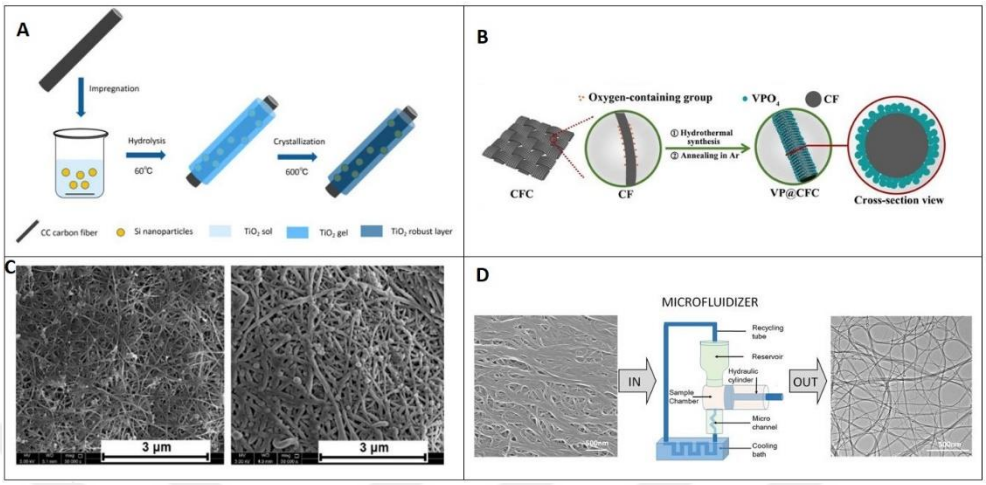


Figure 2.3. Flexible substrate supported anodes. A. Schematic for the 1 Si/TiO2-CC flexible anode (B. Li et al., 2020), B. Schematic illustration of the preparation of composite VP@CFC(Chao Wang et al., 2020)., C. SEM images of Si-based anodes obtained by deposition using RF sputtering, C, D. Microfluidizer Schematic Diagram (Aziz et al., 2020).

2.1.1.2. Flexible Substrate Supported Cathodes

The fabrication of flexible cathodes is one of the main confrontations in the research and development of flexible LIBs. The commonly used cathode materials, such as LiCoO2, LiMn2O4 and LiFePO4, are generally manufactured in environments with high temperatures (> 500°C). Most flexible substrates or materials used to make flexible substrates are chemically unstable at these elevated temperatures. For example, although carbon is able to remain stable at temperatures above 1000 °C, it may react with cathode materials (for example, LiCoO2 and LiMn2O4), resulting in failure to obtain optimal crystallization, and cathode material deterioration, thus low battery performance.

The preparation of flexible cathode materials usually relies on deposition methods such as sputtering and laser ablation, whereby nano-cathode materials can be successfully produced. However, these processes are high-cost and low-efficient.

Therefore, the innovation of new processes for preparing flexible cathodes remains an important research topic.

In the study (Y. Zhu et al., 2020), V2O5 hollow multi shelled structures (HoMSs) prepared by sequential templating are used as active materials, and conductive metallic fabrics are used as current collectors and flexible substrates, as shown in Figure 2.4-A. The prepared fabric exhibits excellent electrochemical performance and ultrahigh stability by leveraging the desirable structure of V2O5 HoMSs, which effectively buffers volume expansion and alleviates stress/strain during repeated Li-insertion/extraction processes, as well as the robust, flexible metallic-fabric current collector. Even after 500 charge/discharge cycles, the capacity retains a high value of 222.4 mA h g^{-1} at a high mass loading of 2.5 mg cm^{-2}, and no obvious performance degradation is observed after hundreds of cycles of bending and folding. These findings suggest that the V2O5 HoMSs/metallic-fabric cathode electrode is a promising candidate for highly flexible lithium-ion batteries (Y. Zhu et al., 2020).

The preparation of carbonized cotton fibers (CCFs) via the carbonization of commercial cotton at different temperatures has been reported by Wang, B., (2020), as in Figure 2.4-b. The carbonization temperatures determine the properties of the produced CCFs. The high aspect ratio and high conductivity of the CCFs make them suitable for use as conductive agents in the integrated organic cathodes of LIBs. The conventional LIB cathodes presented high specific capacities at the optimized CCF ratio of 900 °C; they also exhibited good cyclizing stability by retaining 90.5% of their maximum capacity value after 500 cycles at 0.5 A g^{-1}. This material is suitable for flexible LIBs fabrication due to its good mechanical strength, as manifested by the stable performance at various bent states (B. Wang et al., 2020).

The study by Ma, X., (2019), reported the preparation of $Na_4Fe_3(PO_4)2(P_2O_7)$@$NaFePO_4$@C core-double-shell structures grown on flexible

carbon cloth using a facile sol-gel fabrication approach followed by heat treatment; the prepared structure acts as a binder-free cathode in Na^+ batteries.

The thickness of the $NaFePO_4$ shell in the composite can be fixed at about 15 nm to promote electrochemical activation and ensure high reversible capacity. The working voltage of the $Na_4Fe_3(PO_4)2(P_2O_7)$ core was relatively high & the ion transport capability was fast. Furthermore, the external carbon shell and the carbon cloth conjointly produce a fast 3D electronic conducting network. Adding to the compositional and structural advantages of the $Na_4Fe_3(PO_4)2(P_2O_7)$@$NaFePO_4$@C carbon cloth cathode, its discharge capacity was also high (136 mAh g^{-1} at 0.1 C), as well as excellent cycling stability for over 3000 cycles at 10C without performance decay; the rate capability of the structure was also good at 68 mAh g^{-1} at 100C (see Figure 2.4-c) (Ma et al., 2019).

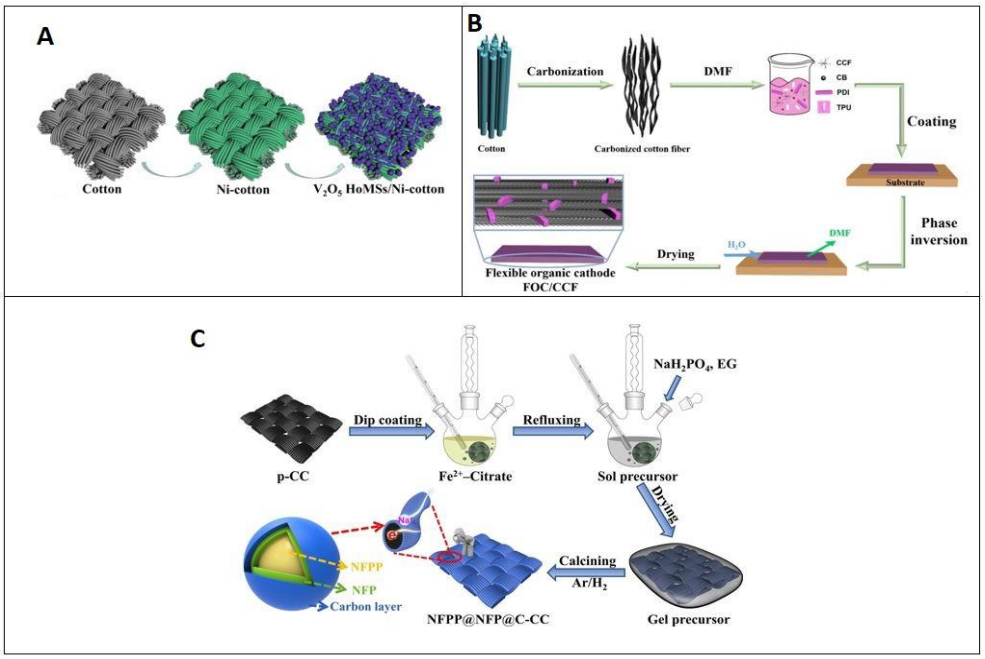


Figure 2.4. Flexible substrate supported cathodes. A schematic of the V2O5 HoMSs/Ni-cotton fabric electrode fabrication process (Y. Zhu et al., 2020), B. schematic illustration of the fabrication processes for the CCF supported flexible organic cathodes (B. Wang et al., 2020), and C. schematic illustration of the preparation process of the NFPP@NFP@C-CC flexible electrode (Ma et al., 2019).

2.1.2. Flexible Freestanding Electrodes

Generally, freestanding electrodes are combinations of 1D and 2D nanostructured active materials, such as nano carbons (like carbon fibers, graphene, CNTs), metal oxide nanowires (NWs) and nanoparticles (NPs), Si NWs & NPs, etc.

Most of the time, a filtration process is required to achieve some of these assemblies. The application of such FEs is restricted by their low efficiency, coupled with their low mechanical strength. This has restricted studies on such flexible electrodes to the laboratory scale, with few studies on full battery constructions.

2.1.2.1. Flexible Freestanding Anodes

The preparation of a binder-free anode for LIB has been reported by Wang, M. (2019)'s study. The polyacrylonitrile (PAN) in the anode serves as a binder and a conductive agent after pyrolysis to improve the specific capacity and conductivity in the absence of any other insulator (see Figure 2.5-a). The study obtained a stable anode with high battery performance at the optimal active material size and Si -PAN ratio (M. Wang et al., 2019). Another study published in 2018 by Yao, Y., created an electrode by halide ion intercalated electrodeposition of Co(OH)2 nanosheet precursors on graphene foam. The final product of the process, which is the Co_3O_4/graphene foam electrode, exhibited good mechanical strength and flexibility.

The Br:Cl ratio was adjusted to regulate the specifications of the final product. The electrode recorded a maximum specific capacity of 790 mAh g^{-1} after 100 cycles at a 0.1 C current density and 0.2−3.0 V voltage range. The similar particle size distribution of the Co_3O_4 nanosheets also reduced the pore structure effect on the electrochemical performance (Yao et al., 2018).

The Zhu, K., (2018), study reported the design and fabrication of a flexible freestanding $Li_4Ti_5O_{12}$-rGO film as seen in Figure 2.5-b. The produced film exhibited a mesoporous structure, high $Li_4Ti_5O_{12}$ load, and good conductivity. The cycling stability and rate performance of the electrodes were also high, even though the rate performance was affected by the sequence of graphene oxide (GO) additions in the hybrid film (K. Zhu et al., 2018).

A flexible felt that consists of amorphous SiO_2 & electrospun anatase TiO_2 nanofibers was prepared by Wang, X., (2016). The nanofibers also contained anatase TiO_2 NPs and were considered a novel anode material for LIBs (see Figure 2.5-c). Upon half-cell electrochemical characterization of the flexible felt, the felt exhibited excellent rate capability and a high initial discharge capacity. Furthermore, 84% of the initial capacity value was retained after 100 cycles at a 1 A g^{-1} charge/discharge rate. The electrochemical performance of the binder-free composite felt remained

high, coupled with good flexibility/robustness after 5000 bending cycles (X. Wang et al., 2016).

The study by Li et al. (2017) prepared a flexible & free collector-current of Si-based anode via coating with carbon black (CB) and Si layer-by-layer. The tri-layer CB/Si/CB electrode was prepared via re-coating on polymethyl methacrylate (PMMA) film, as seen in Figure 2.5-d. A casting process can also be used to prepare the PMMA film. The PMMA-film is coated with the prepared CB slurry and heated for 30 min at 80 °C; then the Si-slurry and CB-slurry are sequentially coated on the above materials.

The prepared tri-layer CB/Si/CB electrode is composed of a single Si material in the middle-layer and double CB layers. Lastly, the PMMA-based film is dissolved in ethyl acetate. The obvious difference between the flexible CB/Si/CB electrode is the presence of the Si/foil, as well as the use of the double CB-layers to shield the Si material (C. Li et al., 2017).

Xia et al. (2020) employed the hydrothermal approach to produce Mo-doped δ-MnO_2 powders. During the study, $MnSO_4 \cdot H_2O$ & $KMnO_4$ were added into 40 mL deionized water at a molar ratio of 1:6; various amounts of $(NH_4)_6MO_7O_{24}\cdot 4H_2O$ were also added into the mixture at different Mo^{6+} and Mn^{2+} molar ratios. The mixture was stirred at room temperature for 5 min before being put in a 50 mL stainless-steel autoclave (Teflon-lined) for hydrothermal treatment at 160 °C for 16 h. The obtained product was rinsed several times using DW and ethanol, then dried for 12 h at 70 °C.

The obtained samples were labeled based on their respective molar ratios as Mo 1%, Mo 3%, Mo 5%, Mo 7%, and Mo 10%. A similar process was also used to prepare pure δ-MnO_2 but $(NH_4)6Mo_7O_{24}\cdot 4H_2O$ was not added to the mixture. From the results, Mo ions with + 6 valances partially substituted Mn4+ ions in the crystal lattice. The best electrochemical performance was delivered by Mo 5%; it also achieved a high specific charge capacity value of 476.8 mAh g^{-1} after 100 cycles at

1000 mA g^{-1}. It also retained 112.7% of its initial capacity. The electrochemical performance was improved by the appropriate Mo doping in δ-MnO_2 as it improves the electrical conductivity, specific surface area, and diffusion rate of Li^+. However, the δ-MnO_2 lattice structure was damaged by excess Mo doping, which deteriorated the electrochemical performance (Xia et al., 2020).

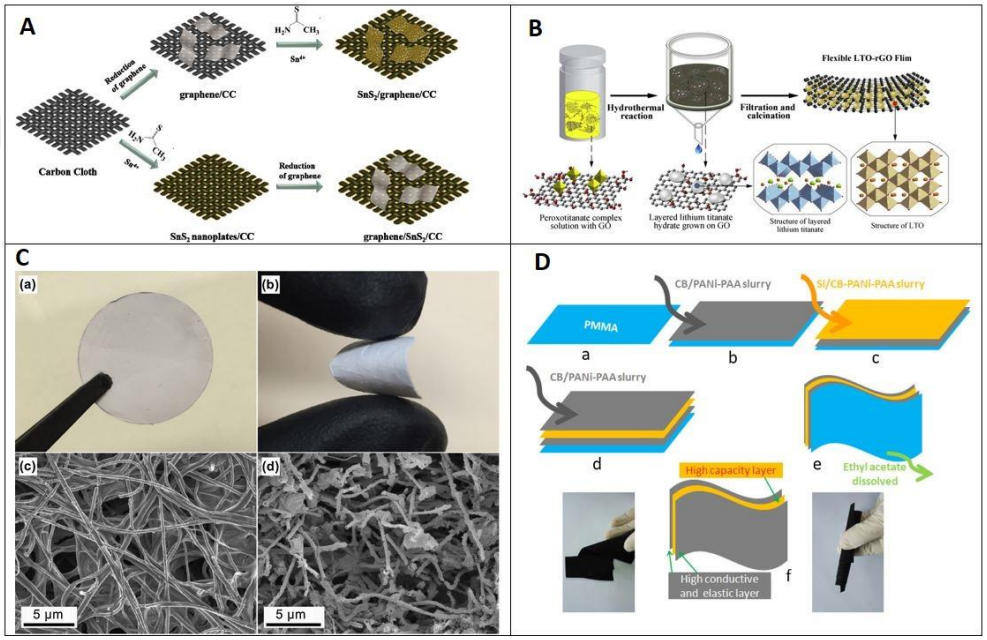


Figure 2.5. Flexible freestanding anodes. A. Schematic illustration of the fabrication of SnS2/graphene/CC and graphene/SnS2/CC electrodes (Wang, M., 2019); B. Schematic illustration of the fabrication process of free-standing LTO-rGO film (K. Zhu et al., 2018); C. Electrospun TiO2 and SiO2 nanofibers infused with TiO2 nanoparticles for lithium ion battery anode (X. Wang et al., 2016); D. Schematic of the fabrication process for CB/Si/CB electrode (C. Li et al., 2017).

2.1.2.2. Flexible Freestanding Cathodes

The fabrication of flexible binder-free composite cathode with SWCNTs (PDHBQS–SWCNTs) through the vacuum filtration method has been reported by Amin, K.(2018). The electrochemical evaluations showed the PDHBQS–SWCNTs

cathode to deliver up to 182 mAh g^{-1} discharge capacity at 50 mAg^{-1} current rate, as well as a potential difference of 1.5 V–3.5 V (Amin et al., 2018). The Li et al., (2019) study reported the synthesis of several multicarbonyl conjugated polymers via the coupling polymerization reaction; then, a vacuum-filtration technique was used to convert the polymers into carbonyl-conjugated polymer/carbon nanotube hybrid films.

The prepared hybrid films could be used as a binder-free, flexible, and free-standing organic cathode for the fabrication of LIBs that can offer good cycling stability, high reversible discharge capacity, and high capacity retention after several cycles. The theoretical calculation further proved that four Li^+ can be accommodated in the symmetrical conjugated structure during electrochemical reactions. The assembled full cell and the flexible battery were found capable of powering small devices, meaning that they can be used in wearable and bendable energy-storage devices (Qiang Li et al., 2019).

A free-standing and binder-free CuS/MWCNTs film cathode (F-CuS-CNT) has been employed in conjunction with Mg-Li dual-salt electrolyte and dendrite-free Mg anode for magnesium-lithium-ion batteries (MLIBs) fabrication by Zhang, Y. (2019).

The study reported that the F-CuS-CNT electrode at up to 70 % CuS content exhibited a high initial specific capacity of 479 mAh g^{-1} and acceptable cycling stability of 165 mAh g^{-1} after 100 cycles at 30 mA g^{-1} current density; this is considerably higher than that of the traditional CuS electrodes. The abundant pores and the flexible network architecture of the F-CuS-CNTs electrode contributed to its electrochemical performance as they provided more stable buffering layers for the CuS particles; they also facilitated higher diffusion of Li^+ during the charging/discharging cycle. Hence, it was suggested that a free-standing flexible film electrode could be fabricated to improve the electrochemical capabilities of MLIBs; they are also an ideal choice for the fabrication of flexible MLIBs (Y. Zhang et al., 2019). Another study published in 2017 by Bao, J. J.; presented the fabrication of

several flexible & free-standing cathodes using different $LiFePO_4$ mass ratios, super P (SP) (LFP/TPU/SP), and thermoplastic polyurethane (TPU) via a phase separation technique.

The study showed that the prepared cathode membranes had porous interwoven network structures and exhibited good rate capability and cycling stability. Tests on electrochemical impedance spectra (EIS), electrolyte uptake, and Li^+ diffusion coefficient (D_{Li^+}) showed accelerated electrolyte infiltration and Li^+ transformation due to the porous nature of the material. The rate capability of the prepared cathode at 4:5:1 (wt:wt) LFP/TPU/SP ratio was better than that of the traditional cathode as it exhibited a discharge capacity of 93 mAh g^{-1} at 10 C and 153 mAh g^{-1} at 0.2C. As an environmentally friendly and cost-efficient process, the phase separation process is a potential way of fabricating freestanding and flexible cathodes (Bao et al., 2017).

Bendable LIBs with paper-like free-standing V2O5-polypyrrole as cathodes were prepared by Lukman; a vacuum filtration process was employed to prepare the flexible cathodes. The length of the V_2O_5 NWs during the fabrication of the free-standing films was controlled using a modified hydrothermal method. The preparation of the V_2O_5- polypyrrole (PPy) composite was done via pyrrole monomer polymerization in the presence of V_2O_5NWs. The uniformity of the prepared product was ensured by dispersing the V_2O_5- polypyrrole (PPy) material in Triton X-100 surfactant via ultrasonication, followed by a filtration step under vacuum. Then, the resultant Polyvinylidene Fluoride (PVDF)-coated membrane was washed in ethanol and dried before peeling off the membrane.

A gel electrolyte containing Poly (vinylidenefluoride-co-hexafluorpropylene) P(VDF-HFP), N-Methylpyrrolidinone (NMP), & 30 nm Al_2O_3 powders was prepared for the full battery assembly. Then, the casting of the gel electrolyte slurry was done on the freestanding V_2O_5-PPy electrode surface before vacuum drying to evaporate the NMP. The NMP-free electrode was immersed in

LiPF6/EC-DMC while the gel electrolyte-based processing of the electrode into flexible bendable cells was done with a lithium foil counter-electrode (Noerochim et al., 2012).

The bendable cell was assembled using flexible and soft aluminum laminated pack materials. A schematic depiction of a flexible and bendable cell. The repeatedly bent cell exhibited similar battery performance to the conventional cell. However, the reversible capacity of the V_2O_5- PPy film was significantly higher than that of the pristine V_2O_5 film; it also achieved good cycling stability after several cycles. Qian et al. also presented the preparation of free-standing, flexible V_2O_5 - graphene composite films via the simple filtration of graphene sheets and V_2O_5 NWs.

The study preferentially oriented the V_2O_5 NWs along the film plane as they were placed in-between sheets of graphene in the film. To adjust the V_2O_5 content of the composites, the relative amount of the dispersions was simply varied. The conductivity of the composite films was improved by the thermal annealing process at 300°C. The composites were evaluated for electrochemical cycling at a voltage range of 2.1 -4.0 V at a rest period of 5 minutes before each charge/discharge step. The discharge capacities of the sandwich-type LIB cells at the binder-free state were 283 mAh g^{-1} and 252 mAh g^{-1} cathode at 50 mA g^{-1} current density during the 1^{st} and 50^{th} cycles, respectively. Furthermore, a composite film prepared with 42.8 wt% V_2O_5 exhibited a 189 mAh g^{-1} discharge capacity at 750 mA g^{-1} due to the higher graphene content; hence, it exhibited high electrical conductivity.

The study by Ding, et al. reported the preparation of flexible LiBs using 3D GLFP as the cathode material. The utilized GLFP was prepared via a solvent evaporation technique. The GLFP composites (90%) and PVdF (10 wt%) were mixed in a beaker that contained NMP before drying in a vacuum. The FEs were prepared by peeling off the dried material from the base of the beaker.

The thickness of the electrode was maintained at 200 μm. Before assembling the cell, the FEs were symmetrically bent to different bending angles (45°, 90° & 120°); this was repeated 100 times. The assembling of the test cells was done using

flexible GLFP as the cathode, Celgard 2300 film as a separator, and lithium metal as the anode. For the electrolyte, 1 M $LiPF_6$ was dissolved in EC+DMC at a 1:1 (v/v) ratio and used. Experiments on the charge/discharge cycles were conducted at 25°C within a voltage range of 2.4-4.2 V. The results showed that the graphene/$LiFePO_4$ nanostructures exhibited significant flexibility and high electrochemical properties. The capacity of the low-graphene-containing composites was higher even in the absence of any conductive agent (Ding et al., 2013).

2.2. Solid-state Electrolytes

Since the 1970s, solid polymer electrolytes (SPEs) have been regarded as a promising material for lithium batteries (Qingfeng Li et al., 2003). SPEs based on poly (ethylene oxide) (PEO) and mixed with various alkali metal salts have received the most attention.

The primary disadvantage of PEO-based SPEs is their low ion conductivity at room temperature. Studies on the conduction mechanism of these SPEs systems are therefore critical. Ionic conductivity of PEO-based solid polymer electrolytes was widely assumed to occur primarily in the amorphous phase above the glass-transition temperature Tg, driven by the local random Brownian motion of amorphous polymer chains [8]. In the meantime, the crystalline phase was thought to be the insulator.

3. MATERIAL AND METHOD

In this chapter, the materials used to produce electrodes and batteries will be described. The methods for assembling the electrodes and the battery will also be described, as will the methods for evaluating the electrochemical properties of electrodes and batteries, and the test tools and equipment used.

3.1. Material

Cotton yarns and carbon yarns were used as the core material for fiber/yarn electrodes. Cotton fabric and carbon cloth were used as the core material for 2D electrodes. Different metal oxides were used as active materials to obtain the positive and negative electrodes. Multi-Walled Carbon Nanotubes (MWCNTs) Carbon Black, Super P, and Graphite were used to increase the conductivity of the electrodes.

Both Table No. 3.1 and Figure No. 3.1 show the materials used to fabricate the electrodes and the cell battery.

Table 3.1. The materials used to produce the electrodes and the battery and where they were purchased.

No	Material	Description	The use	Purchased from
1	LiNiCoMnO2	Lithium Nickel Manganese Cobalt Oxide (LiNiCoMnO2) Powder, (Ni:Co:Mn=5:2:3)- NG08BE1406	Active materiel for Li- ion Battery Cathode	Nanografi Nano Technology
2	Li4Ti5O12	Lithium Titanate Oxide (Li4Ti5O12) Micron Powder (LTO)- NG08BE0306	Active materiel for Li-ion Battery Anode	Nanografi Nano Technology
3	PVDF Binder for Li-ion Battery	PVDF Binder (set: 80g) - NG08BE1101	Binder materiel for Li-ion Battery Electrodes	Nanografi Nano Technology
4	CNT	Multi Walled Carbon Nanotubes, Purity: > 96%, Outside Diameter: 8-18 nm - NG01MW0301	Conductive materiel for Li-ion Battery Electrodes	Nanografi Nano Technology
5	LiFePO4	Lithium Iron Phosphate (LiFePO4) Powder - NG08BE1404	Active materiel for Li-ion Battery Cathode	Nanografi Nano Technology
6	TiO2	Titanium Dioxide (TiO2) Micron Powder, Purity: 99.99 %, Size: 325 Mesh - NG01OM2503		Nanografi Nano Technology
7	CC	Carbon cloth - 600 gr/m2 12k–twill En: 100cm	Carrier material	Dost Kimya Endüstriyel Hammaddeler
8	Cotton yarn	Ne 15/1 Open end	Carrier material	Hateks
9	CMC	carboxymethyl cellulose sodium	Binder materiel	Chemical department
10	NMP	N-Methylpyrrolidone	Solvent materiel	Chemical department
11	Graphite	Graphite Powder <20 µm.	Conductive materiel for	Aldrich Chemistry

			Li-ion Battery Electrodes	
12	Carbon fiber paper	Thickness 0.02mm, density 0.78 g*cm^{-3}, resistivity 2.5 mΩ *cm^2	Carrier material	Teknotip analitik sistemler ltd. Sti.
13	Carbon Black, Super P	Conductive, 99+% (Metals Basis)	Conductive materiel	Alfa Aesar
14	Lithium perchlorate	Lithium perchlorate, anhydrous, 99%	For Electrolyte	Acros
15	Diethylene carbonate	Ethylene carbonate for synthesis.	For Electrolyte	Merck
16	Ethylene carbonate	1,3-Dioxolan-2-one, Ethylene carbonate	For Electrolyte	Merck



Figure 3.1. The materials used to fabricate the electrodes and the battery.

3.2. Method

Samples were prepared and tested in the laboratories of the Textile and Chemical Departments at Çukurova University, in addition to the battery systems research laboratory at Osmaniye Korkut Ata University.

All tests were conducted at standard atmospheric conditions, i.e., 20 ± 2^0C temperature and 65 ± 2 % relative humidity.

Several inks have been made that can be used to make conductive yarns and fabrics that store and release energy. Initially, yarns and fabrics were prepared to receive the inks. To ensure a good coating, various coating methods were used. The influence of different factors on the chemical properties of the resulting electrodes was investigated.

3.2.1. Conductive Cotton-Based Electrodes Production

The textile-based Li-ion battery has the same main components (electrodes, cathode and anode, current collectors, electrolyte and separator) as any traditional battery. As the components will be produced from coated fabrics and yarns, some components will be combined so that each electrode can function as both an electrode and a current collector. As a result, the electrodes must be highly conductive. The lower conductivity will have a negative impact on the battery's performance.

Flexible substrate supported electrodes have been fabricated by using cotton yarns, cotton fabrics, carbon cloth, and carbon fiber paper. Both carbon cloth and carbon fiber paper have good conductivity, but cotton yarn and fabrics are considered insulating materials, so they must be coated with an electrical conductive material to obtain the required conductivity in order to make the battery.

Many experiments have been conducted in order to achieve the highest conductivity of cotton yarns and fabrics. Various coating ink samples that contain carbon in different forms have been prepared as shown in Figure 3.2 and Table 3.2.

Table 3.2. The coating ink samples for conductive cotton yarns and fabrics

Sample No	Conductive additive and its percentage	The Binder and its percentage	Solvent
1	CNTs (90%)	PVDF (10%)	NMP
2	CNTs (90%)	CMC (10%)	Distilled water
3	Graphite (90%)	CMC (10%)	Distilled water
4	Graphite (95%)	CMC (5%)	Distilled water



Figure 3.2. Photos of the procedure for preparing ink samples; A: CNTs weighing process, B: PVDF weighing process, C: The consistency of the final ink

A cotton yarns were covered by passing the thread through a path containing the coating ink samples several times, as shown in the Figure 3.3.

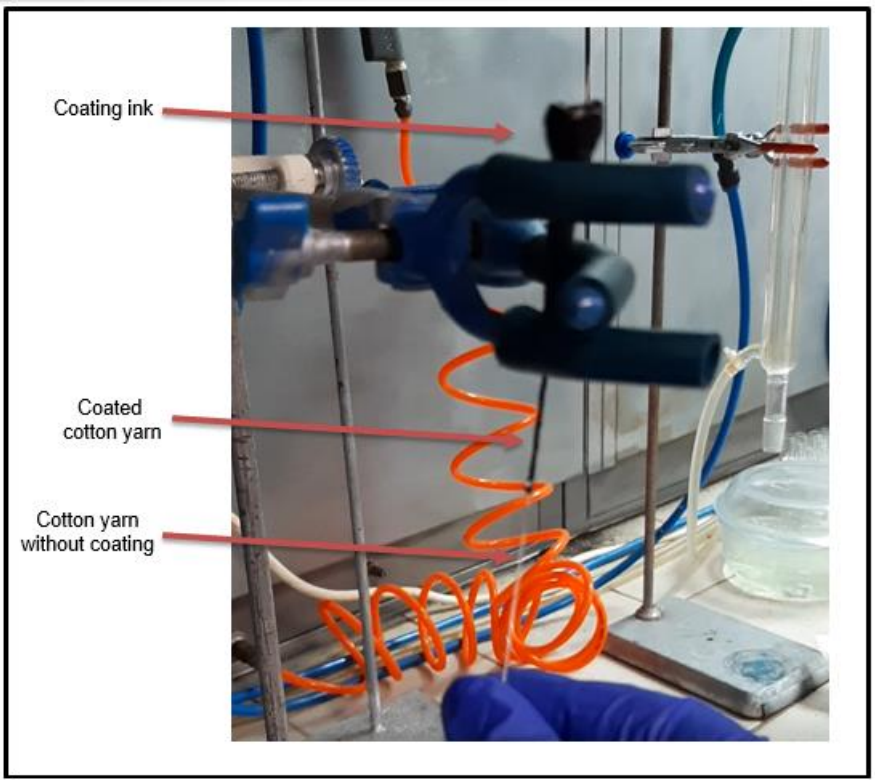
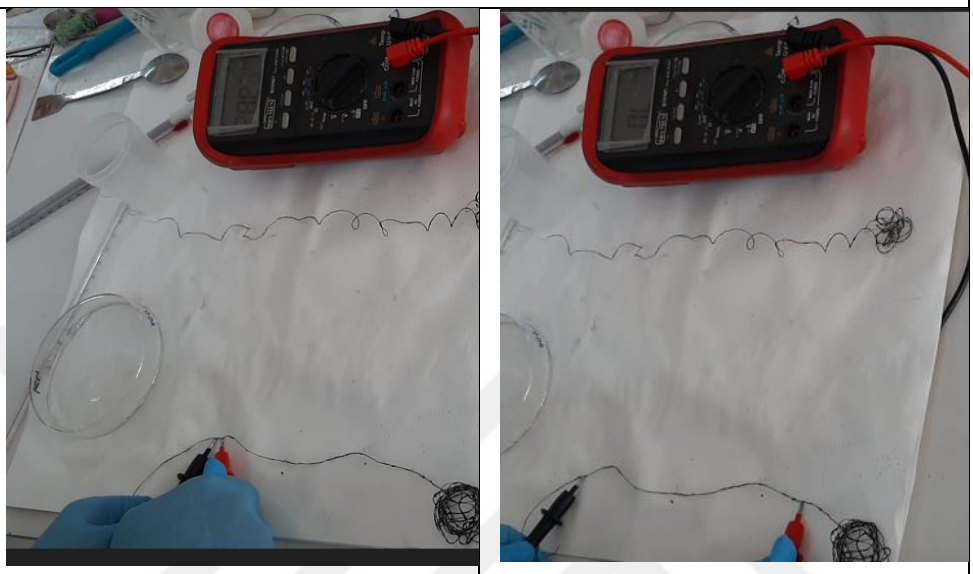


Figure 3.3. Cotton yarns coating process

Then, the threads were dried using an oven at 100°C for 2 hours for samples which have been used CMC as a binder and 12 hours for samples which have been used PVDF as a binder.

The conductivity of the resulting yarns was determined by using digital multimeter, where the resistance was measured, which is the reciprocal of the conductivity, as it is clear in Figure 3.4.

conductivity of the coated yarn with a mixture of PVDF and MWCNTs, with 10% of PVDF and 90% of MWCNTs.



Conductivity of the coated yarn with a mixture of CMC and MWCNTs, with 10% of CMC and 90% of MWCNTs.

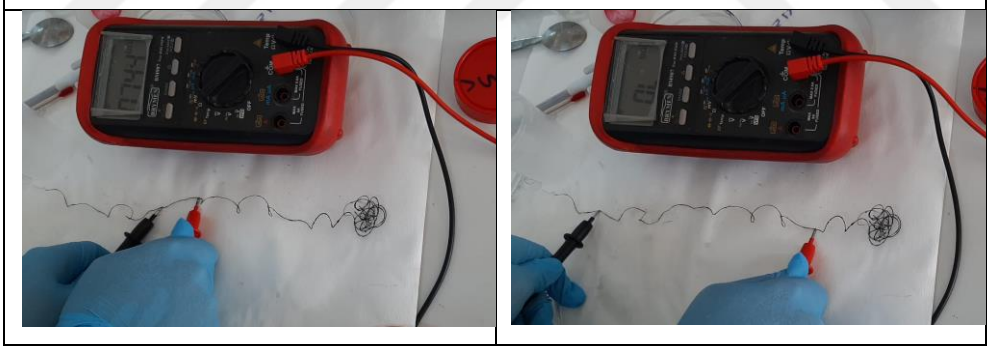


Figure 3.4. Yarn conductivity testing

Cotton fabrics also were coated with ink samples as in Figure 3.5, and the conductivity was measured in the same way.

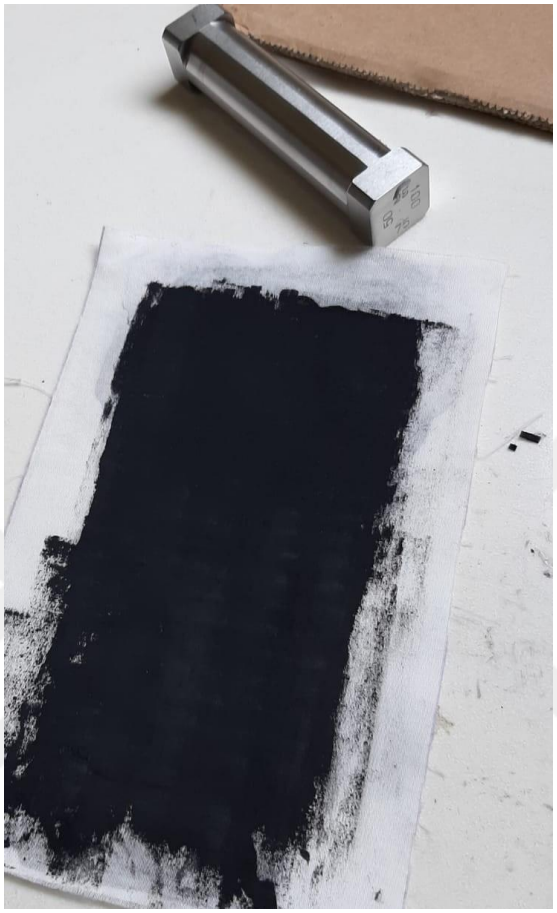


Figure 3.5. Cotton fabrics samples

3.2.2. Anode Production

Production of the anode involves several partial steps, including preparing the ink, preparing the yarn or fabric to receive the ink, the coating process, and testing the anode's properties.

3.2.2.1. Preparation of Anode Inks

Different coating inks for textile-based LIBs anodes were prepared according to the ratios in Table 3.3.

Also inks has been prepared in two different ways:

In first way, a specified amount of the active material was mixed with a specified amount of the conductive material, and they were mixed well using a mortar and pestle. A quantity of a solution containing binder and solvent was prepared at a ratio of 100 mg per 10 mL. A quantity of the previous solution was added to the mixture containing the active material and the conductive material by using a pipet so that the following ratio was achieved: 80:10:10 active material, conductive material, and binder. An illustration was made for the method of preparing the ink as shown in Figure 3.6. The resulting mixture (ink) was mixed using ultrasound for 20 minutes. The inks were shaken by hand several times during the sonication period for better mixing.

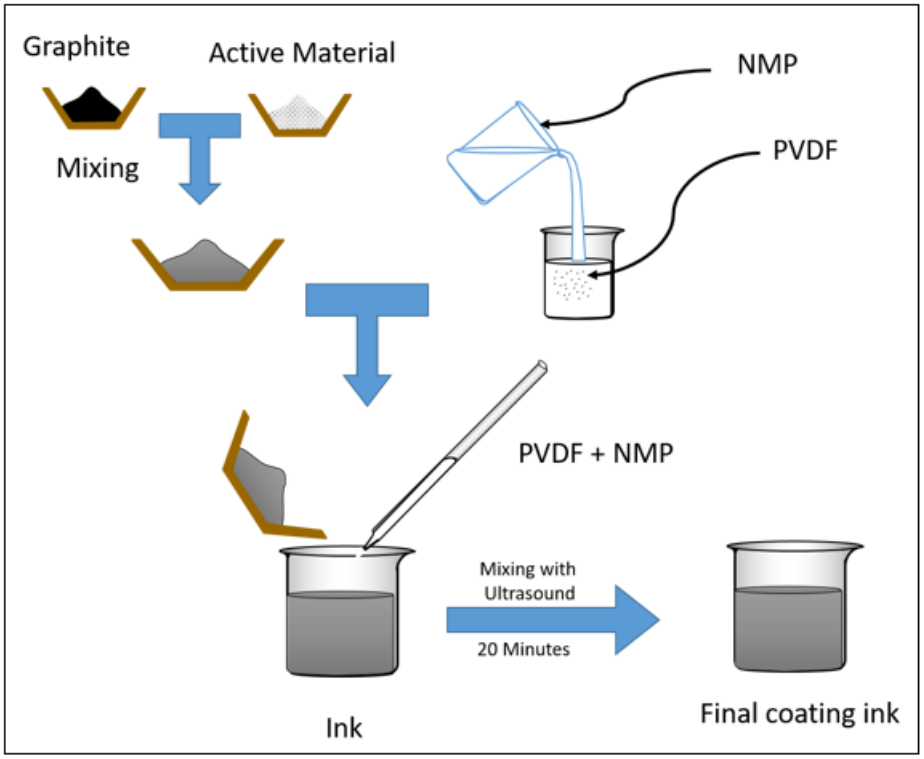


Figure 3.6. The first way for preparing inks samples for textile-based LIBs electrodes.

In the second way, a specified amount of the graphite was mixed with a specified amount of binder (CMC) for 12 hours by using a mechanical mixer (Figure 3.7). The ratio is 95% graphite and 5% CMC. After that a distilled water was added to the mixture. The resulting mixture (ink) was mixed using magnetic mixer for 30 minutes as shown in Figure 3.8.

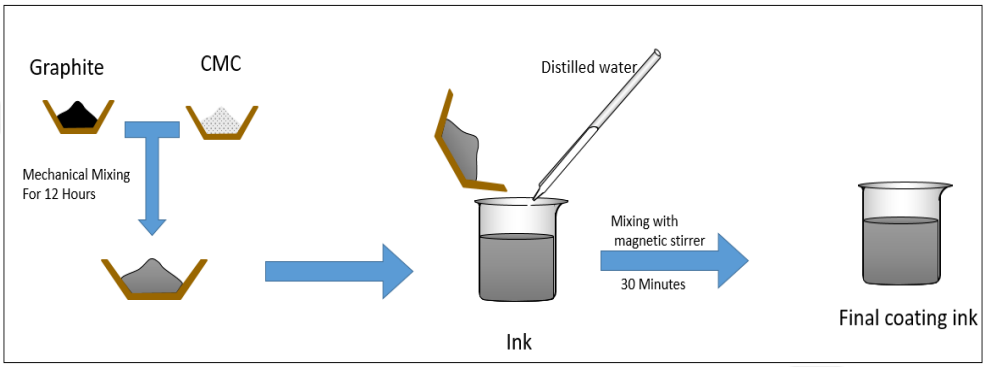


Figure 3.7. The second way for preparing anode inks samples

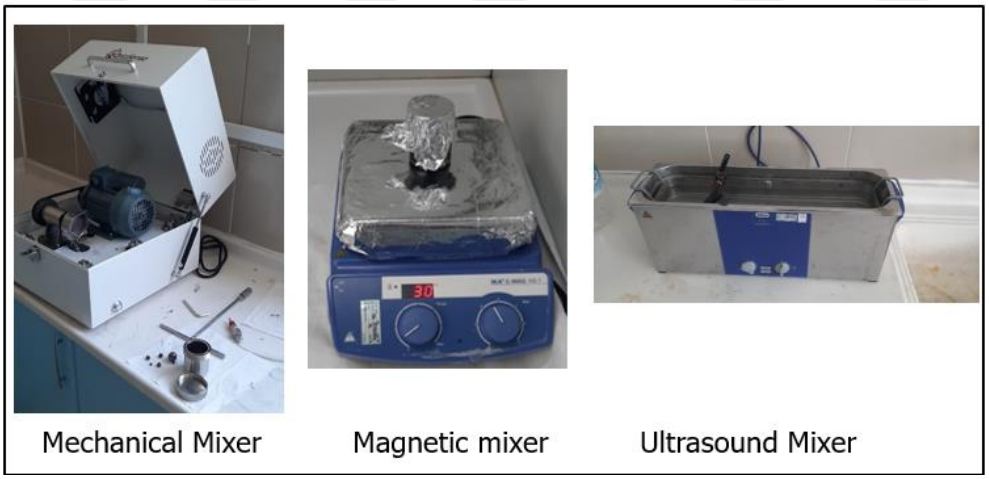


Figure 3.8. The used Mixers for preparing the coating inks

Table 3.3. The coating inks samples for textile-based LIBs anodes

Sample No	Active marital and its percentage	conductive additive and its percentage	The Binder and its percentage	Solvent
1	-	Graphite (95%)	CMC (5%)	Distilled water
2	-	CNTs (90%)	PVDF (10%)	NMP
3	-	Graphite (90%)	CMC (10%)	Distilled water
4	-	CNTs (95%)	PVDF (5%)	NMP
5	Li4Ti5O12 (20%)	CNTs (70%)	PVDF (10%)	NMP
6	Li4Ti5O12 (20%)	Graphite (70%)	CMC (10%)	Distilled water

3.2.2.2. Coating Process for Anode Samples

1D and 2D flexible substrate supported anodes have been fabricated by using cotton yarns, cotton fabrics, carbon cloth, and carbon fiber paper.

Flexible substrate supported anodes (yarn-shaped):

By using different inks, cotton and carbon yarns were covered by passing the thread through a path containing the ink several times, as shown in Figure 3.9. After that, the yarns were dried by placing it in an oven at a temperature of 100 ℃ for 6 hours.

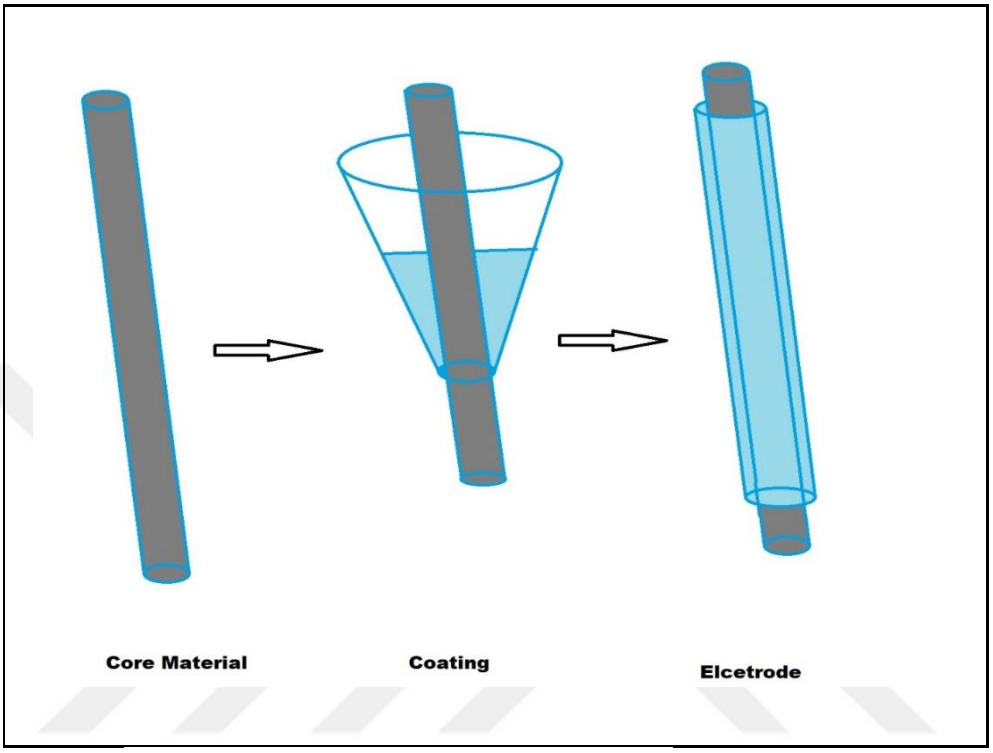


Figure 3.9. Coating Process for Yarn-Shaped LIBs anodes

As it is clear is Figures 3.10 flexible substrate supported anodes (yarn-shaped) was made by coating with different ink samples. The yarn was covered by passing through a path containing the solution several times.



Figure 3.10. Coating process for yarn-shaped anodes

2D flexible substrate supported anodes:

Fabric samples were made from various fabrics (cotton, carbon cloth, and carbon fiber paper), and coated in the Doctor Blade way (Reynolds et al., 2021) as

in Figure 3.11, Figure 3.12 and Table 3.4 shows the 2D flexible substrate-based anodes that were made and the inks that were used.

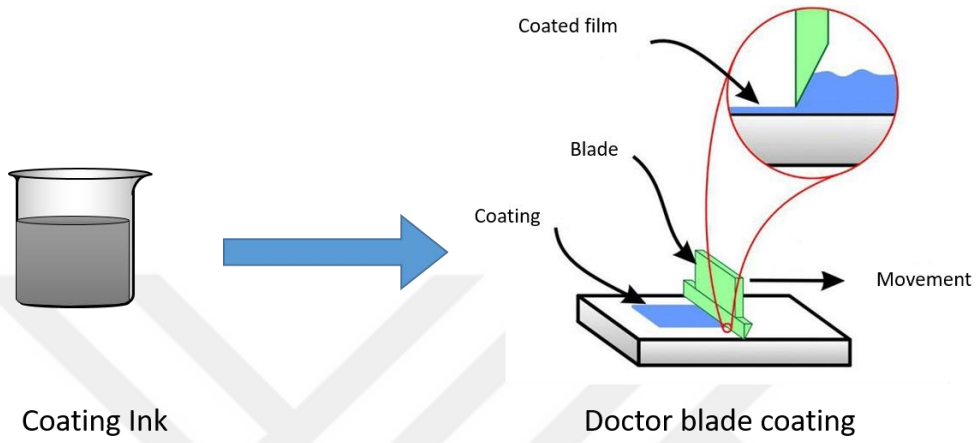


Figure 3.11. Coating Process 2D LIBs anodes

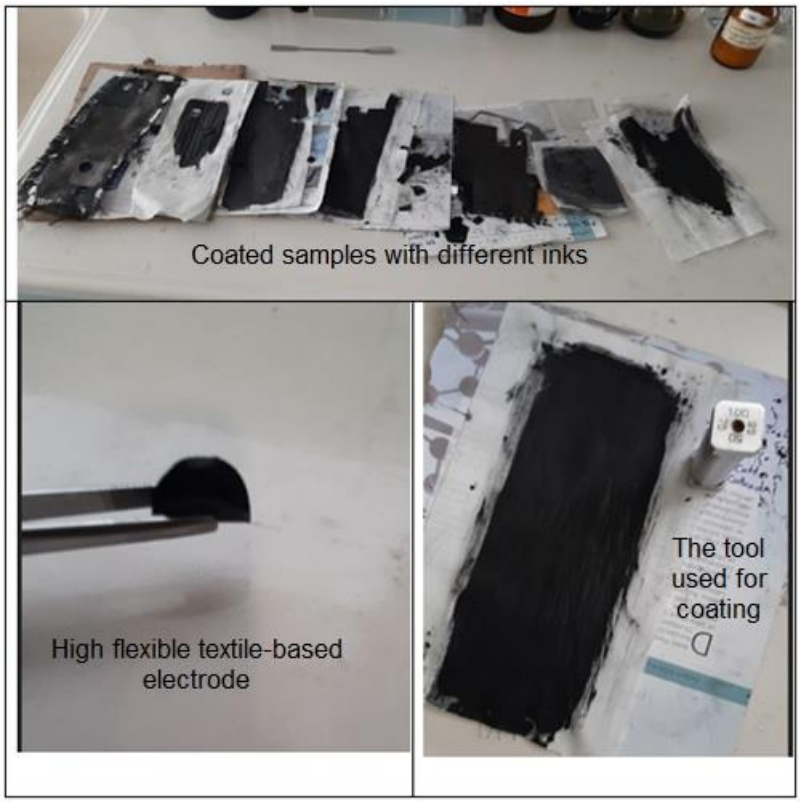


Figure 3.12. 2D coated samples

Table 3.4. The 2D flexible substrate-based anodes that were made and the inks that were used.

Sample No	Active marital and its percentage	conductive additive and its percentage	The Binder and its percentage	Solvent	Carrier material
1	-	Graphite (95%)	CMC (5%)	Distilled water	CC
2	-	CNTs (90%)	PVDF (10%)	NMP	CC
3	-	Graphite (90%)	CMC (10%)	Distilled water	CC
4	-	CNTs (95%)	PVDF (5%)	NMP	CC
5	Li4Ti5O12 (20%)	CNTs (70%)	PVDF (10%)	NMP	CC
6	Li4Ti5O12 (20%)	Graphite (70%)	CMC (10%)	Distilled water	CC
7	-	Graphite (95%)	CMC (5%)	Distilled water	Cotton fabric
8	-	CNTs (90%)	PVDF (10%)	NMP	Cotton fabric
9	-	Graphite (90%)	CMC (10%)	Distilled water	Cotton fabric
10	-	CNTs (95%)	PVDF (5%)	NMP	Cotton fabric
11	Li4Ti5O12 (20%)	CNTs (70%)	PVDF (10%)	NMP	Cotton fabric
12	Li4Ti5O12 (20%)	Graphite (70%)	CMC (10%)	Distilled water	Cotton fabric
13	-	Graphite (95%)	CMC (5%)	Distilled water	CF
14	-	CNTs (90%)	PVDF (10%)	NMP	CF
15	-	Graphite (90%)	CMC (10%)	Distilled water	CF
16	-	CNTs (95%)	PVDF (5%)	NMP	CF
17	Li4Ti5O12 (20%)	CNTs (70%)	PVDF (10%)	NMP	CF
18	Li4Ti5O12 (20%)	Graphite (70%)	CMC (10%)	Distilled water	CF

3.2.2.3. Electrochemical Characterization of Anode Samples

The electrochemical characterization has been tested by using Gamry Interface 1000 device. Where the 3-electrode method was used to obtain cyclic voltammetry CV curves and electrochemical impedance spectroscopy EIS curves.

Three electrode method

In three electrode mode, the Reference lead is separated from the Counter and connected to a third electrode. This electrode is most often positioned so that it is measuring a point very close to the working electrode (which has both Working and Working Sense leads attached: see Figure 3.13).

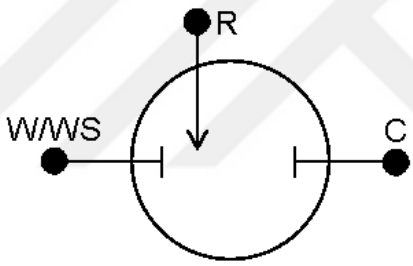


Figure 3.13. 3-electrode cell setup

This isolation allows for a specific reaction to be studied with confidence and accuracy. For this reason, 3-electrode mode is the most common setup used in electrochemical experimentation (Experiments, n.d.).

Cyclic Voltammetry CV

Cyclic voltammetry (CV) is an electrochemical testing method used to investigate the thermodynamics and kinetics of electron transfer in an electrochemical cell. The CV curve is typically a function of potential versus current response. The working electrode potential is ramped linearly versus time during a

CV measurement, and the associated current is collected. When a redox reaction occurs, an obvious peak in the forward or reverse scans can be found due to variations in the current value.

Electrochemical Impedance Spectroscopy EIS

Electrochemical impedance spectroscopy (EIS) is a technique used to study electrochemical processes as they change with frequency, such as electron transfer, mass transport, and chemical reactions. Potentiostatic (PEIS) or galvanostatic (GEIS) EIS measurements were possible. Impedance tests in PEIS mode are carried out by applying a sine wave around a potential E. Its value could be set to a constant or to a value associated with the working electrode's equilibrium potential over a range of frequencies. An impedance spectrum typically contains a high frequency semicircle corresponding to kinetic processes and a low frequency tail corresponding to diffusion processes.

Calculation of specific capacitance (Cp) from CV data

The equation for specific capacitance:

$$C_{\mathrm{p}} = \frac{Q}{\mathrm{mV}} \tag{3.1}$$

Where Q is the charge stored in coulombs, m is the mass of active material in grams. V is the potential and **C**p is the specific capacitance.

As it's known

$$Q = I * t \tag{3.2}$$

By putting equation (3.2) in equation (1) we get,

$$C_{\mathrm{p}} = \frac{(I * t)}{\mathrm{mV}}$$

Dividing nominator and denominator by t,

$$C_{\mathrm{p}} = \frac{(I * t)/t}{\mathrm{mV/t}}$$

or

$$C_{\mathrm{p}} = \frac{I}{\mathrm{m}(\frac{v}{t})}$$

In above equation, $\frac{v}{t}$ is the scan rate of cyclic voltammetry and it can be represent it by k.

$$C_{\mathrm{p}} = \frac{I}{\mathrm{m.k}}$$

$$I = Cp.m.k \qquad (3.3)$$

Now consider a CV curve Figure 3.14.

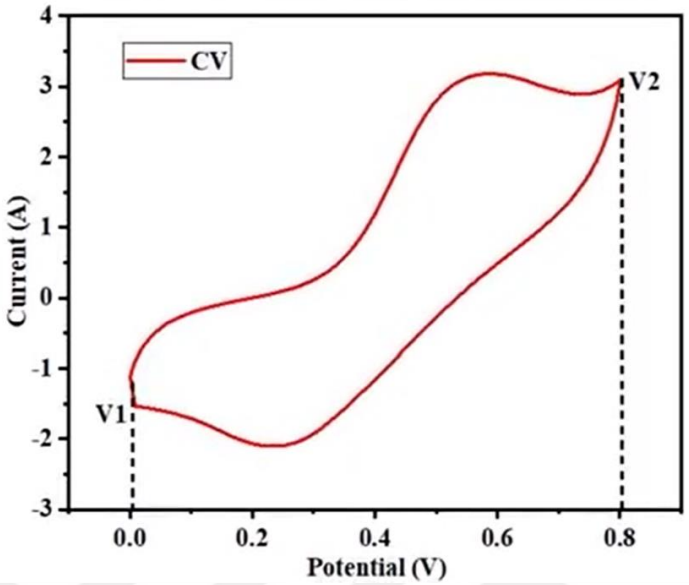


Figure 3.14. CV typical curve

In CV curve, the current changes by changing the potential from V1 to V2.Therefore, equation (3.3) can be written in its integral form as,

$$\int_{V1}^{V2} I(v)dv = \int_{V1}^{V2} (Cp * m * k)dv \quad (3.4)$$

If we look carefully to above equation, the integral on left hand side ($\int_{V1}^{V2} I(v)dv = Area$) represent the area of the CV curve. (I(v) *dv) = Y *X= Area). Therefore, equation (4) can be written as,

$$Area = \int_{V1}^{V2} (Cp * m * k)dv \quad (3.5)$$

For a specific material, the value of $Cp, m, and\ k$ is constant. Therefore, the integral in equation (5) can be solved as,

$$Area = (v2 - v1)Cp * m * k \quad (3.6)$$

In CV curve, there are three areas (see Figure 3.15),

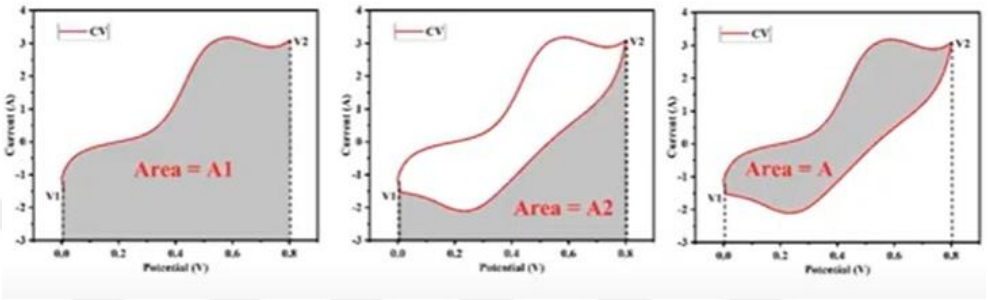


Figure 3.15. The different areas in CV curve.

When cell is charging, then Area= A1 and equation (3.6) can be written as,

$$A1 = (v2 - v1)Cp * m * k \quad (3.7)$$

Similarly, when cell is discharging, then Area= A2 and equation (3.6) can be written as,

$$A2 = (v1 - v2)Cp * m * k \quad (3.8)$$

For the calculation of area (A) inside the CV curve, we have to subtract equation 4.8 from equation 4.7,

$$A = A1 - A2 = [(v2 - v1)Cp * m * k] - [(v1 - v2)Cp * m * k]$$
$$A = 2[(v2 - v1)Cp * m * k]$$

Where **C**p is the specific capacitance, m is mass of active material, k is the scan rate of CV in volts per second and (v2-v1) is the potential window of CV (total voltage range).

By Using Gamry Echem Analyst software (A) Area can be calculated in the CV Curve. The unit of A is C (Coulomb) 1 C = 1 A.s (Ampere-second).

$$Cp = \frac{A}{3.6\ m} \tag{3.9}$$

Where **C**p the specific capacitance in mAh g^{-1}, m is mass of active material in grams, A area in Coulomb.

Preparing the electrolytes:

Using 20 grams of Ethylene carbonate and it was dissolved using 20 grams of Diethylene carbonate and stirred for 10 minutes by a magnetic stirrer, then adding 2 grams of Lithium perchlorate and stirring it by a magnetic stirrer, see Figure 3.16 (L. Zhao et al., 2021).



Figure 3.16. Materials used to prepare the electrolyte

In our tests using the three-electrode technique, platinum plate with a surface area of 2 cm² is used as counter electrode, silver wire as a reference electrode and fabric coated samples as a working electrode as in Figure 3.17.



Figure 3.17. Measurement of electrochemical properties of electrodes using 3-electrode method

3.2.2.4. Scanning Electron Microscopy (SEM)

A scanning electronic microscope (SEM) (FEI Quanta FEG 650) was used to examine the surface morphology of the produced samples. .



Figure 3.18. FEI Quanta model FEG 650 SEM analyzer.

3.2.3. Cathode Production

Production of the cathode involves several partial steps, including preparing the ink, preparing the yarn or fabric to receive the ink, the coating process, and testing the cathode's properties.

3.2.3.1. Preparation of Cathode Inks

In the same way of anode ink preparing, different coating inks for textile-based LIBs cathodes were prepared according to the ratios in Table 3.5.

Also inks has been prepared in two different ways:

In first way, a specified amount of the active material was mixed with a specified amount of the conductive material, and they were mixed well using a mortar and pestle. A quantity of a solution containing binder and solvent was prepared at a ratio of 100 mg per 10 ml. A quantity of the previous solution was added to the mixture containing the active material and the conductive material by using a pipet so that the following ratio was achieved: 80:10:10 active material, conductive material, and binder as in Figure 3.2, and Table 3.3. The resulting mixture

(ink) was mixed using ultrasound for 20 minutes. The inks were shaken by hand several times during the sonication period for better mixing

In the second way, also different coating inks for textile-based LIBs cathodes were prepared according to the ratios in Table 3.4. First, a specified amount of the active material (LiFePO4), a specified amount of the conductive material (Carbon Black, Super P), and a specified amount of binder (PVFD) were mixed well for 12 hours by using a mechanical mixer. After that, an NMP was added to the mixture. The resulting mixture (ink) was mixed using a magnetic mixer for 30 minutes (see Figure 3.19).

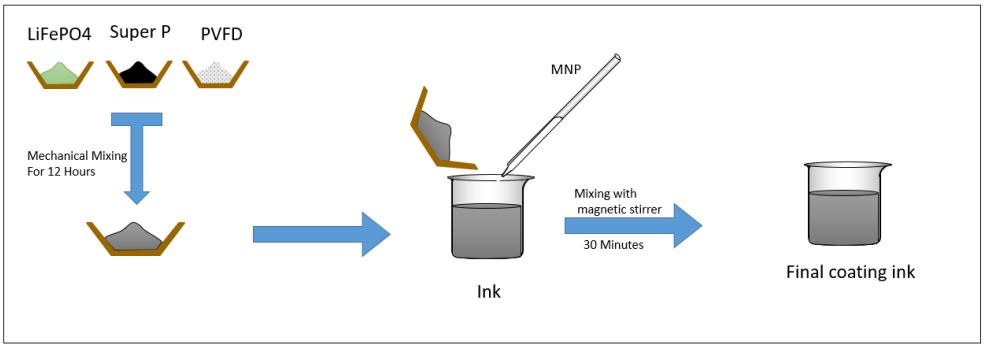


Figure 3.19. The second way for preparing cathode inks samples

Table 3.5. The coating inks samples for textile-based LIBs cathodes

Sample No	Active marital and its percentage	conductive additive and its percentage	The Binder and its percentage	Solvent
1	LiFePO4 (75%)	Carbon Black, Super P (20%)	PVDF (5%)	NMP
2	LiFePO4 (80%)	Carbon Black, Super P 15%)	PVDF (5%)	NMP
3	LiFePO4 (85%)	Carbon Black, Super P (10%)	PVDF (5%)	NMP

3.2.3.2. Coating Process for Cathode Samples

1D and 2D flexible substrate supported cathodes have been fabricated by using cotton yarns, cotton fabrics, carbon cloth, and carbon fiber paper.

Flexible substrate supported cathodes (yarn-shaped):

By using different inks, cotton and carbon yarns were covered by passing the thread through a path containing the ink several times, as shown in Figure 3.6. After that, the yarns were dried by placing it in an oven at a temperature of 100 ℃ for 6 hours.

2D flexible substrate supported cathodes:

Fabric samples were made from various fabrics (cotton, carbon cloth, and carbon fiber paper), and coated in the Doctor Blade way (Reynolds et al., 2021) as in Figure 3.9, Figure 3.10 and Table 3.6 shows the 2D flexible substrate-based cathodes that were made and the inks that were used.

Table 3.6. The 2D flexible substrate-based cathodes that were made and the inks that were used.

Sample No	Active marital and its percentage	conductive additive and its percentage	The Binder and its percentage	Solvent	Carrier material
1	LiFePO4 (75%)	Carbon Black, Super P (20%)	PVDF (5%)	NMP	CC
2	LiFePO4 (80%)	Carbon Black, Super P 15%)	PVDF (5%)	NMP	CC
3	LiFePO4 (85%)	Carbon Black, Super P (10%)	PVDF (5%)	NMP	CC
4	LiFePO4 (75%)	Carbon Black, Super P (20%)	PVDF (5%)	NMP	CF
5	LiFePO4 (80%)	Carbon Black, Super P 15%)	PVDF (5%)	NMP	CF
6	LiFePO4 (85%)	Carbon Black, Super P (10%)	PVDF (5%)	NMP	CF
7	LiFePO4 (75%)	Carbon Black, Super P (20%)	PVDF (5%)	NMP	Cotton Fabric

8	LiFePO4 (80%)	Carbon Black, Super P 15%)	PVDF (5%)	NMP	Cotton Fabric
9	LiFePO4 (85%)	Carbon Black, Super P (10%)	PVDF (5%)	NMP	Cotton Fabric
10	LiFePO4 (75%)	Carbon Black, Super P (20%)	PVDF (5%)	NMP	Cotton Fabric
	-	Graphite (95%)	CMC (5%)	Distilled water	
11	LiFePO4 (80%)	Carbon Black, Super P 15%)	PVDF (5%)	NMP	Cotton Fabric
	-	Graphite (95%)	CMC (5%)	Distilled water	
12	LiFePO4 (85%)	Carbon Black, Super P (10%)	PVDF (5%)	NMP	Cotton Fabric
	-	Graphite (95%)	CMC (5%)	Distilled water	

3.2.3.3. Electrochemical Characterization of Cathode Samples

The electrochemical characterization also has been tested in the same way by using Gamry Interface 1000 device. Where the 3-electrode method was used to obtain cyclic voltammetry CV curves and electrochemical impedance spectroscopy EIS curves.

3.2.3.4. Scanning Electron Microscopy (SEM)

A scanning electronic microscope (SEM) (FEI Quanta FEG 650) was used to examine the surface morphology of the produced samples.

3.2.4. Battery Production

The anode and cathode of the Li-ion coin cell were chosen from samples that had already been made based on the results of electrochemical tests.

Circle samples of electrodes with a diameter of 16 mm were cut by a sample cutting machine (see Figure 3.20).

Table 3.7. Shows electrodes samples that used to produce Li-ion coin cell.

Table 3.7. The electrodes samples that used to produce Li-ion coin cell.

Electrode	ctive marital and its percentage	conductive additive and its percentage	The Binder and its percentage	Solvent	Carrier material
Cathode	LiFePO4 (85%)	Super P (10%)	PVDF (5%)	NMP	CF
Anode	-	Graphite (95%)	CMC (5%)	Distilled water	CF

The Li-ion coin cells were assembled in an argon glove box (see Figure 3.21) with the following structure: anode-separator-electrolyte-anode. These components were protected by a metal jacket (see Figure 3.22). Then, using the crimping machine (see Figure 3.23), the coin cell was sealed



Figure 3.20. Circle sample cutting machine.

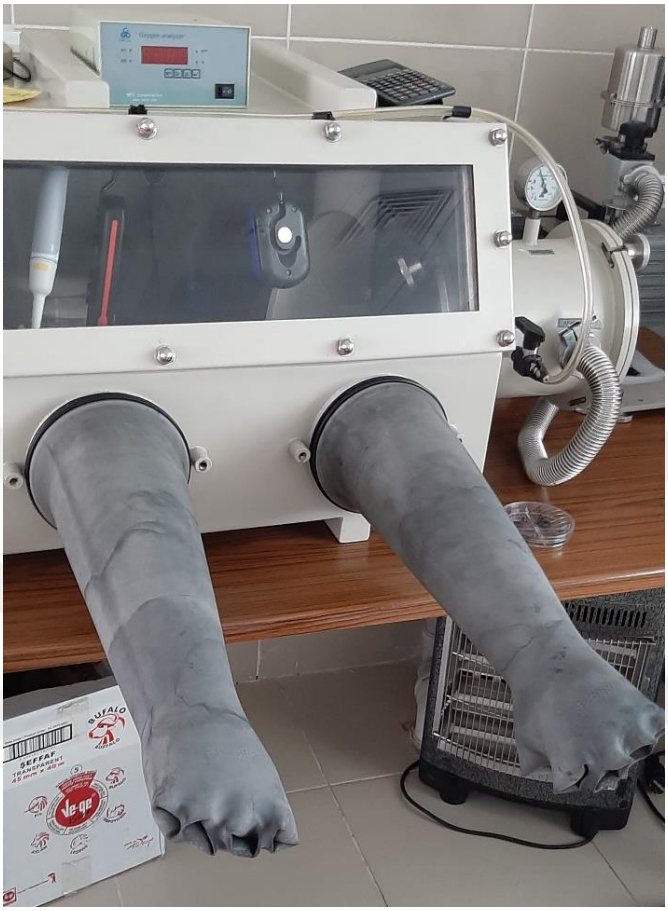


Figure 3.21. Glove box



Figure 3.22. Picture of battery components before assembly. **b.** Diagram showing the order of assembly.



Figure 3.23. Coin cell crimping machine.

3.2.4.1. Lithium-Ion Battery Electrochemical Characterization

The electrochemical characterization has been tested by using the coin cell battery test system OPT-BST8-WA (see Figure 3.24). The charge and discharge capacities of manufactured coin cells have been investigated.



Figure 3.244. Coin cell battery test system OPT-BST8-WA.

.

4. RESULTS AND DISCUSSION

Various test results with analysis have been presented in this chapter. The electrochemical characterization has been tested and discussed by using Gamry Interface 1000 device. Where the 3-electrode method was used to obtain cyclic voltammetry CV and electrochemical impedance spectroscopy EIS curves for different electrode samples. Specific capacity (Cp) was calculated based on CV data.

The charge and discharge capacities of produced lithium ion batteries have been tested and investigated by using the coin cell battery test system.

4.1. Conductivity

Flexible substrate supported electrodes have been fabricated by using cotton yarns, cotton fabrics, carbon cloth, and carbon fiber paper. Both carbon cloth and carbon fiber paper have good conductivity, but cotton yarn and fabrics are considered insulating materials, so they must be coated with an electrical conductive material to obtain the required conductivity in order to make the battery.

The resistance of the produced samples was measured using a digital multimeter, and the conductivity was calculated. Where the conductivity is the reciprocal of the resistance. The results were as follows:

1-The conductivity of the yarn that is coated by using PVDF as a binder is higher than the conductivity of the yarn that is coated by using CMC as a binder.

2-There are cuts in the continuity of the coating that lead to the absence of conductivity over large distances.

3-The continuity of coating resulting from the use of material CMC as a binder is better than the coating resulting from the use of PVDF.

To achieve good conductivity for cotton fabric cathode cotton fabric samples, the samples were coated on both sides. The first side was coated with cathode ink and the other side was coated with graphite to increase the conductivity.

The electrochemical performance of the samples was tested (see Figure 4.1 and Figure 4.2).

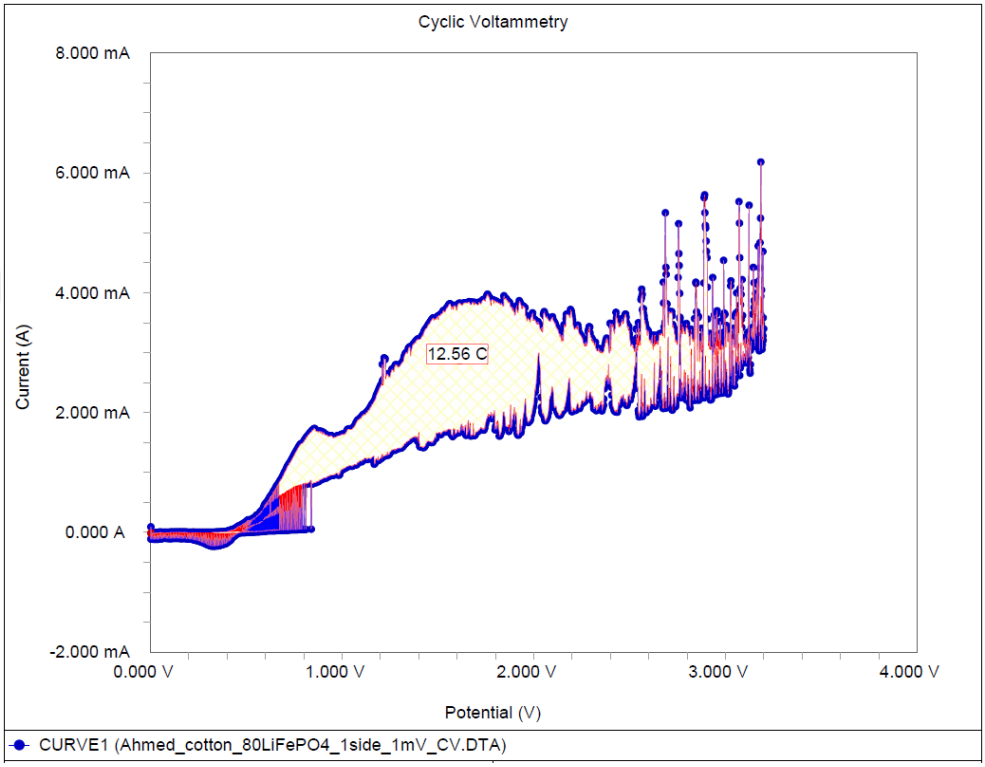


Figure 4.1. CV curve of a cotton fabric cathode sample coated on one side with cathode ink, scan rate of 0.1 mV·s-1.

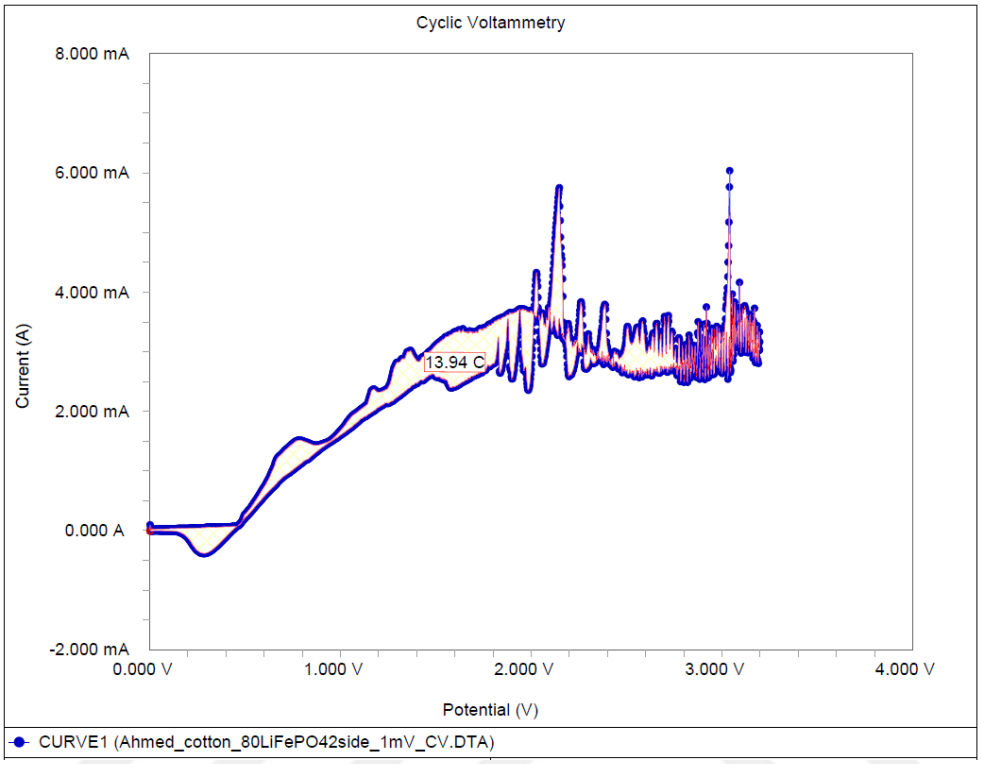


Figure 4.2. CV curve of a cotton fabric cathode sample coated on both sides (first side with cathode ink and the second side with graphite), scan rate of 0.1 mV·s-1.

By comparing the CV curves of samples coated on one side with those coated on two sides, it was found that the capacity of samples coated with two sides is higher than the capacity of samples coated with one side due to the increase in conductivity. As conductivity increases, electrons move more easily, making it easier to transfer ions between electrodes.

4.2. The Effect of the Ink Preparation Method

Ink samples were prepared in two different ways, first the ink samples were prepared as explained in paragraph 3.2.2.1 and the second ink samples were prepared as explained in paragraph 3.2.3.1.

However, in first way for preparing ink samples the coating process was not stable, as after a period of time, part of the ink began to fall off, and the conductivity of the samples decreased significantly, and thus the electrochemical performance of the electrodes.

The samples were prepared by the second way, and the coating process constant was observed due to the homogeneous distribution of the atoms of the binder within the mixture due to the excellent mechanical mixing process. Therefore, the second method was adopted in preparing the samples.

4.3. The Effect of the Concentration of the Active Material

Different samples were produced depending on different concentrations of the active material. The electrochemical performance of the samples was tested and, accordingly, the most appropriate concentration was selected.

The electrochemical characterization has been tested by using the Gamry Interface 1000 device. The 3-electrode method was used to obtain cyclic voltammetry CV curves and electrochemical impedance spectroscopy EIS curves (see appx 1). The capacity was also calculated as follows.

Three samples of carbon cloth were produced depending on three different concentrations of the active material LiFePO4 (75% -80% -85%) and the electrochemical performance of the samples was tested and the specific capacity was calculated by using CV curves (see Figure 4.3). The results show that the cathode carbon cloth sample, which has been coated with 85% active material (LiFePO4) concentration, has the highest specific capacity of 197.065 mAh g^{-1}.

However, it is not possible to go above this ratio in order to ensure the appropriate conductivity of the coating inks, which is secured by the conductive additive.

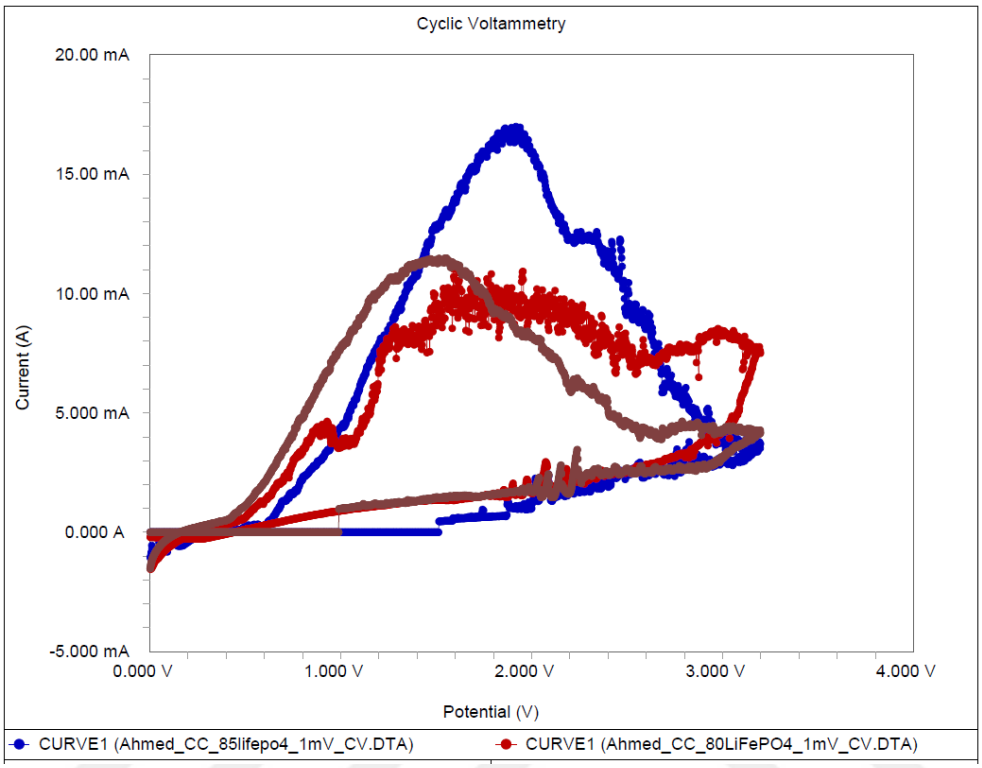


Figure 4.3. CV curves of the 3 different carbon cloth cathode samples, scan rate of 0.1 mV·s-1.

Two samples of carbon fiber were produced depending on three different concentrations of the active material LiFePO4 (75% -85%) and the electrochemical performance of the samples was tested and the specific capacity was calculated by using CV curves (see Figure 4.4). The results show that the cathode carbon fiber sample, which has been coated with 85% active material (LiFePO4) concentration, has the highest specific capacity of 225.785 mAh g^{-1}.

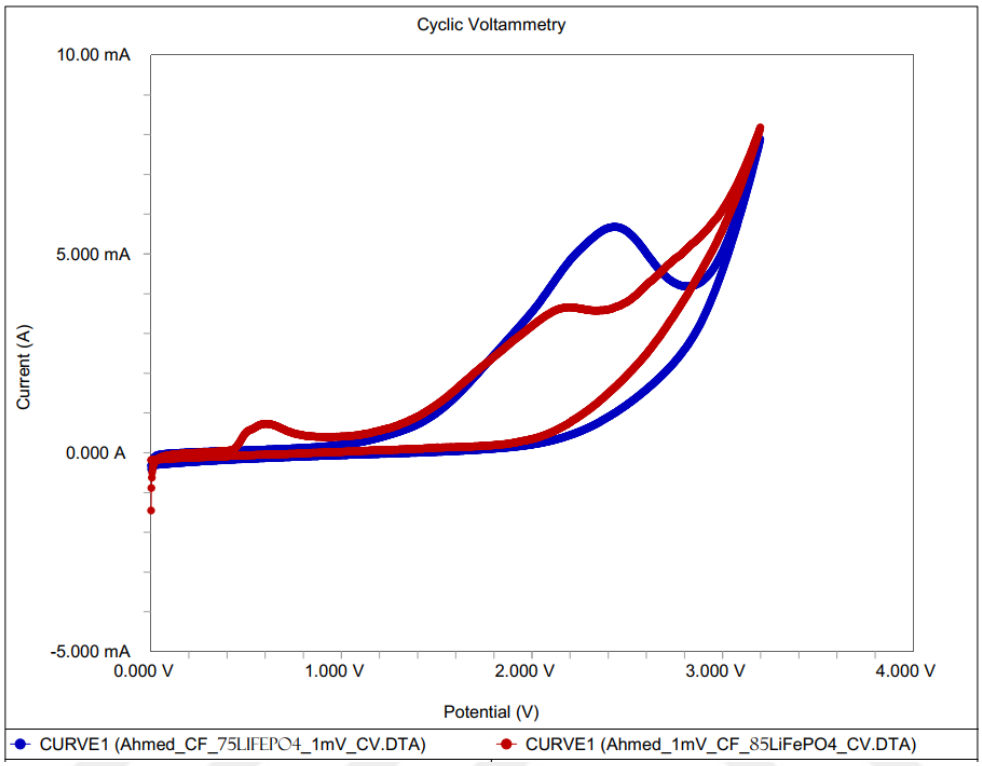


Figure 4.4. CV curves of the 2 different carbon fiber cathode samples, scan rate of 0.1 mV·s-1.

Three samples of cotton fabric were produced depending on three different concentrations of the active material LiFePO4 (75% -80% -85%) and the electrochemical performance of the samples was tested and the specific capacity was calculated by using CV curves (see Figure 4.5). The results show that the cathode carbon cloth sample, which has been coated with 85% active material (LiFePO4) concentration, has the highest specific capacity of 108.374 mAh g^{-1}.

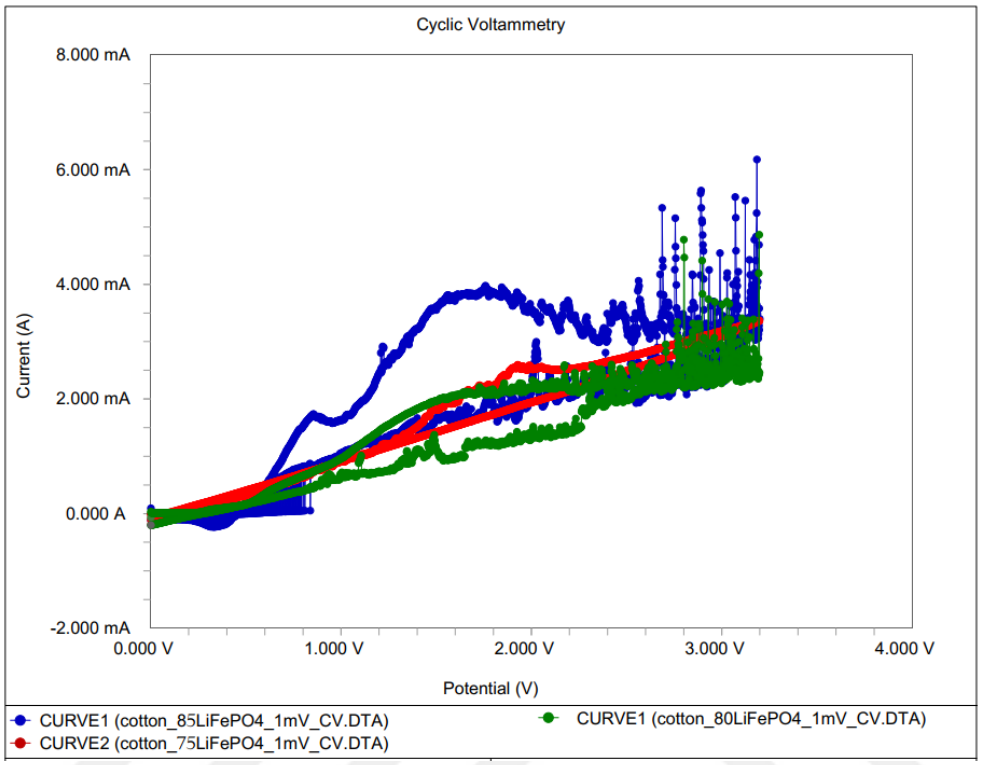


Figure 4.5. CV curves of the 3 different cotton fabric cathode samples, scan rate of 0.1 mV·s-1.

4.3. The Effect of the Carrier Material

Three samples of carbon cloth, carbon fiber and cotton fabric were produced using the same ink and the electrochemical performance of the samples was tested and the specific capacity was calculated by using CV curves (see Figure 4.6). The results show that the cathode carbon fiber sample has the highest specific capacity of 225.785 mAh g^{-1}.

This is due to the following reasons: First, the conductivity of carbon fiber samples is higher than that of cotton fabric and carbon cloth samples. Also, the surface shape of the carbon fiber sample is more homogeneous than that of the carbon and cotton samples.

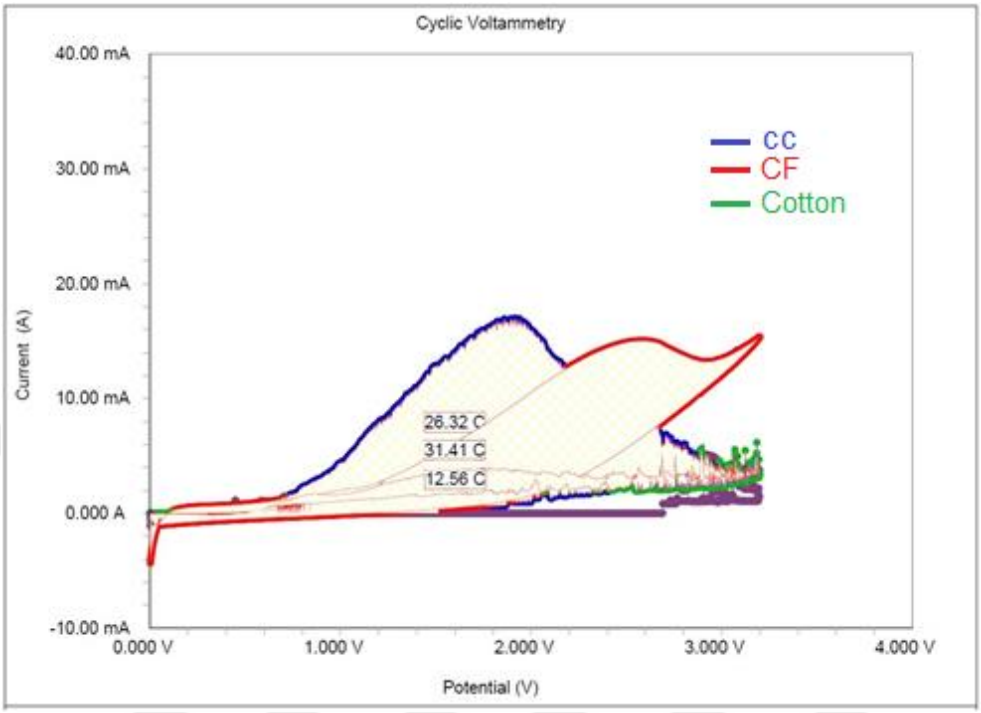


Figure 4.6. CV curves of the 3 different cathode samples of carbon cloth, carbon fiber, and cotton fabric, scan rate of 0.1 mV·s-1.

4.4. Scanning Electron Microscopy (SEM) Results

Figures 4.7 and 4.8 show SEM morphology of 4 different electrode samples.

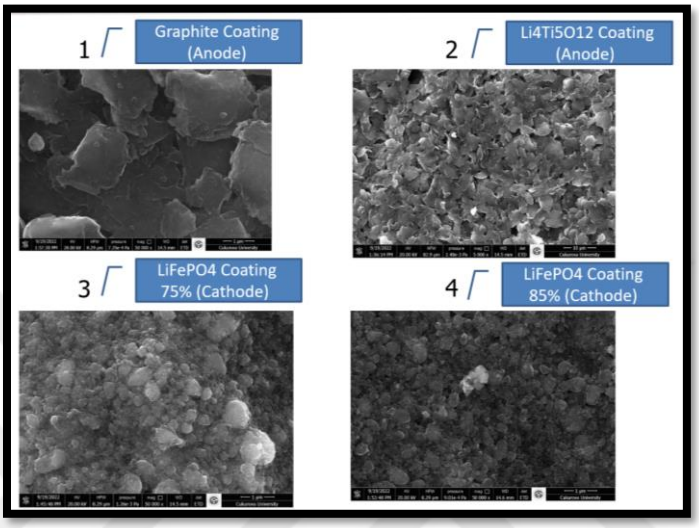


Figure 4.7. SEM morphology of 4 different samples (50000X)

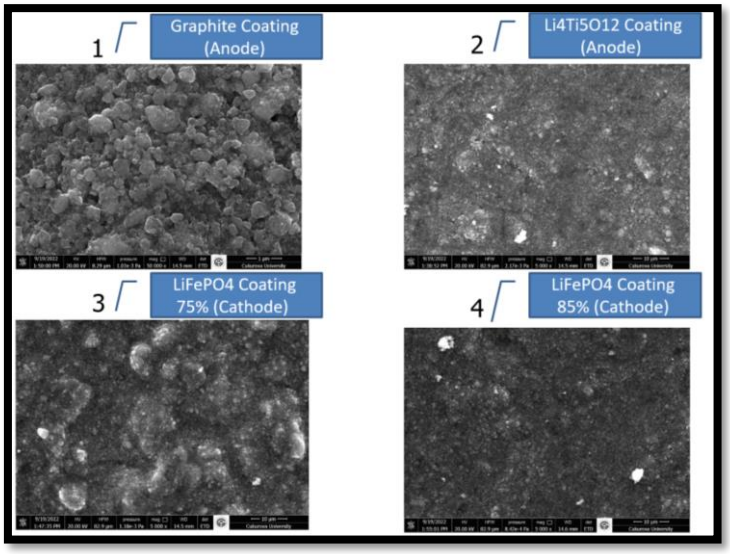


Figure 4.8. SEM morphology of 4 different samples (50000X)

The surface morphology of all samples was examined using a scanning electron microscope. It can be note that the covering process is uniform and the surface is homogeneous.

4.5. Electrochemical Properties of Produced Lithium-Ion Batteries

The produced LIB has been tested by using the coin cell battery test system OPT-BST8-WA. The charge and discharge curve has been drawn by using the coin cell battery test data. The capacitance of the produced battery was 268.43 mAh g^{-1}.

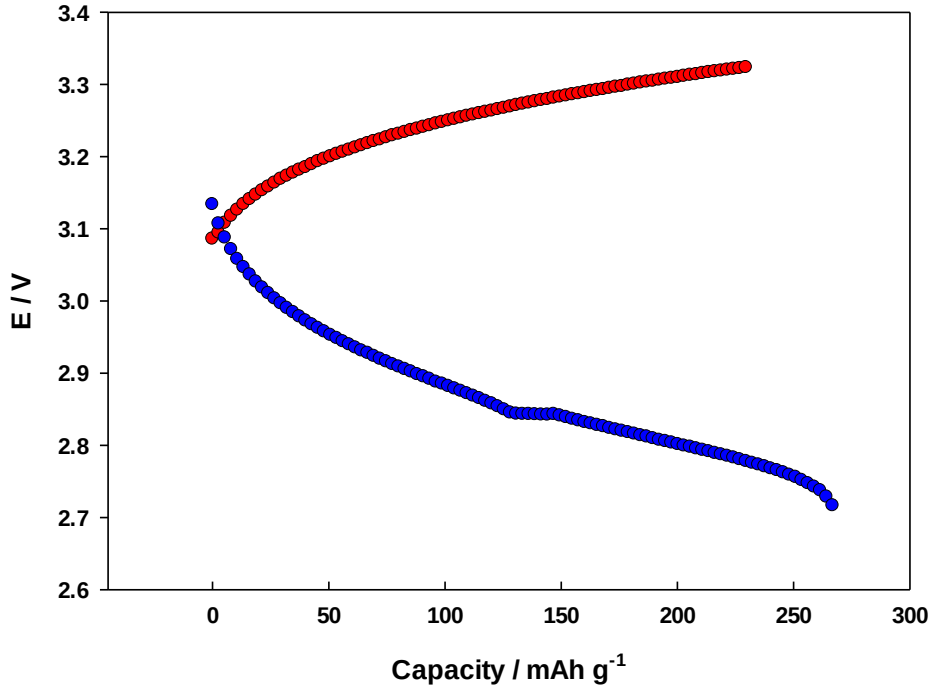


Figure 4.9. Charge-discharge curve for lithium-ion batteries

5. CONCLUSIONS and RECOMMEDATIONS

5.1. Conclusion

Electrodes for lithium batteries have been made by coating carbon cloth, carbon fiber paper, and cotton fabric with different kinds of ink. Several methods for preparing these inks have been tried in order to achieve the highest homogeneity among the ink's components.

Flexible substrate supported electrodes have been fabricated by using cotton yarns, cotton fabrics, carbon cloth, and carbon fiber paper as a carrier material. Both carbon cloth and carbon fiber paper have good conductivity, but cotton yarn and fabrics are considered insulating materials, so they must be coated with an electrical conductive material to obtain the required conductivity in order to make the battery.

To achieve good conductivity for cotton fabric cathode cotton fabric samples, it is better to coat the samples on both sides. The first side should be coated with cathode ink, and the other side should be coated with graphite to increase the conductivity.

Ink samples were prepared in two different ways. However, in first way for preparing inks samples the coating process was not stable, as after a period of time, part of the ink began to fall off, and the conductivity of the samples decreased significantly, and thus the electrochemical performance of the electrodes. But for samples that prepared by the second way, the coating process was constant due to the homogeneous distribution of the atoms of the binder within the mixture due to the excellent mechanical mixing process. Therefore, the second method was adopted in preparing the samples.

Fabric samples were coated with these inks by Doctor Blade method. The electrochemical characterization also has been tested by using Gamry Interface 1000 device. Where the 3-electrode method was used to obtain cyclic voltammetry CV curves and electrochemical impedance spectroscopy EIS curves. The Specific capacitance of produced electrodes has been calculated from CV data.

Different electrode samples were produced depending on different concentrations of the active material (many inks were manufactured with different concentrations of active materials, and then the samples were coated). The electrochemical performance of the samples was tested and, accordingly, the most appropriate concentration was selected.

Three samples of carbon cloth, carbon fiber and cotton fabric were produced using the same ink and the electrochemical performance of the samples was tested and the specific capacity was calculated by using CV curves. The results show that the cathode carbon fiber sample has the highest specific capacity of 225.785 mAh g^{-1}.

- A high flexible substrate supported anode has been made using carbon fiber/Graphite/CMC, which shows an excellent electrochemical performance (a specific capacity of 412 mAh g^{-1}).
- A high flexible substrate supported cathode has been made using carbon fiber/LiFePO4 /Carbon Black, Super P/PVDF, which shows an excellent Li ion storage performance (a specific capacity of 225.785 mAh g^{-1}).
- A textile-based LIB has been made and tested by using the coin cell battery test system OPT-BST8-WA. The capacitance of the produced battery was 268.43 mAh g^{-1}.

5.2. Recommendation

All of the topics discussed in this thesis can be expanded in every way, because each new discovery raises new scientific questions and technological advancements. The recommendations gathered here should be regarded as starting points for future development Textile-based lithium-ion battery.

The experimental work in this thesis was primarily focused on producing electrode materials for use in textile-based lithium-ion batteries. The methods presented here can also be used with other metal oxide nanostructured materials or composite materials.

The issue of solid-state or polymer electrolytes was not addressed in this thesis. In order to obtain the final form of the textile-based lithium battery, it should be studied and the best electrolyte should be chosen.

The textile-based LIBs can provide a suitable source of energy for smart textiles, flexible electronic devices, and sensors that can be integrated into clothes, glasses, watches, and even skin.

REFERENCES

Alahmed, A., & Sabır, E. C. (2021). Textile Based Electrodes for Flexible Lithium-Ion Batteries: New updates. *Current Nanoscience*, *17*(i), 1–9. https://doi.org/10.2174/1573413717666211208143652

Amin, K., Meng, Q., Ahmad, A., Cheng, M., Zhang, M., Mao, L., Lu, K., & Wei, Z. (2018). A Carbonyl Compound-Based Flexible Cathode with Superior Rate Performance and Cyclic Stability for Flexible Lithium-Ion Batteries. *Advanced Materials*, *30*(4), 1–8. https://doi.org/10.1002/adma.201703868

Anonymous. (n.d.). *working principle lithium-ion battery*. E-Lyte Innovations GmbH. Retrieved May 11, 2022, from https://e-lyte-innovations.de/knowledge/working-principle-lithium-ion-battery/

Aziz, A., Bazbouz, M. B., & Welland, M. E. (2020). Double-Walled Carbon Nanotubes Ink for High-Conductivity Flexible Electrodes. *ACS Applied Nano Materials*. https://doi.org/10.1021/acsanm.0c02013

Bao, J. J., Zou, B. K., Cheng, Q., Huang, Y. P., Wu, F., Xu, G. W., & Chen, C. H. (2017). Flexible and free-standing LiFePO4/TPU/SP cathode membrane prepared via phase separation process for lithium ion batteries. *Journal of Membrane Science*, *541*(June), 633–640. https://doi.org/10.1016/j.memsci.2017.06.083

Bates, J. B., Dudney, N. J., Gruzalski, G. R., Zuhr, R. A., Choudhury, A., Luck, C. F., & Robertson, J. D. (1993). Fabrication and characterization of amorphous lithium electrolyte thin films and rechargeable thin-film batteries. *Journal of Power Sources*, *43*(1–3), 103–110. https://doi.org/10.1016/0378-7753(93)80106-Y

Bensalah, N., Kamand, F. Z., Zaghou, M., Dawoud, H. D., & Tahtamouni, T. Al. (2019). Silicon nanofilms as anode materials for flexible lithium ion batteries. *Thin Solid Films*, *690*(December 2018). https://doi.org/10.1016/j.tsf.2019.137516

Bruce, P. G., Scrosati, B., & Tarascon, J. M. (2008). Nanomaterials for rechargeable lithium batteries. *Angewandte Chemie - International Edition*, *47*(16), 2930–2946. https://doi.org/10.1002/anie.200702505

Cecchini, R., & Pelosi, G. (1992). Alessandro Volta and his battery. *IEEE Antennas and Propagation Magazine*, *34*, 30–37.

Ding, Y. H., Ren, H. M., Huang, Y. Y., Chang, F. H., & Zhang, P. (2013). Three-dimensional graphene/LiFePO4 nanostructures as cathode materials for flexible lithium-ion batteries. *Materials Research Bulletin*, *48*(10), 3713–3716. https://doi.org/10.1016/j.materresbull.2013.05.118

Dong, H., Li, J., Guo, J., Lai, F., Zhao, F., Jiao, Y., Brett, D. J. L., Liu, T., He, G., & Parkin, I. P. (2021). Insights on Flexible Zinc-Ion Batteries from Lab Research to Commercialization. *Advanced Materials*, *33*(20). https://doi.org/10.1002/adma.202007548

Downes, R., Wang, S., Haldane, D., Moench, A., & Liang, R. (2015). Strain-induced alignment mechanisms of carbon nanotube networks. *Advanced Engineering Materials*, *17*(3), 349–358. https://doi.org/10.1002/adem.201400045

Experiments, T. (n.d.). *Two-, Three-, and Four-Electrode Experiments*. 1–3.

Flandrois, S., & Simon, B. (1999). Carbon materials for lithium-ion rechargeable batteries. *Carbon*, *37*(2), 165–180. https://doi.org/10.1016/S0008-6223(98)00290-5

Gaikwad, A. M., Whiting, G. L., Steingart, D. A., & Arias, A. C. (2011). Highly flexible, printed alkaline batteries based on mesh-embedded electrodes. *Advanced Materials*, *23*(29), 3251–3255. https://doi.org/10.1002/adma.201100894

Gaikwad, A. M., Zamarayeva, A. M., Rousseau, J., Chu, H., Derin, I., & Steingart, D. A. (2012). Highly stretchable alkaline batteries based on an embedded conductive fabric. *Advanced Materials*, *24*(37), 5071–5076. https://doi.org/10.1002/adma.201201329

Galos, J., Pattarakunnan, K., Best, A. S., Kyratzis, I. L., Wang, C. H., & Mouritz, A.

P. (2021). Energy Storage Structural Composites with Integrated Lithium-Ion Batteries: A Review. *Advanced Materials Technologies*, *6*(8), 1–19. https://doi.org/10.1002/admt.202001059

Gofer, Y., Sarker, H., Killan, J. G., Poehler, T. O., & Searson, P. C. (1997). An all-polymer charge storage device. *Applied Physics Letters*, *71*(11), 1582–1584. https://doi.org/10.1063/1.120074

Gwon, H., Kim, H. S., Lee, K. U., Seo, D. H., Park, Y. C., Lee, Y. S., Ahn, B. T., & Kang, K. (2011). Flexible energy storage devices based on graphene paper. *Energy and Environmental Science*, *4*(4), 1277–1283. https://doi.org/10.1039/c0ee00640h

He, X., Wu, Y., Zhao, F., Wang, J., Jiang, K., & Fan, S. (2013). Enhanced rate capabilities of Co3O4/carbon nanotube anodes for lithium ion battery applications. *Journal of Materials Chemistry A*, *1*(37), 11121–11125. https://doi.org/10.1039/c3ta12608k

Jiang, J., Li, Y., Liu, J., Huang, X., Yuan, C., & Lou, X. W. (2012). Recent advances in metal oxide-based electrode architecture design for electrochemical energy storage. *Advanced Materials*, *24*(38), 5166–5180. https://doi.org/10.1002/adma.201202146

Kasavajjula, U., Wang, C., & Appleby, A. J. (2007). Nano- and bulk-silicon-based insertion anodes for lithium-ion secondary cells. *Journal of Power Sources*, *163*(2), 1003–1039. https://doi.org/10.1016/j.jpowsour.2006.09.084

Kim, H., Auyeung, R. C. Y., & Piqué, A. (2007). Laser-printed thick-film electrodes for solid-state rechargeable Li-ion microbatteries. *Journal of Power Sources*, *165*(1), 413–419. https://doi.org/10.1016/j.jpowsour.2006.11.053

Kim, H. J., Bae, G. H., Lee, S. M., Ahn, J. H., & Kim, J. K. (2019). Properties of lithium iron phosphate prepared by biomass-derived carbon coating for flexible lithium ion batteries. *Electrochimica Acta*, *300*, 18–25. https://doi.org/10.1016/j.electacta.2019.01.057

Lee, K. T., & Cho, J. (2011). Roles of nanosize in lithium reactive nanomaterials for

lithium ion batteries. *Nano Today*, *6*(1), 28–41. https://doi.org/10.1016/j.nantod.2010.11.002

Lee, Y. H., Kim, J. S., Noh, J., Lee, I., Kim, H. J., Choi, S., Seo, J., Jeon, S., Kim, T. S., Lee, J. Y., & Choi, J. W. (2013). Wearable textile battery rechargeable by solar energy. *Nano Letters*, *13*(11), 5753–5761. https://doi.org/10.1021/nl403860k

Li, B., Zhao, W., Yang, Z., Zhang, C., Dang, F., Liu, Y., Jin, F., & Chen, X. (2020). A carbon-doped anatase TiO2-Based flexible silicon anode with high-performance and stability for flexible lithium-ion battery. *Journal of Power Sources*, *466*(May), 228339. https://doi.org/10.1016/j.jpowsour.2020.228339

Li, C., Shi, T., Yoshitake, H., & Wang, H. (2017). A flexible high-energy lithium-ion battery with a carbon black-sandwiched Si anode. *Electrochimica Acta*, *225*, 11–18. https://doi.org/10.1016/j.electacta.2016.12.105

Li, L., Wang, L., Ye, T., Peng, H., & Zhang, Y. (2021). Stretchable Energy Storage Devices Based on Carbon Materials. *Small*, *17*(48), 1–18. https://doi.org/10.1002/smll.202005015

Li, M., Lu, J., Chen, Z., & Amine, K. (2018). 30 Years of Lithium-Ion Batteries. *Advanced Materials*, *30*(33), 1–24. https://doi.org/10.1002/adma.201800561

Li, Qiang, Li, D., Wang, H., Wang, H. G., Li, Y., Si, Z., & Duan, Q. (2019). Conjugated Carbonyl Polymer-Based Flexible Cathode for Superior Lithium-Organic Batteries. *ACS Applied Materials and Interfaces*, *11*(32), 28801–28808. https://doi.org/10.1021/acsami.9b06437

Li, Qingfeng, He, R., Jensen, J. O., & Bjerrum, N. J. (2003). Approaches and Recent Development of Polymer Electrolyte Membranes for Fuel Cells Operating above 100 °C. *Chemistry of Materials*, *15*(26), 4896–4915. https://doi.org/10.1021/cm0310519

Liao, C. L., & Fung, K. Z. (2004). Lithium cobalt oxide cathode film prepared by rf sputtering. *Journal of Power Sources*, *128*(2), 263–269. https://doi.org/10.1016/j.jpowsour.2003.09.065

Liu, T., Kim, K. C., Lee, B., Chen, Z., Noda, S., Jang, S. S., & Lee, S. W. (2017). Self-polymerized dopamine as an organic cathode for Li- and Na-ion batteries. *Energy and Environmental Science*, *10*(1), 205–215. https://doi.org/10.1039/c6ee02641a

Ma, X., Pan, Z., Wu, X., & Shen, P. K. (2019). Na4Fe3(PO4)2(P2O7)@NaFePO4@C core-double-shell architectures on carbon cloth: A high-rate, ultrastable, and flexible cathode for sodium ion batteries. *Chemical Engineering Journal*, *365*(October 2018), 132–141. https://doi.org/10.1016/j.cej.2019.01.173

Marriam, I., Tebyetekerwa, M., Xu, Z., Chathuranga, H., Chen, S., Chen, H., Zheng, J.-C., Du, A., & Yan, C. (2021). Techniques Enabling Inorganic Materials into Wearable Fiber/Yarn and Flexible Lithium-Ion Batteries. *Energy Storage Materials*, *43*(August), 62–84. https://doi.org/10.1016/j.ensm.2021.08.039

Mastragostino, M., Soavi, F., & Zanelli, A. (1999). Improved composite materials for rechargeable lithium metal polymer batteries. *Journal of Power Sources*, *81–82*, 729–733. https://doi.org/10.1016/S0378-7753(99)00152-4

MIT Electric Vehicle Team. (2008). *A Guide to Understanding Battery Specifications*.

Natarajan, B., Stein, I. Y., Lachman, N., Yamamoto, N., Jacobs, D. S., Sharma, R., Liddle, J. A., & Wardle, B. L. (2019). Aligned carbon nanotube morphogenesis predicts physical properties of their polymer nanocomposites. *Nanoscale*, *11*(35), 16327–16335. https://doi.org/10.1039/c9nr03317c

Nathan, A., Ahnood, A., Cole, M. T., Lee, S., Suzuki, Y., Hiralal, P., Bonaccorso, F., Hasan, T., Garcia-Gancedo, L., Dyadyusha, A., Haque, S., Andrew, P., Hofmann, S., Moultrie, J., Chu, D., Flewitt, A. J., Ferrari, A. C., Kelly, M. J., Robertson, J., … Milne, W. I. (2012). Flexible electronics: The next ubiquitous platform. *Proceedings of the IEEE*, *100*(SPL CONTENT), 1486–1517. https://doi.org/10.1109/JPROC.2012.2190168

Noerochim, L., Wang, J. Z., Wexler, D., Rahman, M. M., Chen, J., & Liu, H. K.

(2012). Impact of mechanical bending on the electrochemical performance of bendable lithium batteries with paper-like free-standing V 2O 5-polypyrrole cathodes. *Journal of Materials Chemistry*, *22*(22), 11159–11165. https://doi.org/10.1039/c2jm16470a

Nyholm, L., Nyström, G., Mihranyan, A., & Strømme, M. (2011). Toward flexible polymer and paper-based energy storage devices. *Advanced Materials*, *23*(33), 3751–3769. https://doi.org/10.1002/adma.201004134

O'Heir, J. (2017). Building better batteries. *Mechanical Engineering*, *139*(1), 10–11.

Ohta, S., Komagata, S., Seki, J., Saeki, T., Morishita, S., & Asaoka, T. (2013). Short communication All-solid-state lithium ion battery using garnet-type oxide and Li3BO3 solid electrolytes fabricated by screen-printing. *Journal of Power Sources*, *238*, 53–56. https://doi.org/10.1016/j.jpowsour.2013.02.073

Park, C. M., Kim, J. H., Kim, H., & Sohn, H. J. (2010). Li-alloy based anode materials for Li secondary batteries. *Chemical Society Reviews*, *39*(8), 3115–3141. https://doi.org/10.1039/b919877f

Prosini, P. P., Mancini, R., Petrucci, L., Contini, V., & Villano, P. (2001). Li4Ti5O12 as anode in all-solid-state, plastic, lithium-ion batteries for low-power applications. *Solid State Ionics*, *144*(1–2), 185–192. https://doi.org/10.1016/S0167-2738(01)00891-8

Ren, J., Li, L., Chen, C., Chen, X., Cai, Z., Qiu, L., Wang, Y., Zhu, X., & Peng, H. (2013). Twisting carbon nanotube fibers for both wire-shaped micro-supercapacitor and micro-battery. *Advanced Materials*, *25*(8), 1155–1159. https://doi.org/10.1002/adma.201203445

Ren, W., Wang, C., Lu, L., Li, D., Cheng, C., & Liu, J. (2013). SnO2@Si core-shell nanowire arrays on carbon cloth as a flexible anode for Li ion batteries. *Journal of Materials Chemistry A*, *1*(43), 13433–13438. https://doi.org/10.1039/c3ta11943b

Roy, P., & Srivastava, S. K. (2015). Nanostructured anode materials for lithium ion batteries. *Journal of Materials Chemistry A*, *3*(6), 2454–2484.

https://doi.org/10.1039/c4ta04980b

Sannier, L., Bouchet, R., Grugeon, S., Naudin, E., Vidal, E., & Tarascon, J. M. (2005). Room temperature lithium metal batteries based on a new Gel Polymer Electrolyte membrane. *Journal of Power Sources*, *144*(1), 231–237. https://doi.org/10.1016/j.jpowsour.2004.11.064

Shin, J.-H., Henderson, W. A., & Passerini, S. (2005). PEO-Based Polymer Electrolytes with Ionic Liquids and Their Use in Lithium Metal-Polymer Electrolyte Batteries. *Journal of The Electrochemical Society*, *152*(5), A978. https://doi.org/10.1149/1.1890701

Stenina, I. A., Kulova, T. L., Skundin, A. M., & Yaroslavtsev, A. B. (2018). Effects of carbon coating from sucrose and PVDF on electrochemical performance of Li4Ti5O12/C composites in different potential ranges. *Journal of Solid State Electrochemistry*, *22*(9), 2631–2639. https://doi.org/10.1007/s10008-018-3978-z

Sultana, I., Rahman, M. M., Wang, J., Wang, C., Wallace, G. G., & Liu, H. K. (2012). All-polymer battery system based on polypyrrole (PPy)/para (toluene sulfonic acid) (pTS) and polypyrrole (PPy)/indigo carmine (IC) free standing films. *Electrochimica Acta*, *83*, 209–215. https://doi.org/10.1016/j.electacta.2012.08.043

Sun, H., Zhang, Y., Zhang, J., Sun, X., & Peng, H. (2017). Energy harvesting and storage in 1D devices. *Nature Reviews Materials*, *2*, 1–12. https://doi.org/10.1038/natrevmats.2017.23

Tarascon, J. M., & Armand, M. (2001). Issues and challenges facing rechargeable lithium batteries. *Nature*, *414*(6861), 359–367. https://doi.org/10.1038/35104644

Torres-Torres, C. Mercado-Zúñiga, C. Santos-Fernández, A. M. Martínez-González, C. L. Trejo-Valdez, M. Martínez-Gutiérrez, H. Vargas-García, J. R. Torres-Martínez, R. (2017). Contrast in the Electrical and Opto-Electrical Properties Exhibited by Randomly Distributed Networks and Vertically Aligned Mutil-

Wall Carbon Nanotubes. *Journal of Nanoelectronics and Optoelectronics*, *12*(1), 28-32(5). https://doi.org/10.1166/jno.2017.1972

Vilatela, J. J., Elliott, J. A., & Windle, A. H. (2011). A model for the strength of yarn-like carbon nanotube fibers. *ACS Nano*, *5*(3), 1921–1927. https://doi.org/10.1021/nn102925a

Wang, B., Wang, H., Chen, W., Wu, P., Bu, L., Zhang, L., & Wan, L. (2020). Carbonized cotton fiber supported flexible organic lithium ion battery cathodes. *Journal of Colloid and Interface Science*, *572*, 1–8. https://doi.org/10.1016/j.jcis.2020.03.047

Wang, Caiyun, & Wallace, G. G. (2015). Flexible Electrodes and Electrolytes for Energy Storage. *Electrochimica Acta*, *175*, 87–95. https://doi.org/10.1016/j.electacta.2015.04.067

Wang, Chao, Wang, X., Lin, C., & Zhao, X. S. (2020). Spherical vanadium phosphate particles grown on carbon fiber cloth as flexible anode for high-rate Li-ion batteries. *Chemical Engineering Journal*, *386*(November 2019), 123981. https://doi.org/10.1016/j.cej.2019.123981

Wang, Chunya, Xia, K., Wang, H., Liang, X., Yin, Z., & Zhang, Y. (2019). Advanced Carbon for Flexible and Wearable Electronics. *Advanced Materials*, *31*(9), 1–37. https://doi.org/10.1002/adma.201801072

Wang, J., & Sun, X. (2012). Understanding and recent development of carbon coating on LiFePO 4 cathode materials for lithium-ion batteries. *Energy and Environmental Science*, *5*(1), 5163–5185. https://doi.org/10.1039/c1ee01263k

Wang, M., Huang, Y., Zhu, Y., Wu, X., Zhang, N., & Zhang, H. (2019). Binder-free flower-like SnS2 nanoplates decorated on the graphene as a flexible anode for high-performance lithium-ion batteries. *Journal of Alloys and Compounds*, *774*, 601–609. https://doi.org/10.1016/j.jallcom.2018.09.378

Wang, S., Fan, Y., Stroe, D.-I., Fernandez, C., Yu, C., Cao, W., & Chen, Z. (2021). Lithium-ion battery characteristics and applications. In *Battery System Modeling*. https://doi.org/10.1016/b978-0-323-90472-8.00003-2

Wang, X., Xi, M., Wang, X., Fong, H., & Zhu, Z. (2016). Flexible composite felt of electrospun TiO2 and SiO2 nanofibers infused with TiO2 nanoparticles for lithium ion battery anode. *Electrochimica Acta*, *190*, 811–816. https://doi.org/10.1016/j.electacta.2015.12.123

Wu, K., Niu, Y., Zhang, Y., Yong, Z., & Li, Q. (2021). Continuous growth of carbon nanotube films: From controllable synthesis to real applications. *Composites Part A: Applied Science and Manufacturing*, *144*(July 2020), 106359. https://doi.org/10.1016/j.compositesa.2021.106359

Xia, A., Zhao, C., Yu, W., Han, Y., Yi, J., & Tan, G. (2020). Mo-doped δ-MnO2 anode material synthesis and electrochemical performance for lithium-ion batteries. *Journal of Applied Electrochemistry*, *50*(7), 733–744. https://doi.org/10.1007/s10800-020-01431-2

XIONG, S. (2019). *A STUDY OF THE FACTORS THAT AFFECT LITHIUM ION BATTERY DEGRADATION*.

Yao, Y., Zhu, Y., Zhao, S., Shen, J., Yang, X., & Li, C. (2018). Halide Ion Intercalated Electrodeposition Synthesis of Co3O4 Nanosheets with Tunable Pores on Graphene Foams as Free-Standing and Flexible Li-Ion Battery Anodes. *ACS Applied Energy Materials*, *1*(3), 1239–1251. https://doi.org/10.1021/acsaem.7b00351

Zhang, C., Zhu, J., Lin, H., & Huang, W. (2018). Flexible Fiber and Fabric Batteries. *Advanced Materials Technologies*, *3*(10), 1700302. https://doi.org/10.1002/admt.201700302

Zhang, W. J. (2011). A review of the electrochemical performance of alloy anodes for lithium-ion batteries. *Journal of Power Sources*, *196*(1), 13–24. https://doi.org/10.1016/j.jpowsour.2010.07.020

Zhang, Y., Li, Y., Wang, Y., Guo, R., Liu, W., Pei, H., Yin, G., Ye, D., Yu, S., & Xie, J. (2019). A flexible copper sulfide @ multi-walled carbon nanotubes cathode for advanced magnesium-lithium-ion batteries. *Journal of Colloid and Interface Science*, *553*, 239–246. https://doi.org/10.1016/j.jcis.2019.06.027

Zhao, C., Wada, T., De Andrade, V., Gürsoy, D., Kato, H., & Chen-Wiegart, Y. chen K. (2018). Imaging of 3D morphological evolution of nanoporous silicon anode in lithium ion battery by X-ray nano-tomography. *Nano Energy*, *52*(August), 381–390. https://doi.org/10.1016/j.nanoen.2018.08.009

Zhao, L., Inoishi, A., & Okada, S. (2021). Thermal risk evaluation of concentrated electrolytes for Li-ion batteries. *Journal of Power Sources Advances*, *12*, 100079. https://doi.org/10.1016/j.powera.2021.100079

Zhao, Y., & Guo, J. (2020). Development of flexible Li-ion batteries for flexible electronics. *InfoMat*, *2*(5), 866–878. https://doi.org/10.1002/inf2.12117

Zhu, K., Gao, H., & Hu, G. (2018). A flexible mesoporous Li4Ti5O12-rGO nanocomposite film as free-standing anode for high rate lithium ion batteries. *Journal of Power Sources*, *375*(November 2017), 59–67. https://doi.org/10.1016/j.jpowsour.2017.11.053

Zhu, Y., Yang, M., Huang, Q., Wang, D., Yu, R., Wang, J., Zheng, Z., & Wang, D. (2020). V2O5 Textile Cathodes with High Capacity and Stability for Flexible Lithium-Ion Batteries. *Advanced Materials*, *32*(7), 1–7. https://doi.org/10.1002/adma.201906205

BIOGRAPHY

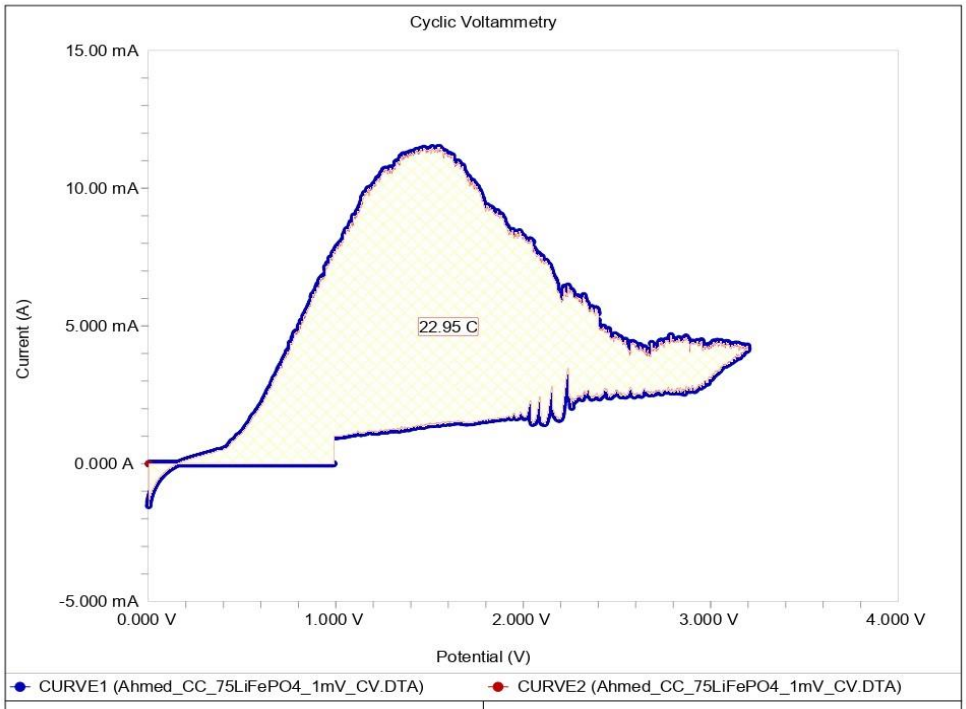
Ahmed Alahmed started his undergraduate education in the Mechanical Engineering - Textile Department at Aleppo University in 2004. He completed his undergraduate education in 2009. He obtained a master's degree in Machinery and Textile Technology from Aleppo University in 2011. He worked as a research assistant at Aleppo University from 2010 to 2014. In 2015, he started his doctorate education at Çukurova University, Institute of Science and Technology, Department of Textile Engineering.

APPENDICES

1- Electrochemical Characterization

The cyclic voltammetry CV curves and electrochemical impedance spectroscopy EIS curves for produced are shown below.

Calculation of specific capacitance (**Cp**) was calculated from CV data for each sample, based on Equation 3.9.

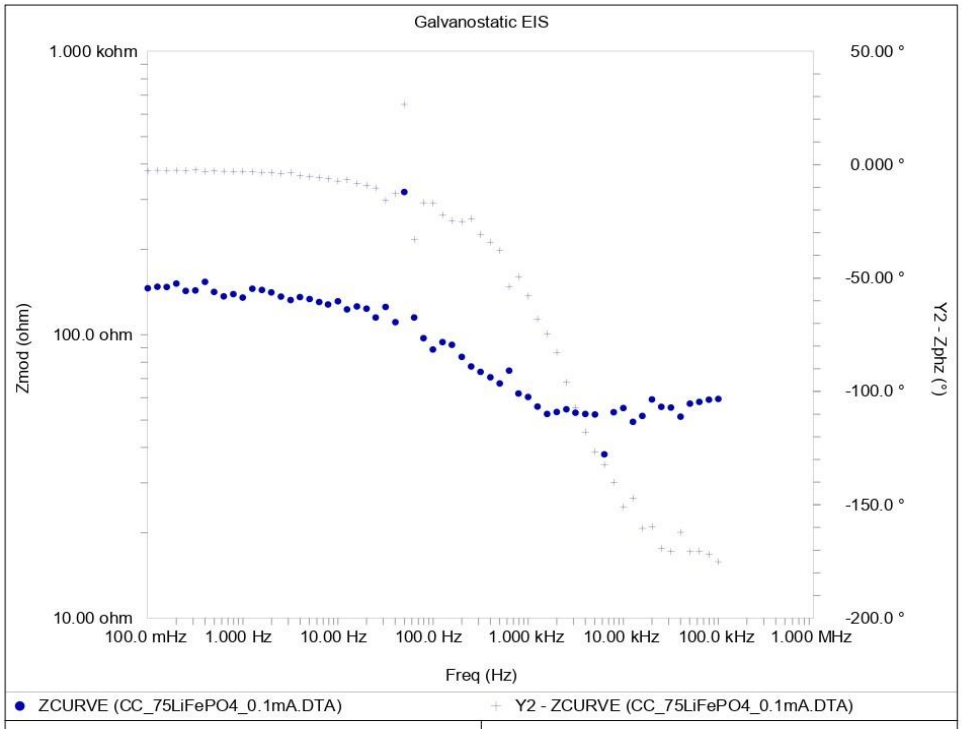


EXPERIMENTAL PARAMETERS

Initial E (V): 0 vs. Eref
Scan Limit 1 (V): 3.2 vs. Eref
Scan Limit 2 (V): 0 vs. Eref
Final E (V): 0 vs. Eref
Cyclic Voltammetry
1.7.2022
15:16:07
Scan Rate (mV/s): 0.999998
Step Size (mV): 2
Electrode Area (cm^2): 1
Equil. Time (s): 5
I/E Range Mode: Auto I/E Range
Max Current (mA): 1000
Conditioning: Off
Init. Delay: Off
IRComp: None
Open Circuit (V): 0
Sampling Mode: Noise Reject

EXPERIMENTAL NOTES

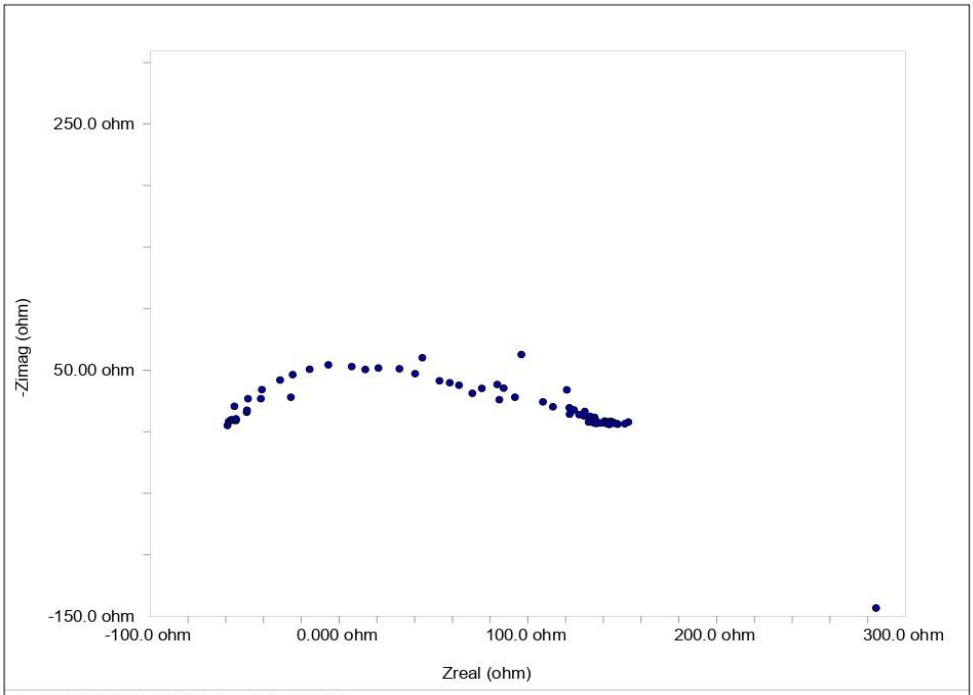
Circle samples of carbon cloth fabric before and after coating with a diameter of 16 mm were cut by a sample cutting machine.
The coating ink consists of the following:
LiFePO4 (75%) -Carbon Black, Super P (20%) -PVDF (5%)
The weight of the ink that was coated was calculated by calculating the weight of the sample before and after the coating process, which is 0.04747 g.
The capacitance was calculated using the following equation:
Cp=A/(3.6 m)
m: The weight of the ink and A: the area within the CV curve
Cp= 134.295 mAh/g



EXPERIMENTAL PARAMETERS

DC Current (A): 0
AC Current (A rms): 0.0001
Galvanostatic EIS
24.6.2022
14:02:42
Initial Freq. (Hz): 100000
Final Freq. (Hz): 0.1
Points/decade: 10
Area (cm^2): 1
Conditioning: Off
Init. Delay: On
Time(s): 10
Stab.(mV/s): 0
Open Circuit (V): 0.4034105

EXPERIMENTAL NOTES

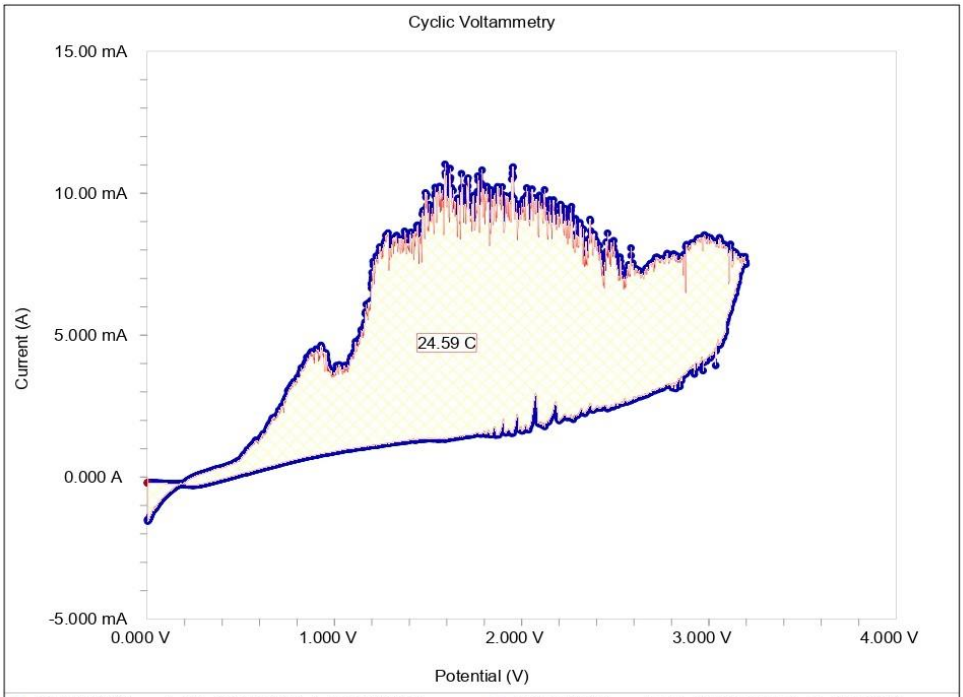


ZCURVE (CC_75LiFePO4_0.1mA.DTA)

EXPERIMENTAL PARAMETERS

DC Current (A): 0
AC Current (A rms): 0.0001
Galvanostatic EIS
24.6.2022
14:02:42
Initial Freq. (Hz): 100000
Final Freq. (Hz): 0.1
Points/decade: 10
Area (cm^2): 1
Conditioning: Off
Init. Delay: On
Time(s): 10
Stab.(mV/s): 0
Open Circuit (V): 0.4034105

EXPERIMENTAL NOTES



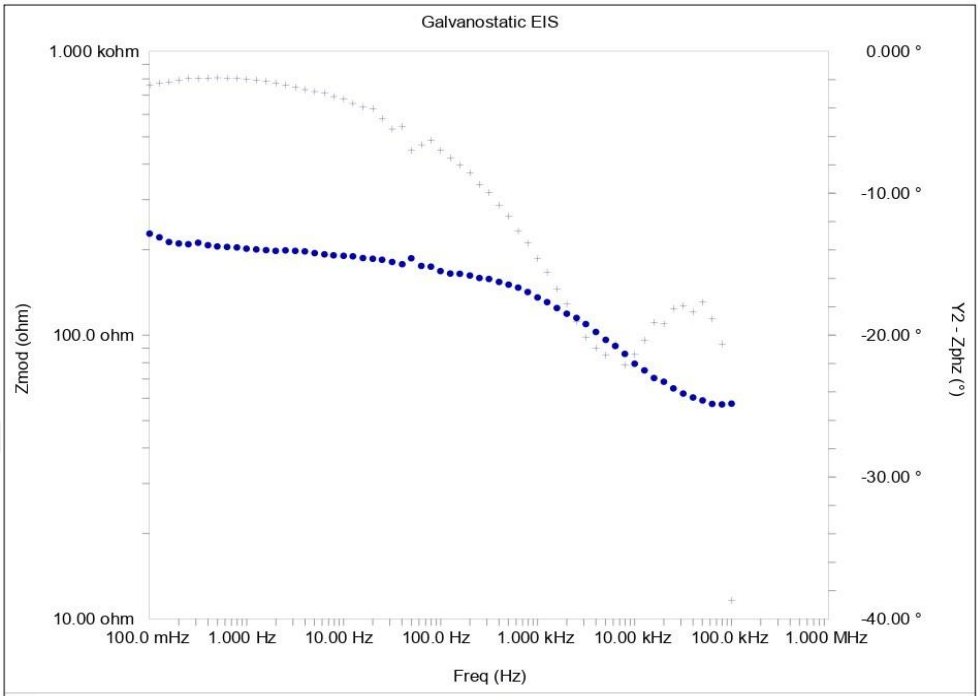
EXPERIMENTAL PARAMETERS

Initial E (V): 0 vs. Eref
Scan Limit 1 (V): 3.2 vs. Eref
Scan Limit 2 (V): 0 vs. Eref
Final E (V): 0 vs. Eref
Cyclic Voltammetry
30.6.2022
15:26:47
Scan Rate (mV/s): 0.999998
Step Size (mV): 2
Electrode Area (cm^2): 1
Equil. Time (s): 5
I/E Range Mode: Auto I/E Range
Max Current (mA): 1000
Conditioning: Off
Init. Delay: Off
IRComp: None
Open Circuit (V): 0
Sampling Mode: Noise Reject

EXPERIMENTAL NOTES

Circle samples of carbon cloth fabric before and after coating with a diameter of 16 mm were cut by a sample cutting machine.

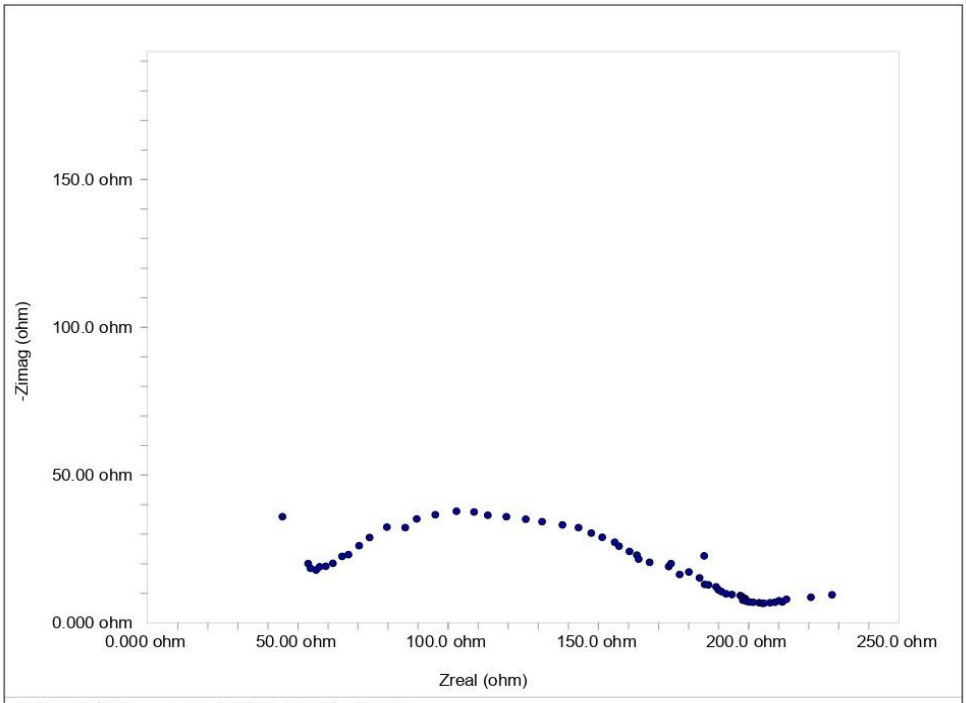
The coating ink consists of the following:
LiFePO4 (80%) -Carbon Black, Super P (15%) -PVDF (5%)
The weight of the ink that was coated was calculated by calculating the weight of the sample before and after the coating process, which is 0.03973 g.
The capacitance was calculated using the following equation:
Cp=A/(3.6 m)
m: The weight of the ink and A: the area within the CV curve
Cp= 171.9244 mAh/g



EXPERIMENTAL PARAMETERS

DC Current (A): 0
AC Current (A rms): 0.0001
Galvanostatic EIS
30.6.2022
15:07:40
Initial Freq. (Hz): 100000
Final Freq. (Hz): 0.1
Points/decade: 10
Area (cm^2): 1
Conditioning: Off
Init. Delay: On
Time(s): 10
Stab.(mV/s): 0
Open Circuit (V): 0.3273135

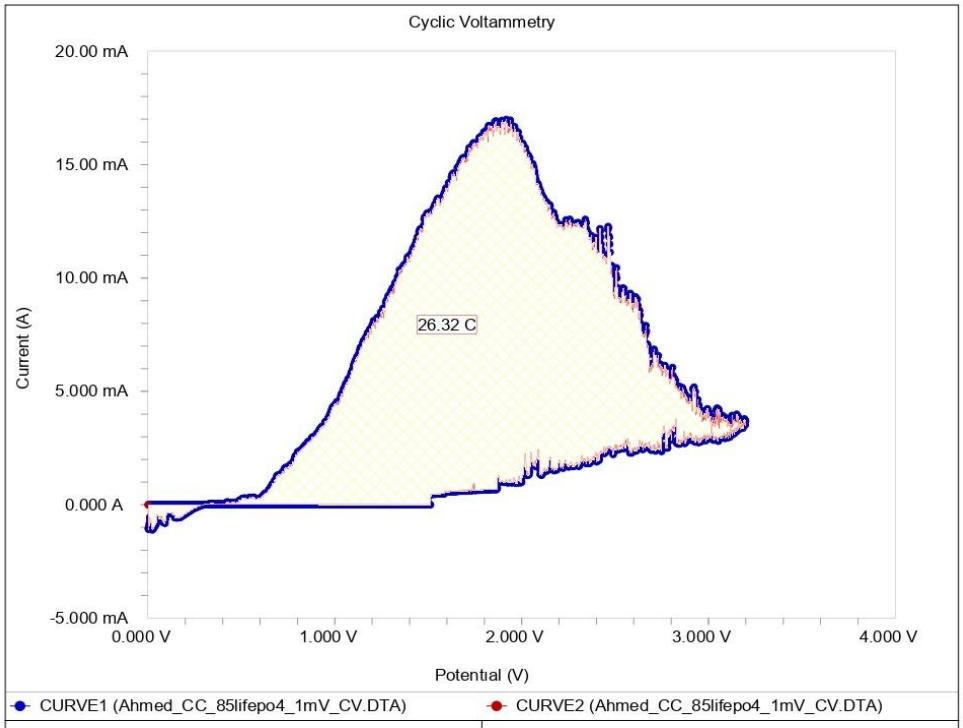
EXPERIMENTAL NOTES



EXPERIMENTAL PARAMETERS

DC Current (A): 0
AC Current (A rms): 0.0001
Galvanostatic EIS
30.6.2022
15:07:40
Initial Freq. (Hz): 100000
Final Freq. (Hz): 0.1
Points/decade: 10
Area (cm^2): 1
Conditioning: Off
Init. Delay: On
Time(s): 10
Stab.(mV/s): 0
Open Circuit (V): 0.3273135

EXPERIMENTAL NOTES



EXPERIMENTAL PARAMETERS

Initial E (V): 0 vs. Eref
Scan Limit 1 (V): 3.2 vs. Eref
Scan Limit 2 (V): 0 vs. Eref
Final E (V): 0 vs. Eref
Cyclic Voltammetry
28.6.2022
18:03:57
Scan Rate (mV/s): 0.999998
Step Size (mV): 2
Electrode Area (cm^2): 1
Equil. Time (s): 5
I/E Range Mode: Auto I/E Range
Max Current (mA): 1000
Conditioning: Off
Init. Delay: Off
IRComp: None
Open Circuit (V): 0
Sampling Mode: Noise Reject

EXPERIMENTAL NOTES

Circle samples of carbon cloth fabric before and after coating with a diameter of 16 mm were cut by a sample cutting machine.

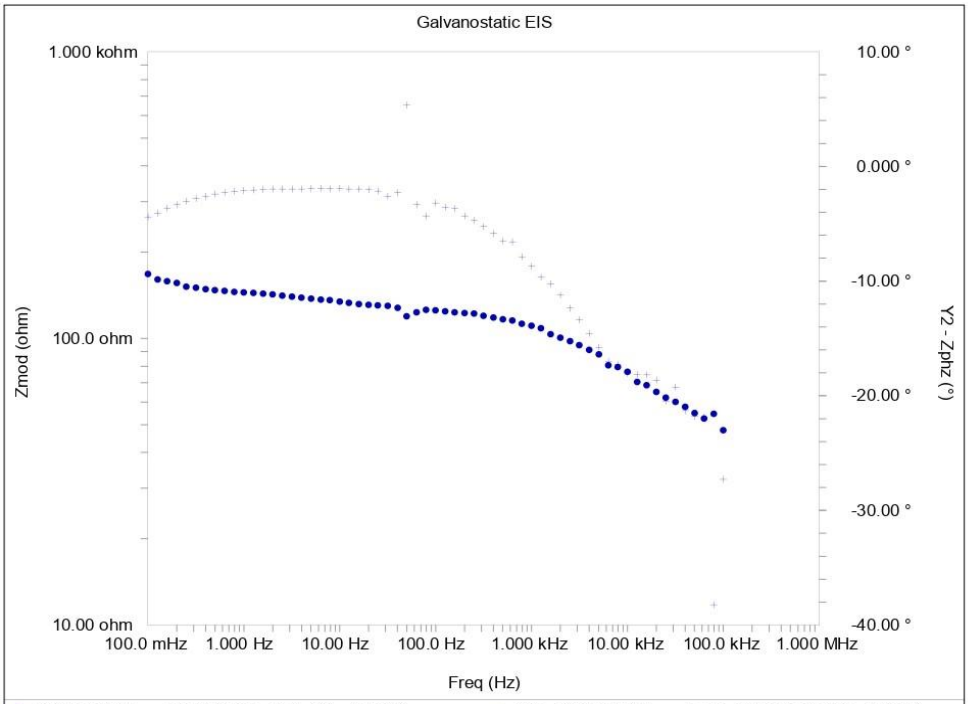
The coating ink consists of the following:
LiFePO4 (85%) -Carbon Black, Super P (10%) -PVDF (5%)

The weight of the ink that was coated was calculated by calculating the weight of the sample before and after the coating process, which is 0.0371 g.

The capacitance was calculated using the following equation:

$$Cp=A/(3.6\ m)$$

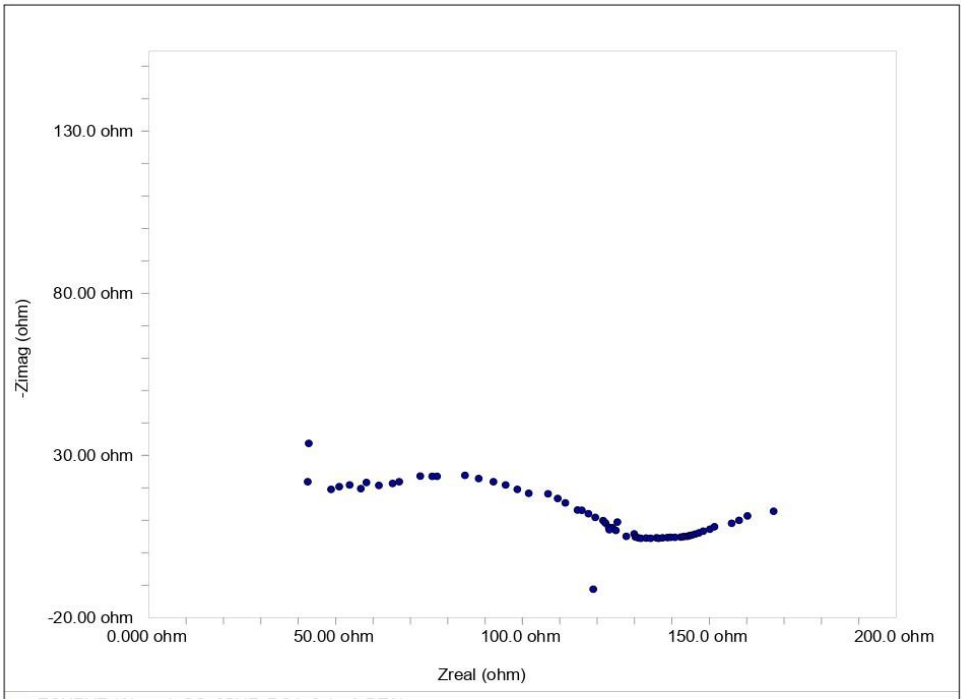
m: The weight of the ink and A: the area within the CV curve
Cp= 197.065 mAh/g



EXPERIMENTAL PARAMETERS

DC Current (A): 0
AC Current (A rms): 0.0001
Galvanostatic EIS
1.7.2022
15:10:32
Initial Freq. (Hz): 100000
Final Freq. (Hz): 0.1
Points/decade: 10
Area (cm^2): 1
Conditioning: Off
Init. Delay: On
Time(s): 10
Stab.(mV/s): 0
Open Circuit (V): 0.2469059

EXPERIMENTAL NOTES

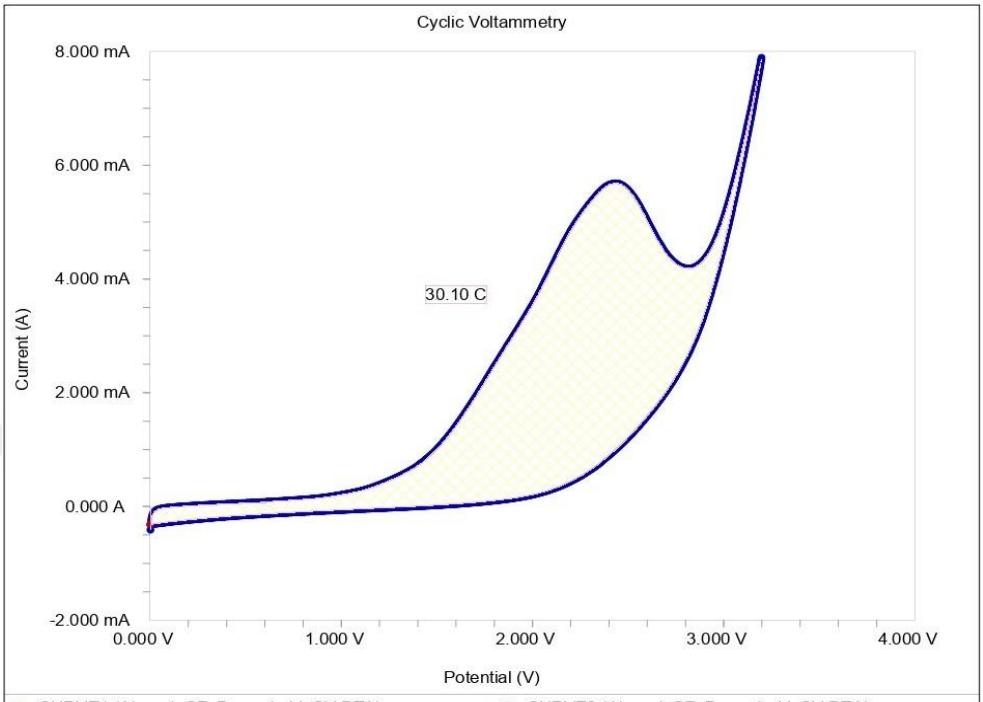


ZCURVE (Ahmed_CC_85LiFePO4_0.1mA.DTA)

EXPERIMENTAL PARAMETERS

DC Current (A): 0
AC Current (A rms): 0.0001
Galvanostatic EIS
1.7.2022
15:10:32
Initial Freq. (Hz): 100000
Final Freq. (Hz): 0.1
Points/decade: 10
Area (cm^2): 1
Conditioning: Off
Init. Delay: On
Time(s): 10
Stab.(mV/s): 0
Open Circuit (V): 0.2469059

EXPERIMENTAL NOTES

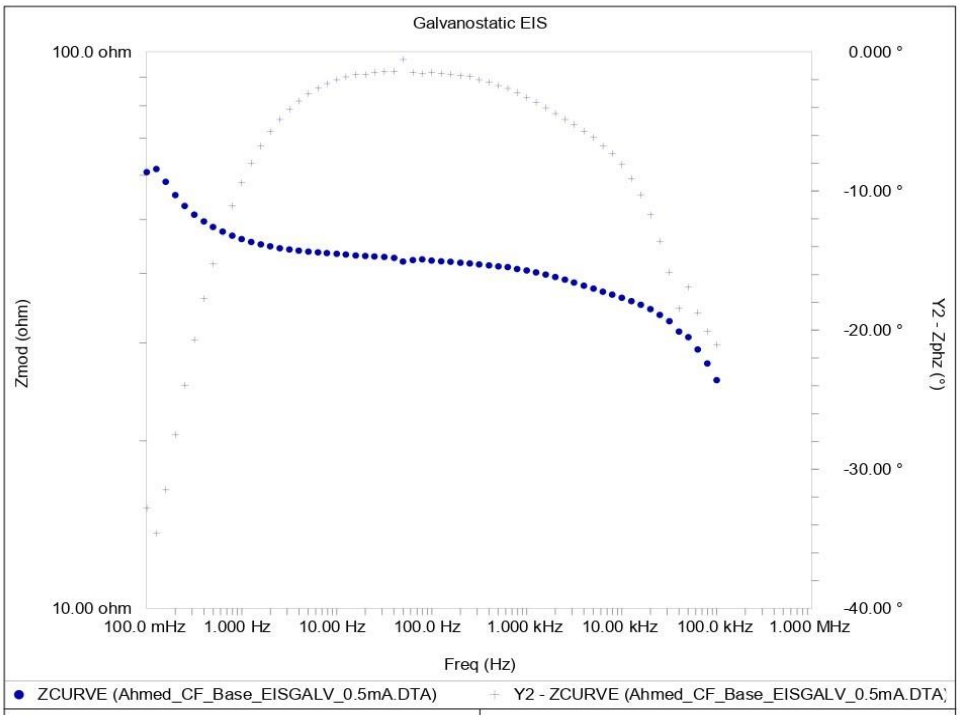


EXPERIMENTAL PARAMETERS

Initial E (V): 0 vs. Eref
Scan Limit 1 (V): 3.2 vs. Eref
Scan Limit 2 (V): 0 vs. Eref
Final E (V): 0 vs. Eref
Cyclic Voltammetry
14.6.2022
16:37:42
Scan Rate (mV/s): 0.999998
Step Size (mV): 2
Electrode Area (cm^2): 1
Equil. Time (s): 5
I/E Range Mode: Auto I/E Range
Max Current (mA): 1000
Conditioning: Off
Init. Delay: Off
IRComp: None
Open Circuit (V): 0
Sampling Mode: Noise Reject

EXPERIMENTAL NOTES

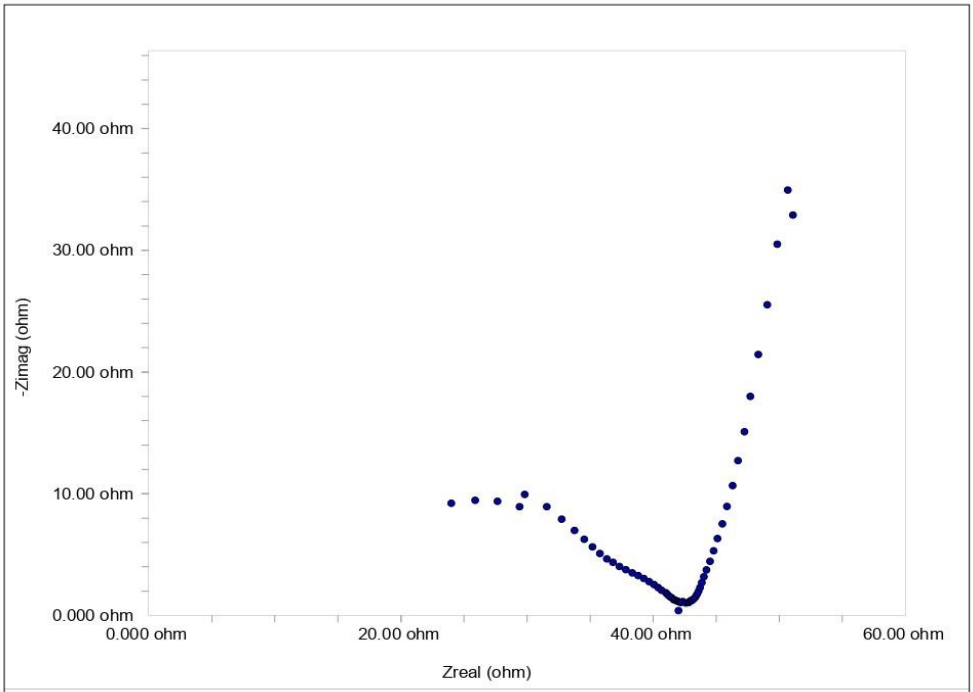
Circle samples of carbon Fiber fabric before and after coating with a diameter of 16 mm were cut by a sample cutting machine.
The coating ink consists of the following:
LiFePO4 (75%) -Carbon Black, Super P (20%) -PVDF (5%)
The weight of the ink that was coated was calculated by calculating the weight of the sample before and after the coating process, which is 0.0381 g.
The capacitance was calculated using the following equation:
Cp=A/(3.6 m)
m: The weight of the ink and A: the area within the CV curve
Cp= 219.4517 mAh/g



EXPERIMENTAL PARAMETERS

DC Current (A): 0
AC Current (A rms): 0.005
Galvanostatic EIS
14.6.2022
15:44:58
Initial Freq. (Hz): 100000
Final Freq. (Hz): 0.1
Points/decade: 10
Area (cm^2): 1
Conditioning: Off
Init. Delay: On
Time(s): 10
Stab.(mV/s): 0
Open Circuit (V): 0.3280096

EXPERIMENTAL NOTES

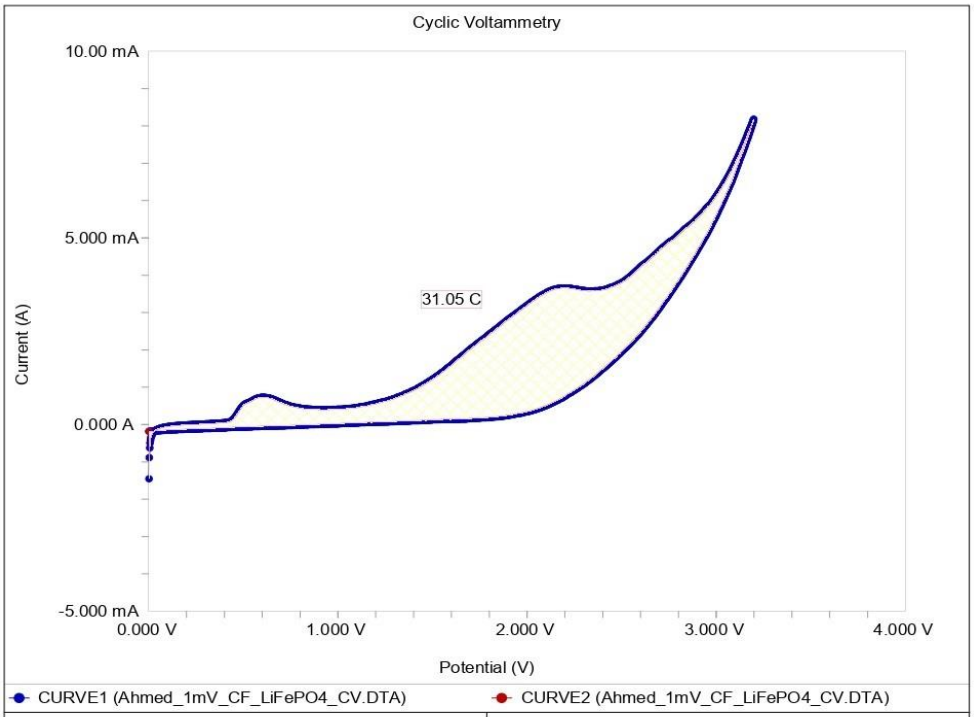


ZCURVE (Ahmed_CF_Base_EISGALV_0.5mA.DTA)

EXPERIMENTAL PARAMETERS

DC Current (A): 0
AC Current (A rms): 0.005
Galvanostatic EIS
14.6.2022
15:44:58
Initial Freq. (Hz): 100000
Final Freq. (Hz): 0.1
Points/decade: 10
Area (cm^2): 1
Conditioning: Off
Init. Delay: On
Time(s): 10
Stab.(mV/s): 0
Open Circuit (V): 0.3280096

EXPERIMENTAL NOTES

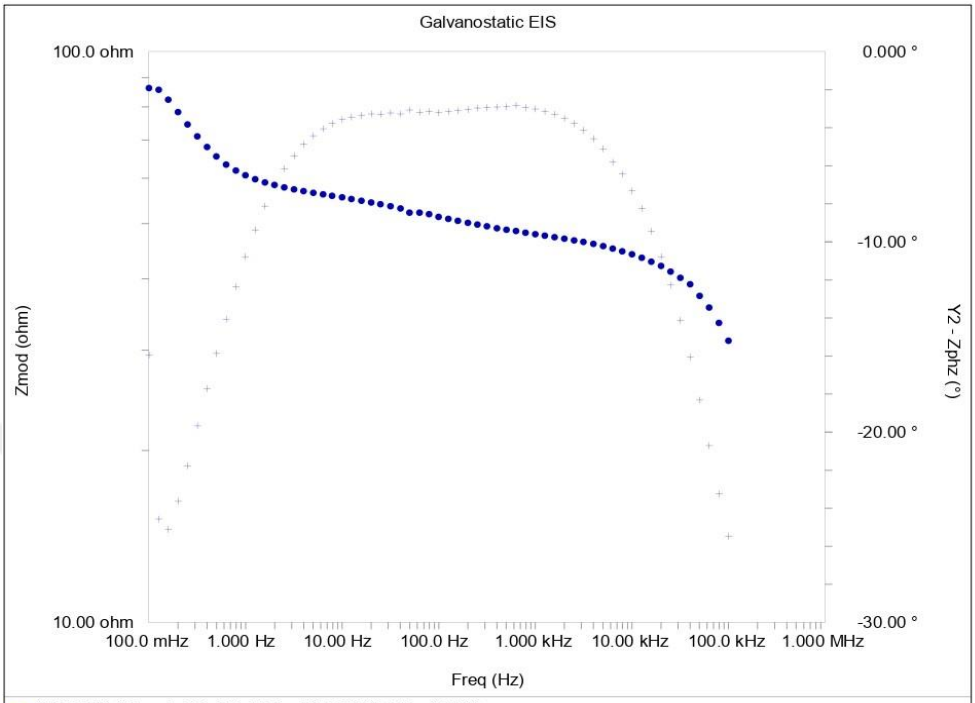


EXPERIMENTAL PARAMETERS

Initial E (V): 0 vs. Eref
Scan Limit 1 (V): 3.2 vs. Eref
Scan Limit 2 (V): 0 vs. Eref
Final E (V): 0 vs. Eref
Cyclic Voltammetry
15.6.2022
11:05:01
Scan Rate (mV/s): 0.999998
Step Size (mV): 2
Electrode Area (cm^2): 1
Equil. Time (s): 5
I/E Range Mode: Auto I/E Range
Max Current (mA): 1000
Conditioning: Off
Init. Delay: Off
IRComp: None
Open Circuit (V): 0
Sampling Mode: Noise Reject

EXPERIMENTAL NOTES

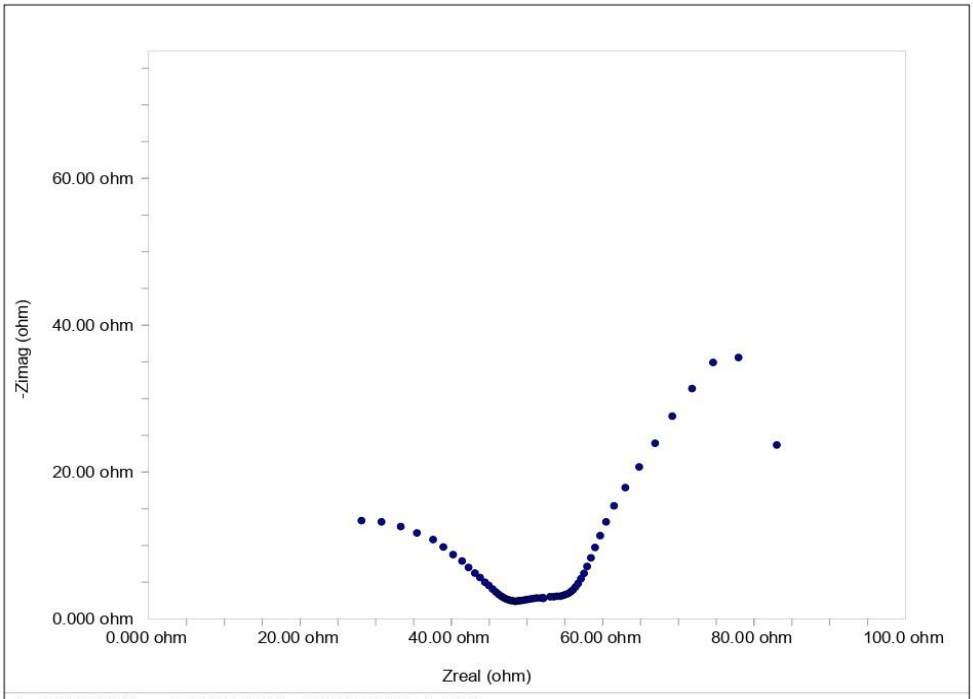
Circle samples of carbon cloth fabric before and after coating with a diameter of 16 mm were cut by a sample cutting machine.
The coating ink consists of the following:
LiFePO4 (85%) -Carbon Black, Super P (10%) -PVDF (5%)
The weight of the ink that was coated was calculated by calculating the weight of the sample before and after the coating process, which is 0.0382 g.
The capacitance was calculated using the following equation:
Cp=A/(3.6 m)
m: The weight of the ink and A: the area within the CV curve
Cp= 225.7853 mAh/g



EXPERIMENTAL PARAMETERS

DC Current (A): 0
AC Current (A rms): 0.005
Galvanostatic EIS
15.6.2022
10:57:29
Initial Freq. (Hz): 100000
Final Freq. (Hz): 0.1
Points/decade: 10
Area (cm^2): 1
Conditioning: Off
Init. Delay: On
Time(s): 10
Stab.(mV/s): 0
Open Circuit (V): 0.3392652

EXPERIMENTAL NOTES

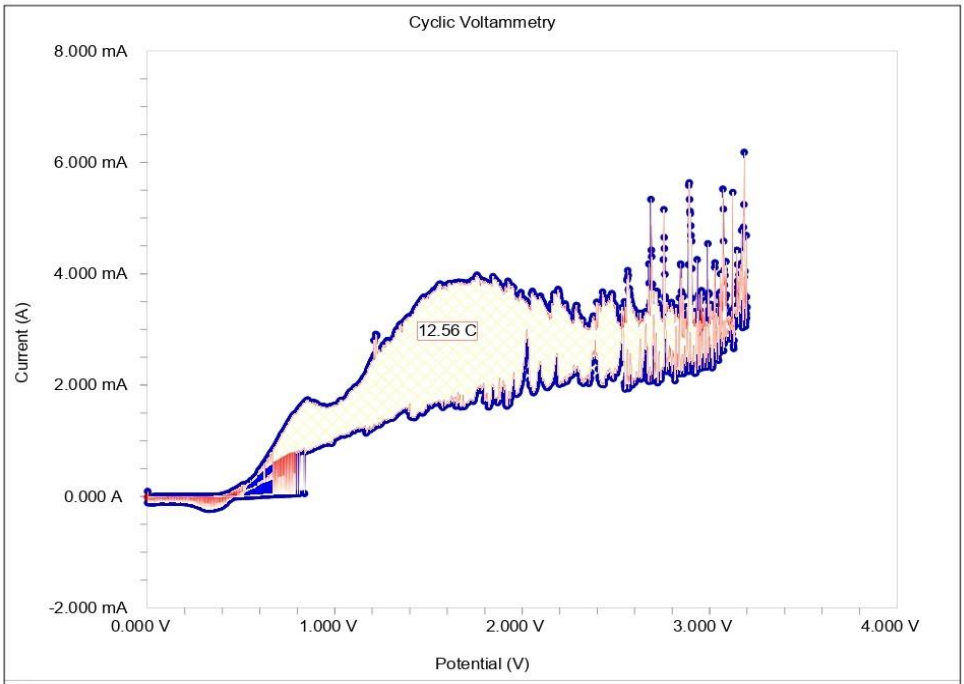


ZCURVE (Ahmed_CF_LiFePO4__EISGALV_0.5mA.DTA)

EXPERIMENTAL PARAMETERS

DC Current (A): 0
AC Current (A rms): 0.005
Galvanostatic EIS
15.6.2022
10:57:29
Initial Freq. (Hz): 100000
Final Freq. (Hz): 0.1
Points/decade: 10
Area (cm^2): 1
Conditioning: Off
Init. Delay: On
Time(s): 10
Stab.(mV/s): 0
Open Circuit (V): 0.3392652

EXPERIMENTAL NOTES

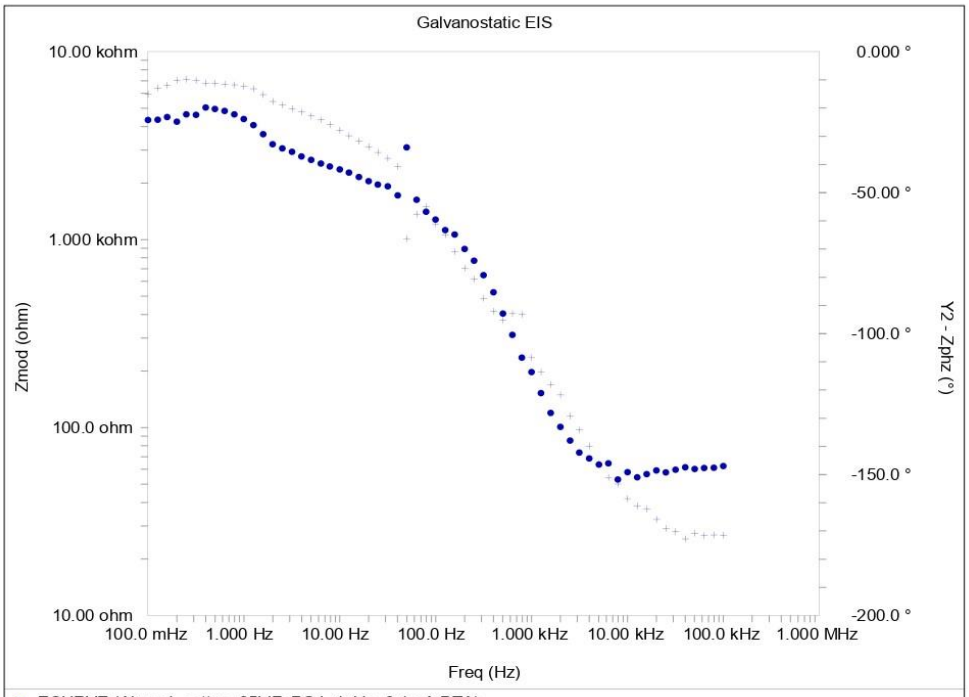


EXPERIMENTAL PARAMETERS

Initial E (V): 0 vs. Eref
Scan Limit 1 (V): 3.2 vs. Eref
Scan Limit 2 (V): 0 vs. Eref
Final E (V): 0 vs. Eref
Cyclic Voltammetry
30.6.2022
13:11:50
Scan Rate (mV/s): 0.999998
Step Size (mV): 2
Electrode Area (cm^2): 1
Equil. Time (s): 5
I/E Range Mode: Auto I/E Range
Max Current (mA): 1000
Conditioning: Off
Init. Delay: Off
IRComp: None
Open Circuit (V): 0
Sampling Mode: Noise Reject

EXPERIMENTAL NOTES

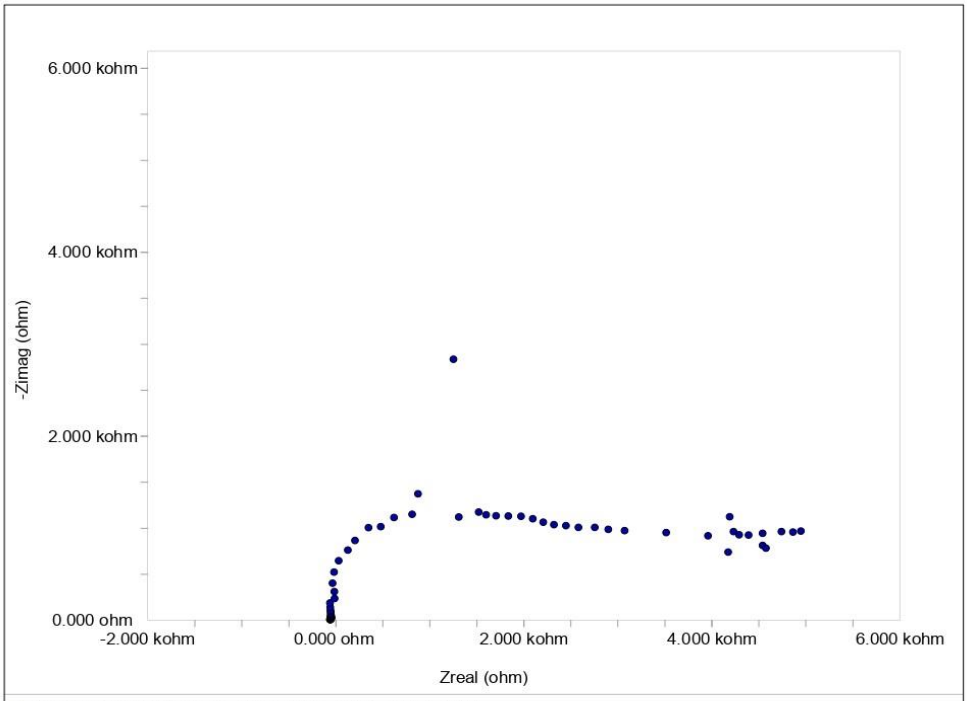
Circle samples of cotton fabric before and after coating with a diameter of 16 mm were cut by a sample cutting machine.
The coating ink consists of the following:
LiFePO4 (85%) -Carbon Black, Super P (10%) -PVDF (5%)
The weight of the ink that was coated was calculated by calculating the weight of the sample before and after the coating process, which is 0.03573 g.
The capacitance was calculated using the following equation:
Cp=A/(3.6 m)
m: The weight of the ink and A: the area within the CV curve
Cp= 108.3745 mAh/g



EXPERIMENTAL PARAMETERS

DC Current (A): 0
AC Current (A rms): 0.0001
Galvanostatic EIS
30.6.2022
13:05:34
Initial Freq. (Hz): 100000
Final Freq. (Hz): 0.1
Points/decade: 10
Area (cm^2): 1
Conditioning: Off
Init. Delay: On
Time(s): 10
Stab.(mV/s): 0
Open Circuit (V): 0.2340472

EXPERIMENTAL NOTES

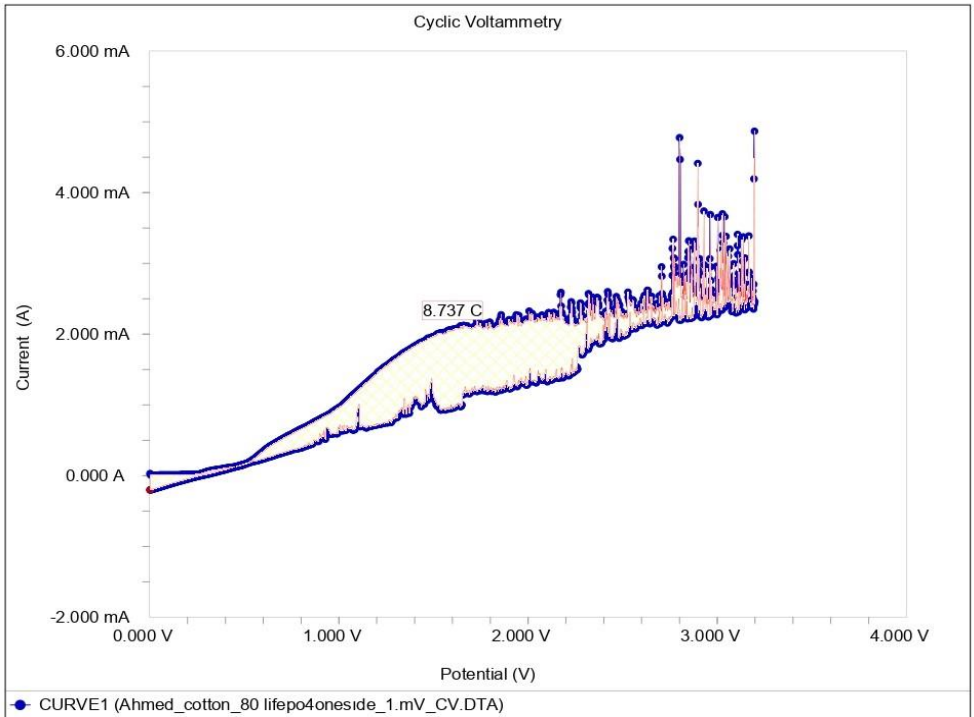


ZCURVE (Ahmed_cotton_85LiFePO4_1side_0.1mA.DTA)

EXPERIMENTAL PARAMETERS

DC Current (A): 0
AC Current (A rms): 0.0001
Galvanostatic EIS
30.6.2022
13:05:34
Initial Freq. (Hz): 100000
Final Freq. (Hz): 0.1
Points/decade: 10
Area (cm^2): 1
Conditioning: Off
Init. Delay: On
Time(s): 10
Stab.(mV/s): 0
Open Circuit (V): 0.2340472

EXPERIMENTAL NOTES

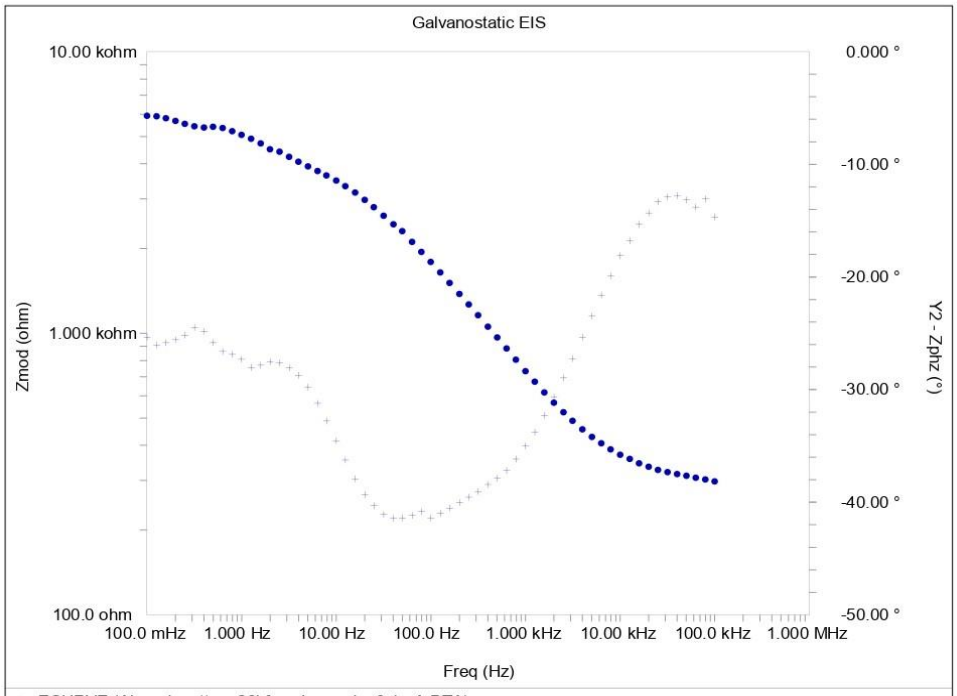


EXPERIMENTAL PARAMETERS

Initial E (V): 0 vs. Eref
Scan Limit 1 (V): 3.2 vs. Eref
Scan Limit 2 (V): 0 vs. Eref
Final E (V): 0 vs. Eref
Cyclic Voltammetry
28.6.2022
16:00:23
Scan Rate (mV/s): 0.999998
Step Size (mV): 2
Electrode Area (cm^2): 1
Equil. Time (s): 5
I/E Range Mode: Auto I/E Range
Max Current (mA): 1000
Conditioning: Off
Init. Delay: Off
IRComp: None
Open Circuit (V): 0
Sampling Mode: Noise Reject

EXPERIMENTAL NOTES

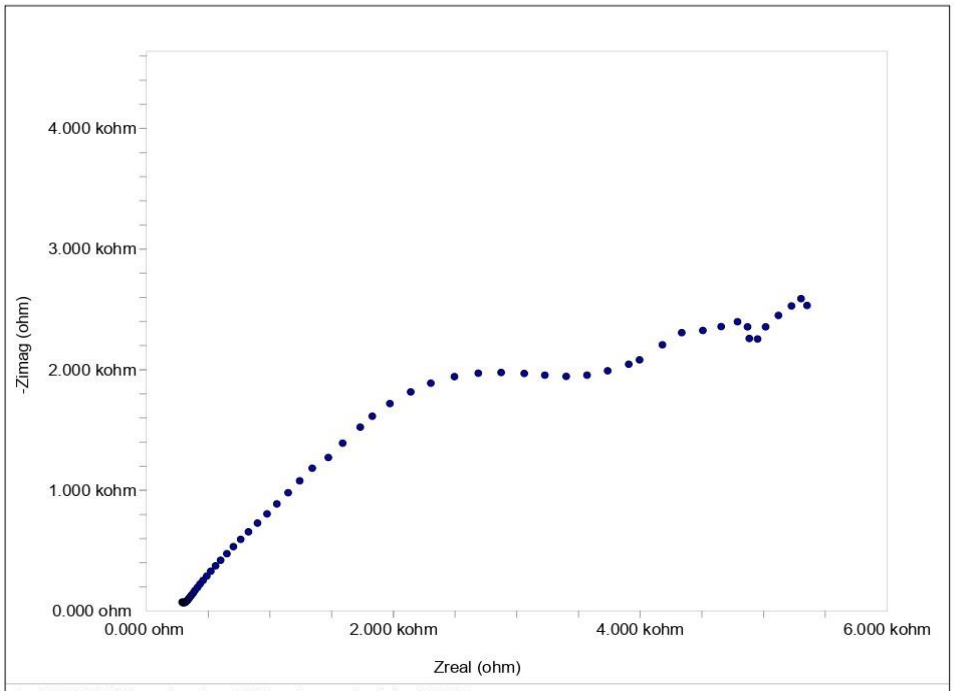
Circle samples of cotton fabric before and after coating with a diameter of 16 mm were cut by a sample cutting machine.
The coating ink consists of the following:
LiFePO4 (80%) -Carbon Black, Super P (15%) -PVDF (5%)
The weight of the ink that was coated was calculated by calculating the weight of the sample before and after the coating process, which is 0.0315 g.
The capacitance was calculated using the following equation:
Cp=A/(3.6 m)
m: The weight of the ink and A: the area within the CV curve
Cp= 77.045 mAh/g



EXPERIMENTAL PARAMETERS

DC Current (A): 0
AC Current (A rms): 0.0001
Galvanostatic EIS
28.6.2022
15:49:34
Initial Freq. (Hz): 100000
Final Freq. (Hz): 0.1
Points/decade: 10
Area (cm^2): 1
Conditioning: Off
Init. Delay: On
Time(s): 10
Stab.(mV/s): 0
Open Circuit (V): -0.2147414

EXPERIMENTAL NOTES

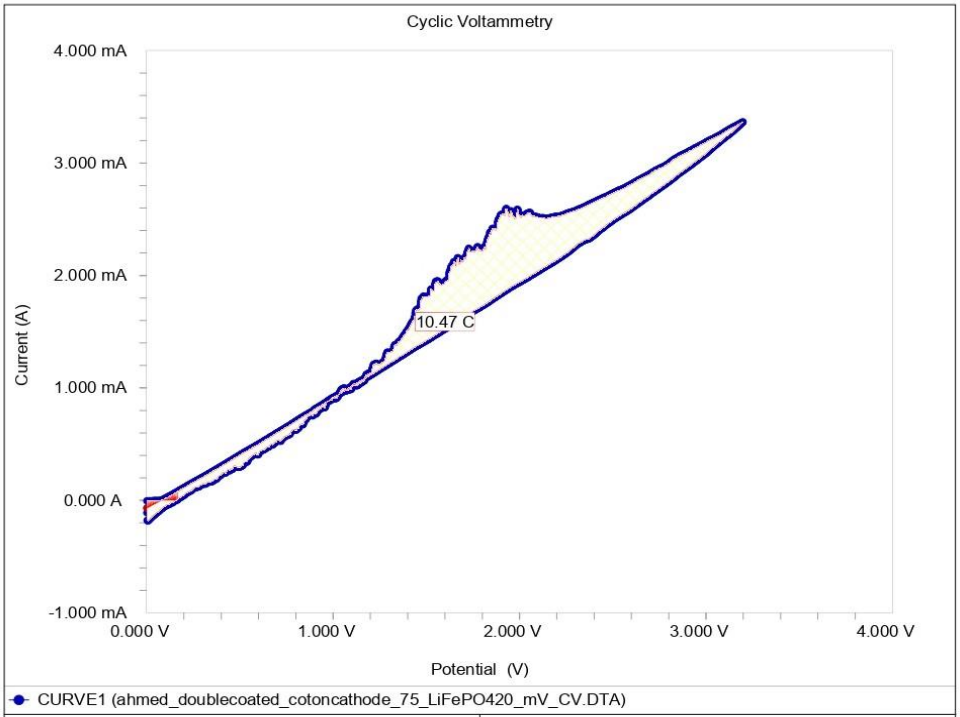


ZCURVE (Ahmed_cotton_80lıfepo4onesıde_0.1mA.DTA)

EXPERIMENTAL PARAMETERS

DC Current (A): 0
AC Current (A rms): 0.0001
Galvanostatic EIS
28.6.2022
15:49:34
Initial Freq. (Hz): 100000
Final Freq. (Hz): 0.1
Points/decade: 10
Area (cm^2): 1
Conditioning: Off
Init. Delay: On
Time(s): 10
Stab.(mV/s): 0
Open Circuit (V): -0.2147414

EXPERIMENTAL NOTES

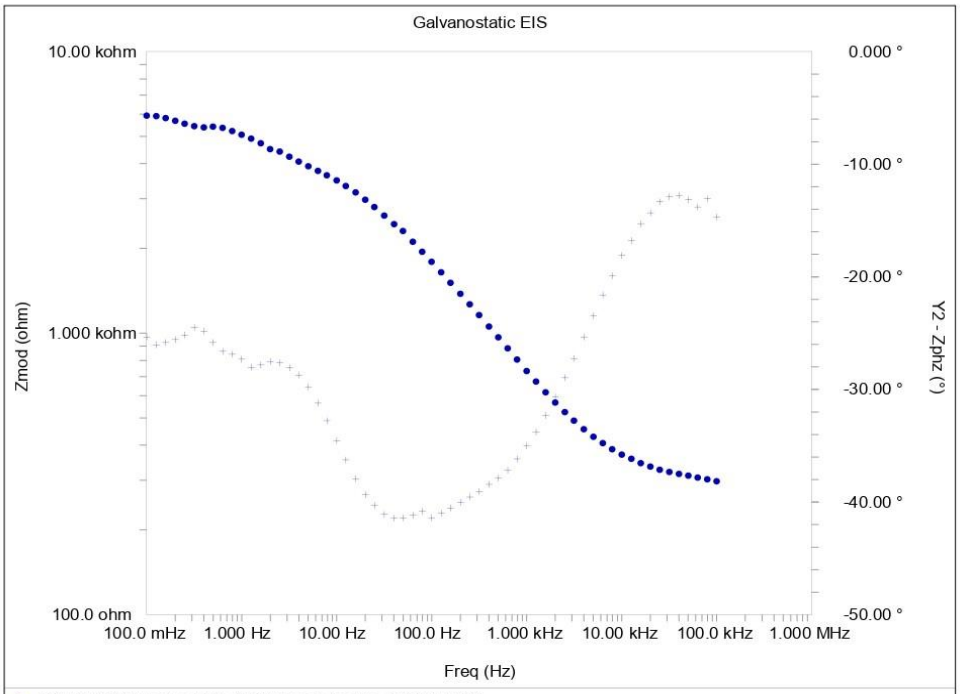


EXPERIMENTAL PARAMETERS

Initial E (V): 0 vs. Eref
Scan Limit 1 (V): 3.2 vs. Eref
Scan Limit 2 (V): 0 vs. Eref
Final E (V): 0 vs. Eref
Cyclic Voltammetry
24.6.2022
16:35:40
Scan Rate (mV/s): 0.999998
Step Size (mV): 2
Electrode Area (cm^2): 1
Equil. Time (s): 5
I/E Range Mode: Auto I/E Range
Max Current (mA): 1000
Conditioning: Off
Init. Delay: Off
IRComp: None
Open Circuit (V): 0
Sampling Mode: Noise Reject

EXPERIMENTAL NOTES

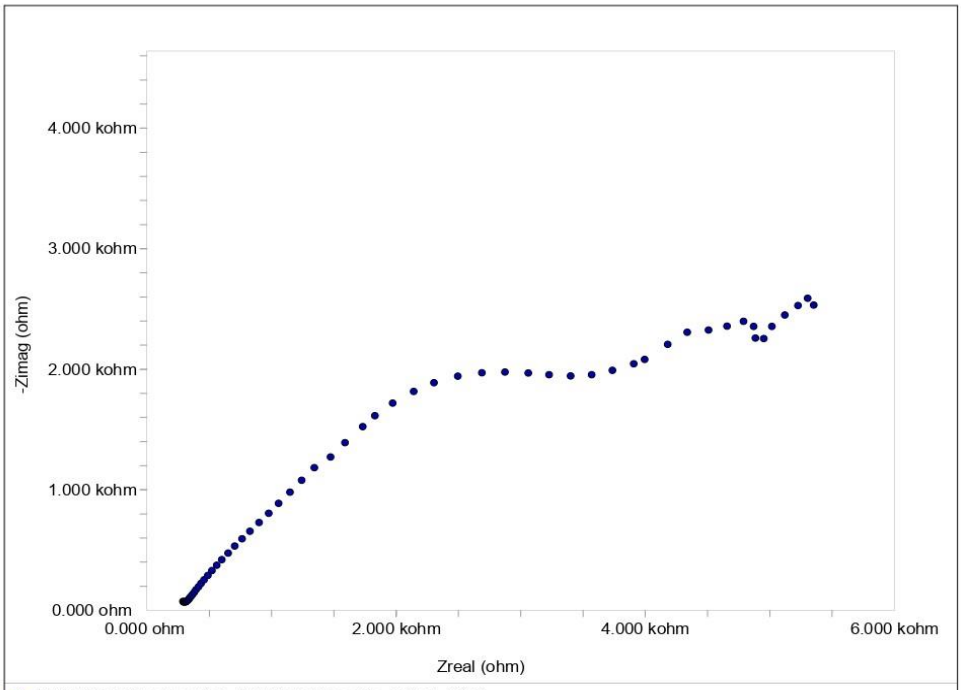
Circle samples of cotton fabric before and after coating
with a diameter of 16 mm were cut by a sample cutting machine.
The coating ink consists of the following:
LiFePO4 (75%) -Carbon Black, Super P (20%) -PVDF (5%)
The weight of the ink that was coated was calculated by calculating
the weight of the sample before and after the coating process,
which is 0.0365 g.
The capacitance was calculated using the following equation:
Cp=A/(3.6 m)
m: The weight of the ink and A: the area within the CV curve
Cp= 79.68 mAh/g



EXPERIMENTAL PARAMETERS

DC Current (A): 0
AC Current (A rms): 0.0001
Galvanostatic EIS
28.6.2022
15:49:34
Initial Freq. (Hz): 100000
Final Freq. (Hz): 0.1
Points/decade: 10
Area (cm^2): 1
Conditioning: Off
Init. Delay: On
Time(s): 10
Stab.(mV/s): 0
Open Circuit (V): -0.2147414

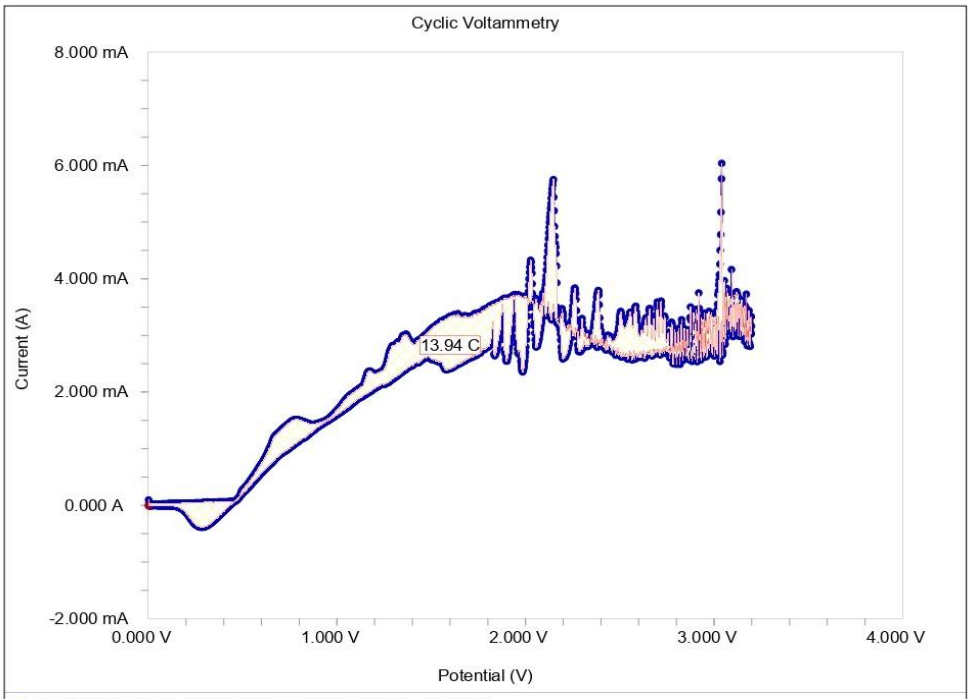
EXPERIMENTAL NOTES



EXPERIMENTAL PARAMETERS

DC Current (A): 0
AC Current (A rms): 0.0001
Galvanostatic EIS
28.6.2022
15:49:34
Initial Freq. (Hz): 100000
Final Freq. (Hz): 0.1
Points/decade: 10
Area (cm^2): 1
Conditioning: Off
Init. Delay: On
Time(s): 10
Stab.(mV/s): 0
Open Circuit (V): -0.2147414

EXPERIMENTAL NOTES

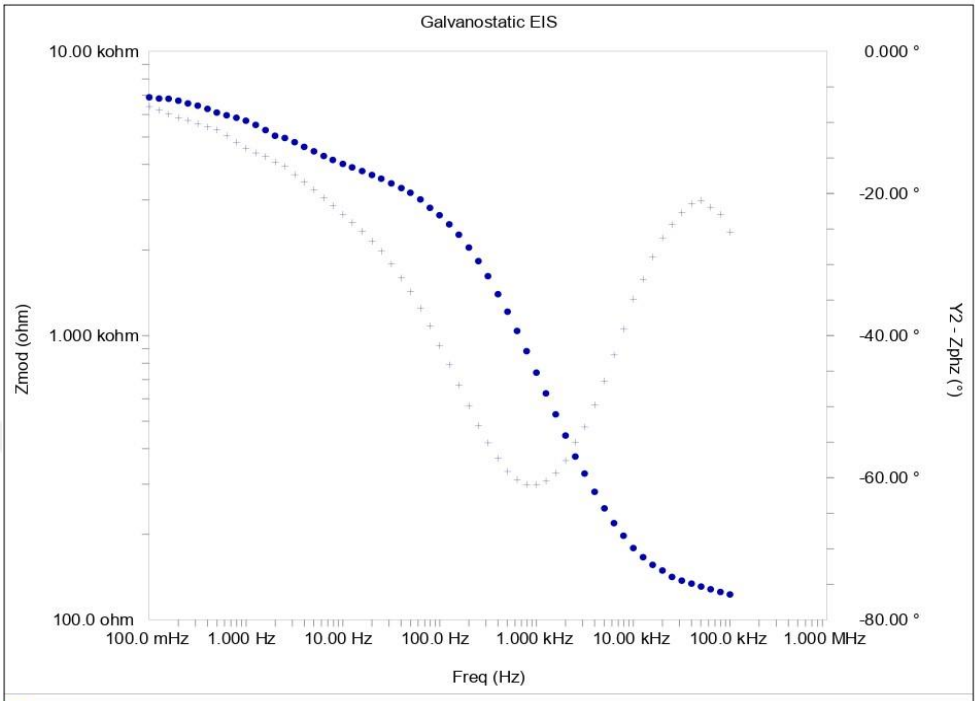


EXPERIMENTAL PARAMETERS

Initial E (V): 0 vs. Eref
Scan Limit 1 (V): 3.2 vs. Eref
Scan Limit 2 (V): 0 vs. Eref
Final E (V): 0 vs. Eref
Cyclic Voltammetry
30.6.2022
11:11:09
Scan Rate (mV/s): 0.999998
Step Size (mV): 2
Electrode Area (cm^2): 1
Equil. Time (s): 5
I/E Range Mode: Auto I/E Range
Max Current (mA): 1000
Conditioning: Off
Init. Delay: Off
IRComp: None
Open Circuit (V): 0
Sampling Mode: Noise Reject

EXPERIMENTAL NOTES

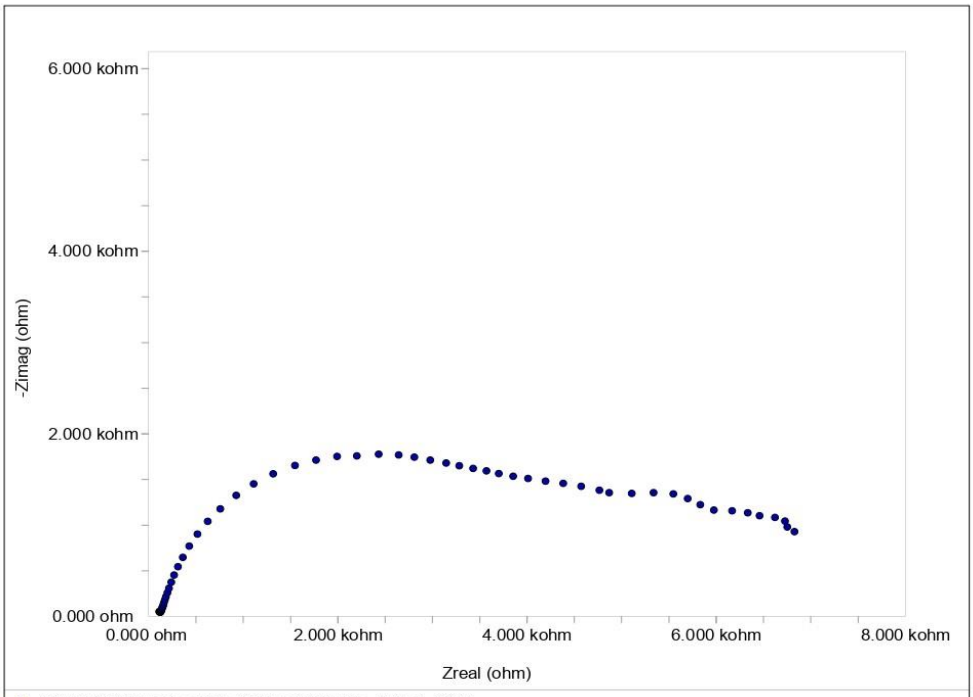
Circle samples of cotton fabric before and after coating with a diameter of 16 mm were cut by a sample cutting machine.
The coating inks consists of the following:
1- LiFePO4 (80%) -Carbon Black, Super P (15%) -PVDF (5%)
2- Graphite (95%) - CMC (5%)
The weight of the ink that was coated was calculated by calculating the weight of the sample before and after the coating process, which is 0.0351 g.
The capacitance was calculated using the following equation:
Cp=A/(3.6 m)
m: The weight of the ink and A: the area within the CV curve
Cp= 110.319 mAh/g



EXPERIMENTAL PARAMETERS

DC Current (A): 0
AC Current (A rms): 0.0001
Galvanostatic EIS
30.6.2022
11:03:22
Initial Freq. (Hz): 100000
Final Freq. (Hz): 0.1
Points/decade: 10
Area (cm^2): 1
Conditioning: Off
Init. Delay: On
Time(s): 10
Stab.(mV/s): 0
Open Circuit (V): -0.1535709

EXPERIMENTAL NOTES



ZCURVE (Ahmed_cotton_80LiFePO42side_0.1mA.DTA)

EXPERIMENTAL PARAMETERS

DC Current (A): 0
AC Current (A rms): 0.0001
Galvanostatic EIS
30.6.2022
11:03:22
Initial Freq. (Hz): 100000
Final Freq. (Hz): 0.1
Points/decade: 10
Area (cm^2): 1
Conditioning: Off
Init. Delay: On
Time(s): 10
Stab.(mV/s): 0
Open Circuit (V): -0.1535709

EXPERIMENTAL NOTES